Impacts of Smoke-Ash from the 2021 Wildfires to the Ecology of Lake Tahoe

Work Order: #107-UNR
TRPA Contract #17C00018
Date of Work Order: July 19, 2022

Authors and Institutions

Dr. S. Chandra, Dr. F. Scordo, E. Suenaga, Dr. J. Blazsczak, Dr. C. Seitz, E. Carlson, and K. Loria
University of Nevada Reno's Global Water Center

Dr. J. Brahney
Utah State University

Dr. S. Sadro, Dr. G. Schladow, Dr. A. Forrest, K. Larrieu, and Dr. S. Watanabe
University of California Davis Tahoe Environmental Research Centre

Dr. Alan Heyvaert
Desert Research Institute

Dr. C. Williamson and E. Overholt
Miami University

Acknowledgements

The Caldor and other large wildfires of 2021 presented an unprecedented opportunity to investigate how major wildfires and their associated smoke conditions influence lake conditions. However, resources to support scientific investigations immediately after large crisis like wildfires are difficult to acquire; scientists rely on contributions from individuals and organizations with flexible funding models. We are grateful to the following organizations and people who supported this work including: League to Save Tahoe (Darcie Goodman-Collins and Jesse Patterson), Tahoe Fund (Amy Berry and Caitlin Meyer), Dr. Stephen Talbot and Dr. Jill Derby , Dr. Mick Hitchcock, Lahontan Water Quality Control Board (Melissa Thaw, Mary-Fiore Wagner), Bently Enterprises (Nick Hinkel, Camille Bently, Carlo Luri), the Parasol Foundation Community Foundation of Northern Nevada (Laura Roche), Geoff and Sally White, Ryan and Karen Dotson, the Tahoe Science Advisory Council (Program Officer Robert Larsen, co-chair Ramon Naranjo).

This project would not have been possible without the help of many people from all the institutions involved these efforts. From Utah State University, we would like to acknowledge and thank Audree Provard for her help in processing and analyzing samples in the Utah State University laboratory. We would also like to thank the Utah State Agricultural Experiment Station Project UTAO1669 for Dr. Janice Brahney's time. From the University of California Davis, we would like to thank the TERC field and laboratory staff who made data collection and analysis possible during the extreme conditions of the Caldor Fire, including Brant Allen, Brandon Berry, Helen Fillmore, Anne Liston, Katie Senft, Steven Sesma, Raph Townsend, Aaron Vanderpool, and Erik Young. We would also like to thank the graduate and undergraduate students from UC Davis, Nick Framsted, Melissa Grim, Carolyn Jones, and Adam Vera for help with the laboratory experiments. From the University of Nevada Reno, we would like to thank our undergraduate technicians Luisa Ortega, Parker Land, Sky Russell, and Wyatt Watson for their assistance in the lab. We would also like to thank members of the Blaszczak Laboratory for their assistance in maintaining and monitoring the nearshore instruments in Lake Tahoe. We are grateful to the stewards of Lake Tahoe who permitted us to deploy and helped monitor our ash collectors during the 2021 wildfire season: Gary and Susan Clemons, Goodman family, Sharon Lane, Alibi Ale Works (Kevin Drake and Rich Romo), Heather Segale, Dan Segan, Rachel Sigman, Shawn Butler, and Scott Attinger.

Table of Contents

Lay Summary including a summary of findings and recommendations

Quantifying the disturbances from wildfire smoke generated from regional to continental wildfires is particularly important as mega-fires are predicted to increase with changes in climate. Understanding the direct influences of wildfire smoke is of particular importance to policymakers who are already confronted with managing ecosystems important to the regional economy, like Lake Tahoe, that are undergoing accelerated environmental change from multiple stresses. Questions remain about how wildfires augment or exacerbate the current changes and whether these disturbances from wildfires have lasting impacts.

In 2021, while still under COVID-19 pandemic conditions and limited capacity at their institutions, a team of 34 scientists and early career trainee students (undergraduate and graduate) from 5 institutions, lobbied for a "rapid response" study which focused on quantifying the influence of wildfire smoke to Lake Tahoe and a smaller lake representative of other lakes in the area. With support from non-profit organizations, agencies, private donors, and their individual institutions, the scientists were able to initiate immediate studies to quantify the impacts of wildfire smoke to the water quality of these ecosystems. Without the support of many organizations who contributed to these efforts, and the staff available at the time from the institutions to conduct such a study, this rapid action to understand the impacts of wildfire smoke could not have occurred. The team used existing information from monitoring programs and publicly available data, opportunistic sampling events using novel technologies, laboratory experiments, and basic concepts in science to determine the impacts of wildfire smoke from the 2021 season to lake dynamics. At the heart of the investigations was the augmentation and interpretation from the long-term monitoring information (physical and biological) collected at Lake Tahoe combined with analysis of freely available weather and air quality monitoring information.

The publicly available "purple air" sensors are useful to understand the air quality conditions around the basin from wildfire smoke. These sensors and resulting calculations for particulate matter of smaller size (2.5 micron in size) can be used to understand the variability in smoke conditions around the lake, which was highly variable over time. In general, smoke conditions interpreted as changes in potential particulate matter deposition and light were strongest in the southern part of the lake, but sites across the lake would exhibit synchronous and asynchronous behavior indicating the potential for changing light conditions across the lake surface. As air quality changes within the basin, we observe differential changes to surface or incident light conditions measured at a continuous sensor in Tahoe City. Changes in surface light influence biological, chemical, and physical conditions in freshwaters. Considering the variability of smoke across the basin exhibited by the publicly available air sensors, having calibrated surface light radiometers across the spectral band paired with weather stations around the basin could assist in determining nearshore and offshore changes around the lake from changes in atmospheric conditions from wildfires.

Climate and snowpack are known to influence the relative loads of particulate matter and nutrients to the lake. Years with higher snow condition led to increased loads of particulate matter to the lake. Thus, we adopted an approach to compare the 2021 wildfire smoke conditions to other climatic years (dry to wet). Since 2021 was a relatively drier year on record, we expected transparency to start relatively high compared to years with larger snowpack. As expected, before smoke conditions were observed in the basin in 2021, we observed high water transparency measured by secchi disk and increased penetration of ultraviolet and visible light, known as photosynthetically active radiation. Ultraviolet light has been shown to control many biological and chemical processes in lakes and photosynthetically active light conditions determine the depth of algal production and organismal foraging behavior. However, after the smoke period, the transparency and ultraviolet and visible light was immediately reduced by 4.5m, 17.5m, and 7.6m, respectively. The reduction in light conditions was similar to years when there was higher snowpack indicating that wildfire smoke and resulting depositional impacts may act similar to years with more snow.

From a single fixed monitoring station at a buoy in the lake, the atmospheric deposition of particles was a relatively small contributor to overall lake particles where the mean addition was approximately 0.2% of the population of particles in the upper 20 meters of the lake each day. It is not known what fraction of the in-lake particle number was organic or inorganic. Evaluating the loading from another view with broader spatial layout using collectors distributed around the lake indicated the highest ash deposition rates occurred during the first sampling period (Aug. 26th – Sept. 10th, 2021) and around the southern end of the lake. Average ash deposition around the lake during this period was 240.5 mg m^{-2} d^{-1}. The heterogeneous deposition in space and time around the lake, differential quality of material, disappearance of this material, and likely contribution of this material to open water productivity and water quality conditions (see below) indicates the need for a more robust atmospheric deposition and air quality measurements around the basin. Using an autonomous vehicle, we were able to determine the concentration of fine particles in space and time after the wildfires. There is a rapid decrease in fine suspended particulate matter concentrations indicating the particles entering the lake are rapidly cleared from the water. As deposition decreased by mid-September, concentrations of small particles in Lake Tahoe followed a similar trend with little lag indicating that these small particles disappear either through physical settling, photodegradation, or consumption.

The deposition and resulting degradation of wildfire smoke-ash material and changes in atmospheric light condition influence the production and composition of open water algae producing organic material in the water column that contributed to the observed decline in clarity and light conditions. The monitoring data suggests changes to where productivity in the water column occurs, the composition of plankton, and the overall amount of phytoplankton production, but little change in algal biomass as measured via chlorophyll. Clearwater lakes with depth can have two layers of algal production, one in the shallower water and one in the deeper waters where light levels are lower, near or below 1 to 0.1% of the surface, and nutrients can be higher in availability. The deep-water layers of algae can be important for zooplankton energy and feeding supporting the flow of carbon to fish consumers. Prior to the

arrival of smoke conditions in the basin, the maximum amount of chlorophyll occurred in the deeper water around the typical summer depth of 60-80 meters. After the arrival of smoke and changes in the surface levels of light and decrease in visible light depth, chlorophyll levels rise in depth. A previous published study at Castle Lake, a moderately productive lake similar to Emerald Bay or other small water bodies in the region, showed smoke in the atmosphere and changes in light conditions in the water column that led to the disappearance of the chlorophyll a maximum. Thus, having a high frequency measurements of water quality, including chlorophyll a in time and space, during these large-scale disturbances can inform us of the changes in ecological conditions in these large lakes which can influence zooplankton.

Together with the change in deep chlorophyll maximum there was a change in the phytoplankton community. Compared to historical information which shows that Lake Tahoe's algal community is predominantly dominated by diatoms, the 2021 information indicates a change to the larger bodied *Leptolyngbya,* which is a cyanobacteria. Some cyanobacteria can fix nitrogen supplying this nutrient to the lake after they die and many also produce toxins that are generally inedible for filter feeding animals like zooplankton due to their size and toxicity. Some have part of their life history in the bottom habitats of the lakes and *Leptolyngbya* is found in the nearshore of Lake Tahoe. Along with changes in composition, likely due to changing light conditions and the addition of nutrients into the lake from ash (see below), the amount of open water algal production was the highest annual value recorded at 334 g carbon meter^{-2} year^{-1}. The value is 20% higher than the record set in 2019 although the data is still provisional by UC Davis. This finding is consistent with the very high algal abundance in 2021, and with the occurrence of very high cell counts of *Leptolyngbya*. Previous studies by Charles R. Goldman and colleagues that evaluated the impacts of wildfire smoke from the Wheeler fire in the 1980s also suggested the highest production on record at the time of the fire. Together this indicates the importance of wildfire smoke in influencing open water algal production.

Information from experiments which manipulated both the light and ash sources, and visual observations by our scientists on the ground nearly each day during the wildfires, complement the lake monitoring data and elucidates the mechanisms affecting production. While there is more ash deposited in the south/east and less in the north/west (see above), the quality of ash deposits varies in space. Generally, less ash is deposited in the north/west part of the lake, but the ash deposited is much higher quality contributing to algal and bacterial production. This occurs when there is simulated reduced light conditions in the atmosphere from wildfire smoke, or normal light conditions for smaller lakes, and we see that ash deposited around the lake along with ash collected from the burn sites, which can run off into the lake at a later time, stimulate net algal production. This suggests that lakes can have complex responses to smoke ash deposits and under different atmospheric light conditions and it may depend on the lake's starting conditions of algal and bacterial community structure and nutrient state at the time of deposition. Future work should couple fields of knowledge and expertise that are exploring the development of wildfires, creation of wildfire smoke and weather, distribution in the atmosphere, deposition of ash deposits, and effects to lake dynamics (light, nutrients, biological production, and behaviour).

Incubating lake water with ash and manipulating light conditions also suggests that the lakes start off as net heterotrophic (dominated by bacteria that consume organic carbon rather than algal dominance). The responses of the lake water quality dynamics during the experiments suggest that the lakes take time to process the organic matter, which is dominated by bacterial and respiration processes. Once this initial flux of organic matter is processed then the phytoplankton and light driven utilization of carbon and nutrients occurs. While the method for using oxygen may be useful for understanding initial changes in water quality, it will take time to detect changes in experiments or the water column unless there is a substantial change to the community. The experimental studies combined with the fact that particles deposited to the lake "disappeared quickly" suggests that the microbial dynamics in the lake are likely very important for processing organic matters. Currently the monitoring and experimental investigations funded at the lake do not include the evaluation of microbial activity, biological players or micro zooplankton grazers which feed on them.

Immediately during the wildfire smoke conditions in the basin and after the wildfire, continuing into the summer of 2022, our teams and many members of the public observed changes to the nearshore environment, specifically reporting increases in nearshore and bottom algal growth in some parts of the lake but not others. During our collections of ash deposited during the wildfire of 2021, we visually observed ash washing up on beaches and trapped between sediment particles at the bottom of the lake. Using high frequency sensing for oxygen and temperature, coupled with a published model, we determined that nearshore productivity (algal and bacteria) increased immediately after the wildfire smoke entered the basin, but the influence was relatively short-lived. We do not have other years to compare nearshore production, nor are there measurements at depth through the lighted zone of the lake (40-50 meters). Given the variability in nearshore algal and bacterial production due to variable habitats around the lake (cobble, sand, rocks) and nearshore and offshore mixing dynamics, we recommend that additional high frequency sensors and models incorporating metabolic and mixing processes are developed to understand how light, ash deposition, and nutrient run off influence the nearshore environments in the lake. We predict that not every part of the nearshore will respond the same way due to the variability within the environment.

While not explicitly required as a part of this study, we did measure metal toxicants in the ash deposited in the lake. We observed higher levels of metal deposits in the north/west sites that exhibited lower loads to the lake compared to the south/east shores. In the future, analyzing information collected by the US Environmental Protection Agency's IMPROVE program, the loading of toxic metals, and conditions pre- and post-wildfire may be warranted. Burning structures associated with wildfire may result in the deposits of metals and other contaminants which influence public health and the ecology of the lake.

In conclusion, this rapid response effort by scientists shows the importance of wildfire connections to fundamental lake processes. The efforts would not have been possible without the generous support of private donors, our local non-governmental organizations and resources provided to the Tahoe Science Advisory Council). Current funding models do not allow scientists to access funding during times of crisis even though they are ready to

contribute to understanding how a crisis can change the management of a lake. In this study, while we find that the overall deposition of smoke-ash from fires in the region and watershed may occur proximate to the source of a fire (e.g., Caldor), the quality of that material is highly variable with the highest quality of some materials deposited furthest from the fires. The quality of available nutrients for production may vary with differential contributions of variable ash sources. Furthermore, areas of deep-water algal mass change their location within the lake likely due to changes in light in the atmosphere. Overall, particles introduced into the lake are lower compared to other sources but may be rapidly transformed after degradation or consumption for use by bacteria and algae. The nutrients available from the ash stimulate changes to production and algal composition to less desirable species like cyanobacteria. Certain types of ash deposits are more available to production depending on the lake type which brings a cautionary note of investigating the influences of wildfire generated smoke-ash and deposits left on the ground which can run off into the water or become aerosolized and deposited on the lake at another time. Changes to the nearshore production can occur but longer-term influences on this habitat are not known. Increased algal growth in 2022 in select beaches of Tahoe suggests a contribution of wildfire ash to metabolic (bacterial and algal) dynamics. There are inherently complex connections between the wildfire smoke, air quality and resulting changes in light condition, and nutrients deposited to the lake. If we are going to quantify the impacts of these regional wildfires and their smoke-ash deposition on the lake then we need to expand programs related to air quality monitoring, connections to lake production and not biomass, and enhance our scientific understanding of whole lake processes (nearshore and offshore, bacterial and algal) not only through monitoring but developing a mechanistic understanding of changes through experiments and model evaluations.

BACKGROUND

Conserving Lake Tahoe's water clarity is, and historically has been, a major priority of managers and scientists alike. Efforts to understand the drivers of offshore water clarity include, but are not limited to, understanding the type of particles (algal, terrestrial organic or inorganic) which contribute to the loss of clarity, understanding the inter- and intra-annual particulate loading from watersheds, storm water runoff, the role of lake mixing and physical processes, including alterations to these dynamics due to climate change, and the role of animals in controlling planktonic biomass. Efforts to understand nearshore water quality, including clarity and periphyton growth, have been more limited than pelagic water clarity but do include long-term monitoring of algal biomass in the nearshore edge of the lake, modeling of hydrodynamics, studying the connections between groundwater to surface waters, and investigating the role of invasive crayfish in the nearshore food web. There is growing realization that other external anthropogenic effects, such as smoke and atmospheric deposition of particles from wildfires, drive changes in water clarity and affect ecological connections within the lake in both nearshore and offshore habitats.

The smoke generated from the 2021 wildfires presents a unique opportunity to understand how major disturbances near and within the basin influence short and long-term water quality dynamics in Lake Tahoe. The Tamarack, Caldor, and Dixie Fires burned outside of the Lake Tahoe basin and impacted the air quality for weeks to months in the summer and fall of 2021 (Figure 1). Ultimately, the Caldor Fire burned eastward until it crossed over the Sierra Nevada range into the south Tahoe basin. Understanding these disturbances at regional scales is becoming particularly important for policymakers as mega-wildfires become a more frequent occurrence with changing climate and as we try to contextualize the impacts of large-scale disturbances with the finer scale impacting Lake Tahoe's ecosystem.

There have been limited efforts to explore how indirect effects from wildfire smoke influence lake clarity in Lake Tahoe or other water bodies. Typically, smoke plumes from previous wildfires were limited in their duration and frequency of exposure, although some insights can be gained on how they affected the lake. For example, Goldman et al. (1990) found that the Wheeler Fire in Southern California in 1985 increased algal production in July to its highest level reported at the time. The increase in algal production was attributed to changes in incident (surface) light and to stimulation of growth from nutrients, including micro and macronutrients, although these were not directly measured during the study. Williamson et al. (2016) found direct changes to light reaching Lake Tahoe's surface (incident ultraviolet to visible light ratio) in July to early August 2014 during the King Fire. These changes influenced the depth distribution of zooplankton, an important food resource for fish (Urmy et al. 2016). Most recently, a study at Castle Lake in Northern California compared the impacts of smoke from multiple fires in 2018 in a small subalpine lake in Northern California (Scordo et al. 2021) to hydroclimatic periods without smoke. In those studies, wildfire smoke cooled the lake and decreased ultraviolet light in the upper waters that typically suppresses algal growth. The algal productivity increased by 109% in the upper part of the lake and the deep-water algal production was near zero. Animals responded in different ways with slight changes to the composition of zooplankton and changes

in the behavior of trout. These limited studies of wildfire smoke suggest that there can be several complex, yet direct, changes to lake productivity in the offshore and changes in animal behavior. No published study to date has evaluated changes to nearshore water quality in Lake Tahoe or elsewhere. Observations by Chandra (report author) the week of Sept 10, 2021, suggested a greening of the nearshore in South Lake Tahoe along Baldwin Beach, Bijou, and South of Cave rock to Glenbrook. In addition, orange aquatic fungus was observed collecting on top of ash that was washing up on beaches around the lake.

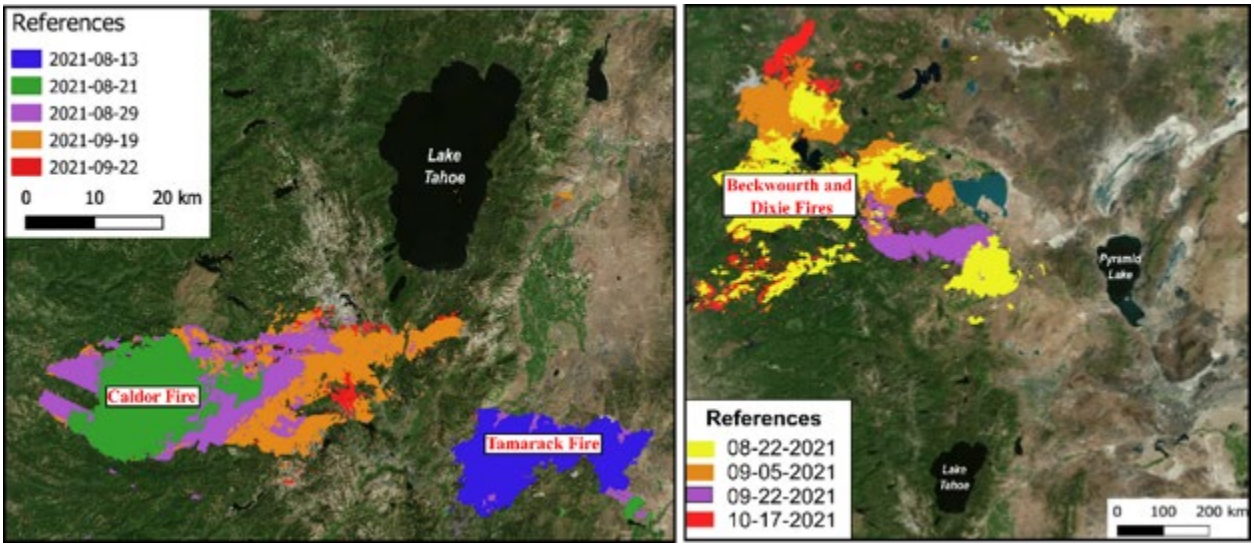

Figure 1. Location of Lake Tahoe in north-west California and the area burned by the Caldor, Tamarack, Dixie and Beckwourth fires in 2021, within 400 km radius from the lake.

Objectives

Our project explores direct connections of wildfire smoke and their interrelationships across different components of the lake ecosystem (Figure 2). Our main objectives will be as follows:

1. Quantify the changes in air quality and light regime during periods of smoke over Lake Tahoe during the 2021 fire season (Task 1 & 7).
2. Determine the composition and "lability" of ash particles deposited around the lake during the 2021 fire period (Task 2)
3. Quantify the effects of smoke on algal growth and productivity in the pelagic (Task 3 & 8) and nearshore (Task 4) zones of Lake Tahoe.
4. Assess changes in water quality and phytoplankton in comparison to years without prolonged smoke coverage using UC Davis long term monitoring data (Task 5).
5. Measure the particle size distribution and concentrations in the water column affecting clarity (Task 6)

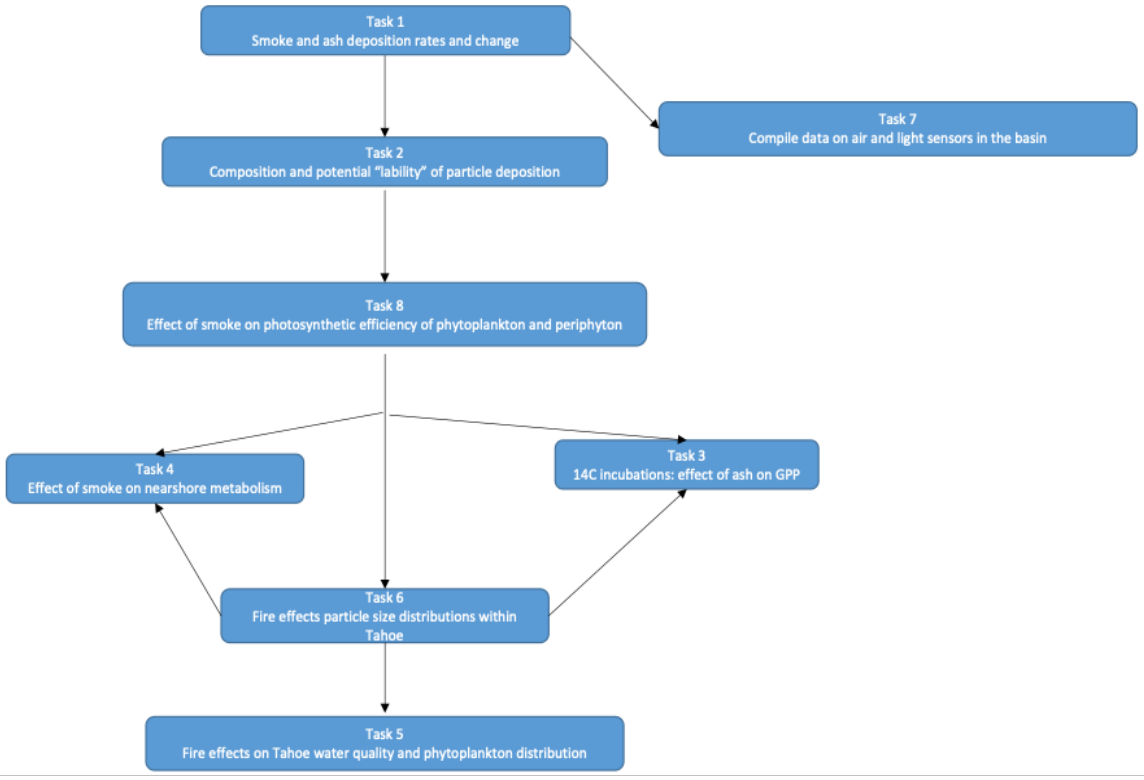

Figure 2. Conceptual linkages between Tasks 1-7 associated with this project as described in the original Task Order created for this project.

We have added a plain language summary under the objective or task to facilitate a basic understanding of key findings and recommendation for each section.

OBJECTIVES OF THIS STUDY AND FINDINGS

Objective 1: Quantify changes in the air and light regime during periods of smoke at Lake Tahoe in the 2021 fire season (Tasks 1 & 7).

Plain Language Summary: The Caldor fire led to heavy ashfall in the Lake Tahoe region. The amount of ash that fell was highly variable around the lake with more ash falling in the first sampling period post-fire. Ash deposition rates fell by 70% in the following two sampling periods. Wind trajectories and proximity to the fire influenced the location of the ash deposition, with five times more ash falling in the south and eastern areas of the lake as compared to the north and west. Air monitoring stations around the basin indicated diminished air quality, suggesting an exceedance of both the Federal and the State of California's $PM_{2.5}$ air quality standards (50 and 30 μg m^{-2} in 24-hour $PM_{2.5}$, respectively). Lower air quality persisted for a longer period closest to the fire near the southern end of the lake. The elevated concentrations of ash in the air altered the light conditions around the basin, specifically by diminishing the amount of solar radiation that reached the lake, including both the ranges of light wavelengths needed for photosynthesis (PAR) as well as harmful ultraviolet light (UV). Since light conditions near the surface of the lake are often too intense for algal communities, it is anticipated that reduced PAR and UV may lead to increases in algal production as well as the movement of algal communities up in the water column towards the surface.

Task 1. Quantify areal estimates of particulate deposition on the surface of the basin and collection of ash particles.

J. Brahney, F. Scordo, C. Seitz, E. Suenaga, E. Carlson, S. Chandra

To quantify areal estimates of particulate deposition around Lake Tahoe, we placed atmospheric dry deposition samplers at 10 locations encircling the basin. The locations were selected based on their proximities to the Caldor fire (e.g., southern end of the lake was closest location) and were also placed around the east, west, and north shores to include the entire basin.

Ash deposition rates were determined using standard bulk deposition samplers where glass marbles are used to retain deposited material within the collection vessel (Reheis 1997; Figure 3). Samplers were mounted on the ground surface or placed atop buildings. At the end of each sampling period, fine synthetic brushes were used to collect the dry particulates from the marbles and collection vessel for nutrient analyses and experimentation. Dry recovered sample mass was determined gravimetrically by brushing the ash into pre-weighted containers. The samplers were then triple rinsed with deionized (DI) water and filtered through pre-weighed PES (0.2 μm) filters to obtain the total deposition mass. In total there were three sampling periods ranging from 8 to 16 days starting August 22nd through October 7th, 2021, to reflect typical atmospheric deposition sampling periods. Deposition rates within each sample period were calculated using the mass recovered, the sampling interval, and the area of the bucket

(0.066m^2). Ash deposition rates were used to quantify nutrient and metal deposition rates (see Objective 2). Additional ash was collected directly from the ground, hereafter "ground ash", from southeastern locations of the Tahoe Basin where heavy accumulation occurred (Table 1).

Ash deposition when summarized by lake region (south/west, north/east, and all sites) was highly variable in both space and time around Lake Tahoe (Figure 4 & 5, Tables 1 and 2). Deposition rates varied from 20.0 to 694 mg m^{-2} d^{-1}. The highest deposition rates occurred during the first sampling period (Aug. 26th – Sept. 10th, 2021) and around the southern end of the lake (Table 3.2). Average ash deposition around the lake during this period was 240.5 mg m^{-2} d^{-1}. From September 10th-24th, deposition rates fell by 71% to 69.6 mg m^{-2} d^{-1}. Through the following weeks (Sep 24th - Oct 7th), ash deposition rates fell only slightly to 61.5 mg m^{-2} d^{-1}. Deposited ash in the north and western areas was visibly different from ash collected in the south and eastern areas of Lake Tahoe. Northern and western deposition was brown in color and contained visible plant fragments, whereas ash collected in the southern and eastern areas were finer grained and darker in color, particularly samples collected at sites in South Lake Tahoe (SLT) and South Lake Basin (STB), and the Tahoe Regional Planning Agency (TRPA, Figure 4)

Figure 3. A) Ash on beaches around Lake Tahoe. B & C) Bucket method used to collect atmospheric deposition using 5-gallon buckets with glass marbles.

Table 1. Location and ash loading rates (mg of dry weight of material*m^{-2} * day^{-1}) of the atmospheric deposition samplers at 8 locations around the Tahoe Basin. *Location where ash was collected on the ground, no bucket deposition collectors at this site. **Take home:** Ash deposition rates (mg m^{-2} d^{-1}) were highest in the south-east regions of the lake at the end of August/early September, with rates over 5 times higher than in the north-west regions.

	Latitude	Longitude	Aug 26 – Sep10	Sep 11 – Sep 18	Sep 25 –Oct 7
South Tahoe Basin (STB)	38.8818	-120.0223	536	76	134
South Lake Tahoe (SLT)	38.9404	-119.9449	694	71	45
Tahoe Regional Planning Agency (TRPA)	38.9662	-119.931	579	134	86
Cave Rock (CR)	39.0309	-119.949	86	45	20
Glenbrook (GB)	39.0871	-119.9396	68	131	57
Alibi Brewery (AB)	39.247	-119.9535	36	104	72
Tahoe City field station (TC)	39.185	-120.1217	22	35	23
Tahoma (TH)	39.063	-120.1285	100	31	71
Rubicon Bay (RB)	39.0112	-120.1157	121	42	87
Cascade Lake (CL)	38.9469	-120.0887	164	25	21
Ground ash (GA)*	38.8679	-119.9638	NA	NA	NA

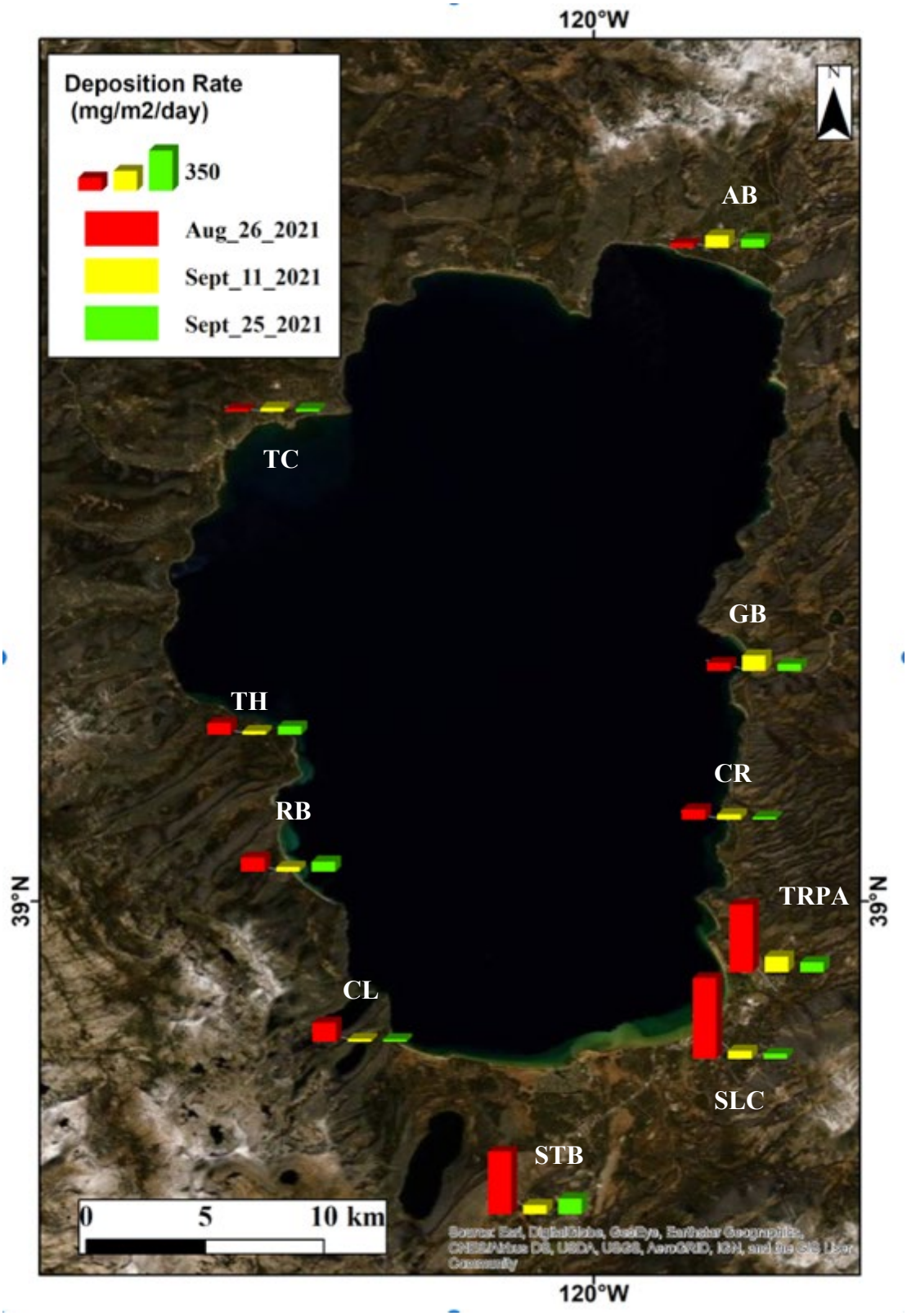

Figure 4. Ash deposition rates at 10 locations around the Lake Tahoe Basin from three time periods between August 26th through October 7th, 2021, during the Caldor Fire.

Table 2. Average ash deposition rates (mg m^{-2} d^{-1}) during three sampling periods from 10 sites encircling Lake Tahoe. Deposition rates in the south and east sites closer to the fire experienced higher rates of deposition during late August and early September. **Take Home:** Deposition fell predominantly during the first week of sampling and deposition rates in the south/east were 5x higher than the north/west.

All Sites	Average Rate	Std. dev.
Aug 26 - Sept 10, 2021	240.46	256.17
Sept 10 - Sept 24, 2021	69.59	41.12
Sept 24 - Oct 7, 2021	61.49	36.19
South/East Sites	Average Rate	Std. dev.
Aug 26 - Sept 10, 2021	469.07	275.84
Sept 10 - Sept 24, 2021	103.22	34.29
Sept 24 - Oct 7, 2021	80.55	39.34
North/West Sites	Average Rate	Std. dev.
Aug 26 - Sept 10, 2021	88.05	52.76
Sept 10 - Sept 24, 2021	47.52	32.18
Sept 24 - Oct 7, 2021	54.53	30.55

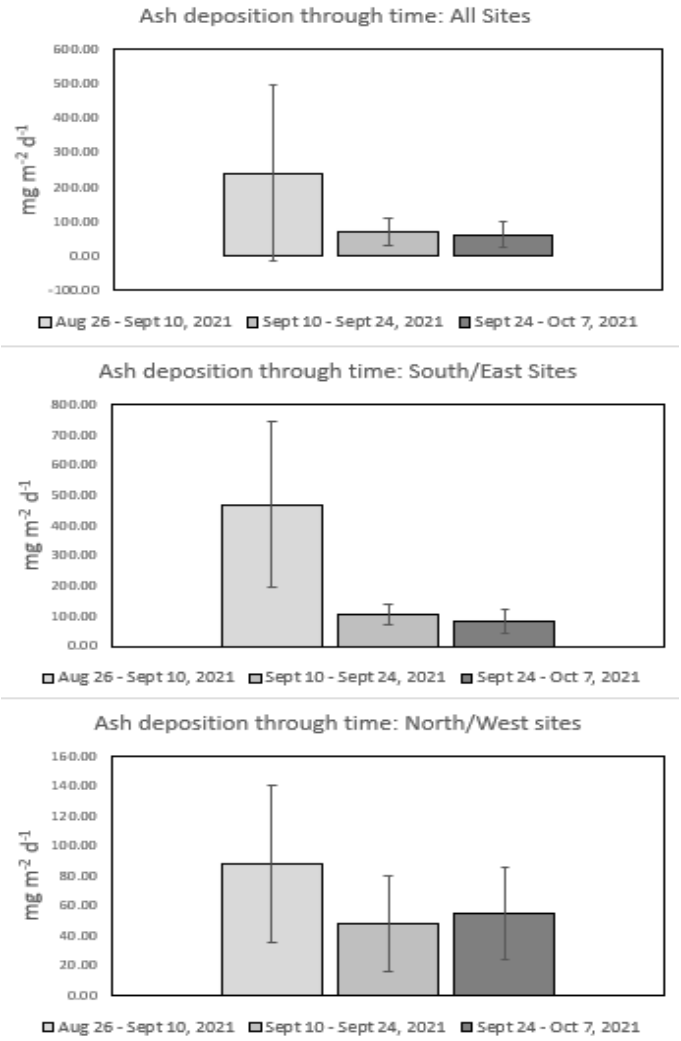

Figure 5. Determined from Table 1, these are the average ash deposition rates (mg m^{-2} d^{-1}) during three sampling periods compiled from 10 sites encircling Lake Tahoe (Table 1, Figure 3). Deposition rates in the south and east sites closer to the fire experienced higher rates of deposition during late August and early September. **Take home:** Deposition fell predominantly during the first week of sampling and deposition rates in the south/east were 5x higher than the north/west.

Task 7. Compile information from air and light sensors within the Tahoe basin to compare changes in 2021 fire season to "historical" conditions without fire.

F. Scordo, S. Chandra, C. Seitz, A. Heyvaert

Tahoe Basin data collected on light regime and air particulate before and after the fires are fundamental to understanding the influence of smoke and its potential impacts on the lake. Changes to light and atmospheric deposition regimes can influence lake water temperature, clarity, and productivity. We identified and synthesized data from existing air quality measurements throughout the 2021 fire season, which included data from the US Environmental Protection Agency in Tahoe City and four "Purple Air" $PM_{2.5}$ sensors located in Tahoe City, Incline Village, Glenbrook, and South Lake Tahoe. We also obtained weather data from stations E3758, F9917, G0254, and HMDC1 located near the PM2.5 sensors. We quantified the spatial variability of air quality (particle concentrations) and light regimes on land and water surfaces within the basin and evaluated the wet-dry deposition from the long-term fixed station managed by UC Davis. Comparisons were made to years with differences in snow water equivalent and hydroclimatic conditions since drier versus wet years can influence the water clarity and quality dynamics of the lake.

Atmospheric air quality data

From our analysis of smoke-related particulate material ($PM_{2.5}$), solar radiation, and temperature before and after the smoke period, we observed a $PM_{2.5}$ concentration higher than 20 µg m^{-3} around Lake Tahoe starting August 5th, which continued to intensify until August 15th (Figure 6). In fire prone areas, concentrations of $PM_{2.5}$ greater than 20 µg m^{-3} indicates smoke presence (Liu et al. 2017). Between August 21st and 26th, all sites had $PM_{2.5}$ higher than 200 µg m^{-3}, however we observed that air quality was heterogeneous in time and space. The southern part of the lake, closest to the Caldor Fire, showed the highest concentrations of $PM_{2.5}$ for the longest period of time (until September 8th), followed by the eastern side of the lake, and the northern and western parts of the lake had shorter periods of higher concentrations of $PM_{2.5}$. The periods of increased $PM_{2.5}$ coincided with periods of decreased solar radiation and air temperature around the lake. The data suggest the utility of using $PM_{2.5}$ to understanding changes in atmospheric conditions but also indicates the importance of having calibrated air sensor data by the Environmental Protection Agency.

Lake transparency (measured via Secchi disc, Ultraviolet light B, and Photosynthetically Active Radiation)

Both incident and underwater ultraviolet B radiation (UVB) and photosynthetically active radiation (PAR) light decreased during the smoke period in 2021 in Lake Tahoe (Figure 7). Having fixed sensors around the lake that monitoring light conditions (UVB and PAR) could provide further insights as to how light changes are occurring across the watershed and thus influencing lake dynamics. The April 1st snow water equivalent (SWE) in 2021 was low (480mm) at the beginning of spring, similar to 2018 and 2020 (Figure 7a). SWE influences important

ecosystem traits (i.e., water temperature, nutrient and light availability, biomass, and community composition of consumers) in western mountain lakes of the United States (Melack et al. 2020; Sadro et al. 2018; Scordo et al. 2021). SWE in the early spring has been shown to affect inter-annual open water transparency and productivity in small lakes, including the timing and level of gross primary productivity and respiration (Goldman et al. 1989; Jassby et al. 1990; Park et al. 2004; Strub et al. 1985). Therefore, as expected, before the fires in 2021, Lake Tahoe had high water transparency, depth of 1% UVB, and 1% PAR (Figure 7 d, e, f). During the smoke period, however secchi disk, 1% UVB, and 1% PAR depth were reduced by 4.5m, 17.5m, and 7.6m, respectively. Peaks of smoke cover coincided with low incident PAR and UVB values in 2021 when compared to the previous four years (Figure 7 b, c).

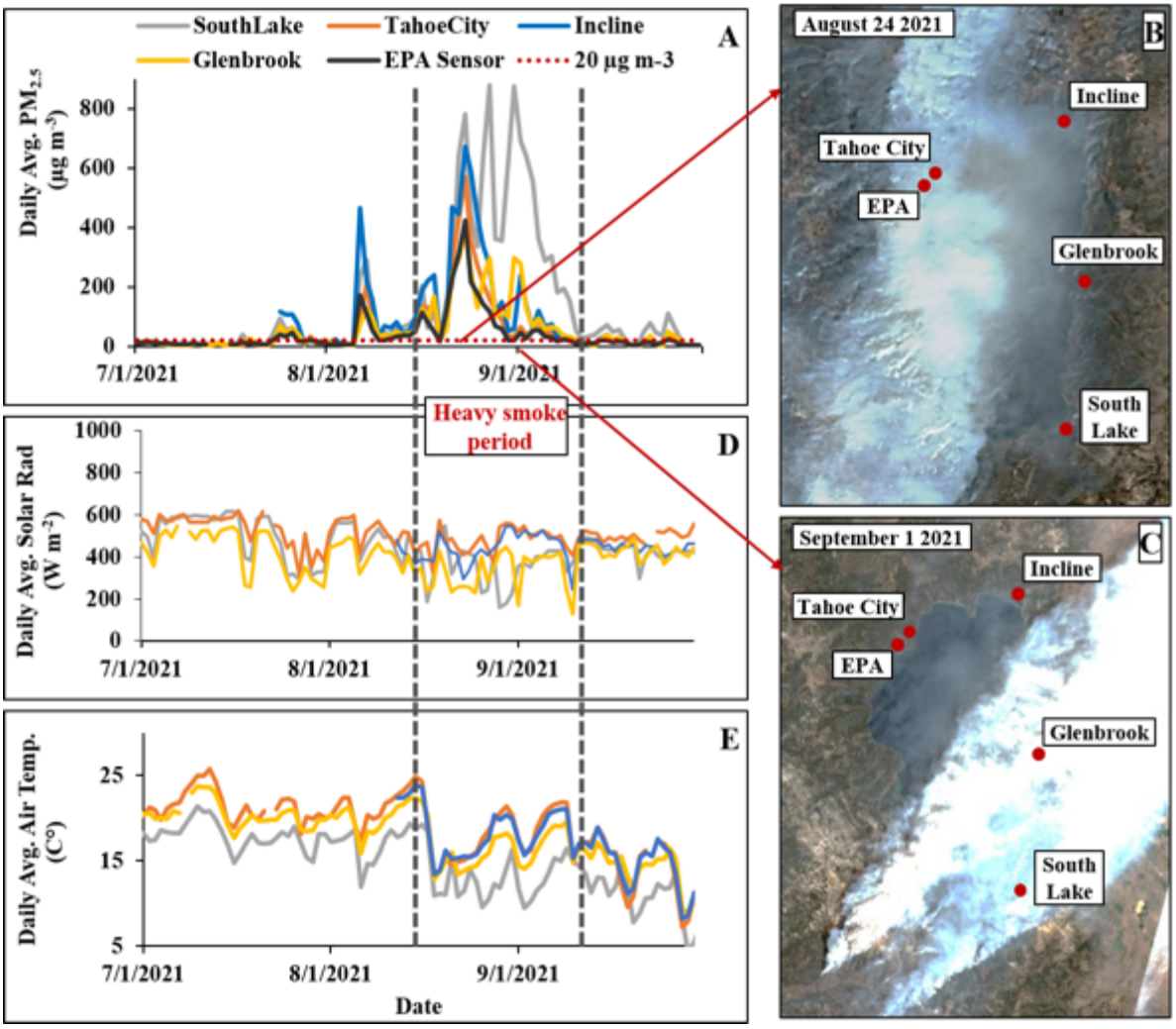

Figure 6. Particulate matter (a), light (d), and air temperature (e) data from station around the Lake Tahoe basin. Spatial heterogeneity of smoke cover during two days in August and September 2021 (b, c). **Take home:** Sensors show variable smoke cover over the basin through the 2021 summer season at Lake Tahoe with regions experiencing heavy smoke coinciding with slightly lower air temperatures and solar radiation.

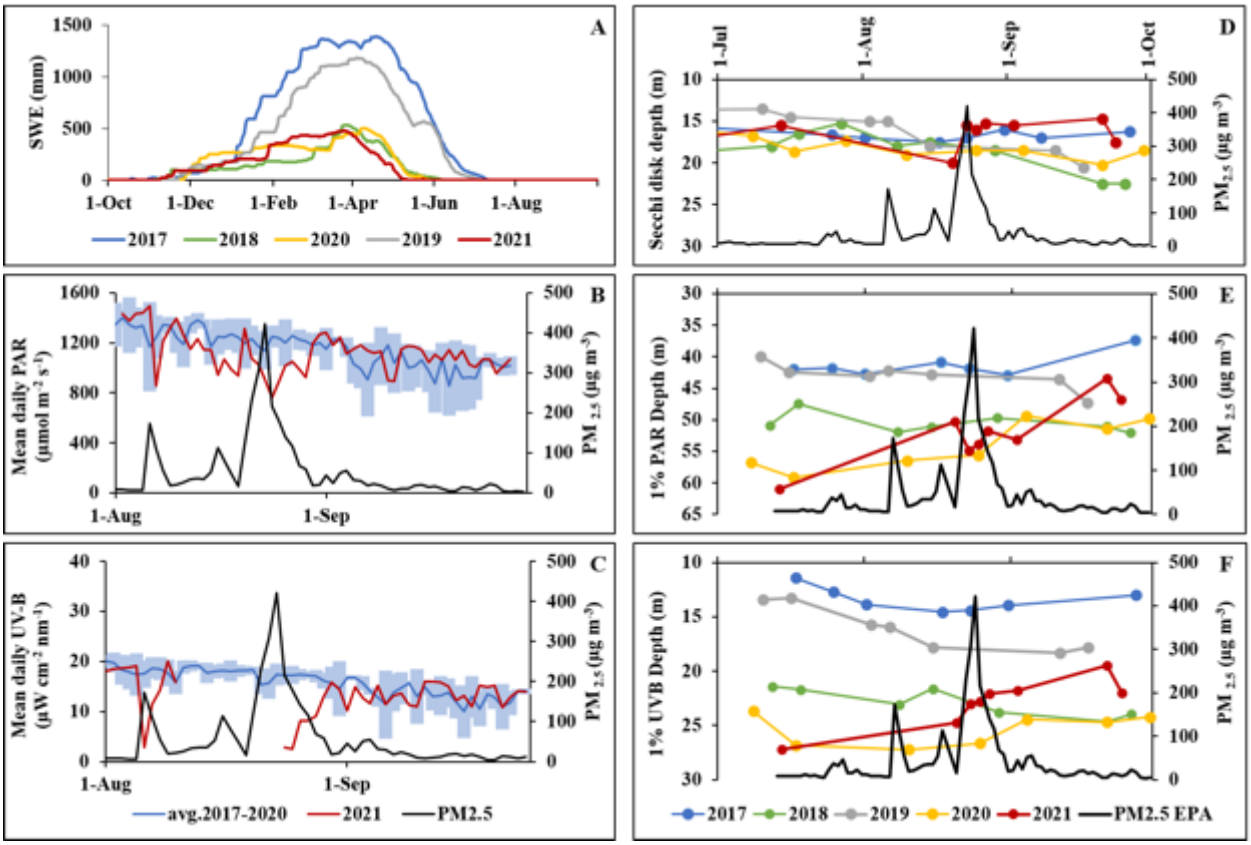

Figure 7. a) Snow water equivalent (SWE) and light regimes above and under lake water during heavy smoke cover in 2021 and in the previous four years (2017-2020). B & C) Surface photosynthetically active radiation (PAR), and ultraviolet B radiation (UVB) in 2021 compared to the mean and 95% confidence intervals of the previous four years. D, E, & F) A time series of Secchi Disk depth and depth of 1% PAR and UVB in Lake Tahoe. Black lines indicate PM2.5 estimations from the EPA sensor in Tahoe City. **Take home:** In 2021, before the smoke period, water clarity was similar to previous years. During the period of smoke cover over the lake the clarity decreased rapidly. Surface light conditions of UVB and PAR also change immediately after smoke enters the basin as indicated by the PM2.5 sensos (black line).

Objective 2: Determine the composition and "lability" of ash particles deposited around the lake during the 2021 fire period.

Plain Language Summary: Not all ash is created equal. As with the rate of ash fall around the lake, the composition of the ash that fell was highly variable in space and time. The composition of the ash was related to the degree to which it had burned where particles still identifiable as burned vegetation, dominantly brown in color, contained higher concentrations of leachable nutrients. Whereas ash that was gray in color and fine-grained contained lower concentrations of bioavailable nutrients. Interestingly, the brown ash fell further from the fire at the northern and western portions of the lake. Despite the lower concentrations of bioavailable nutrients in the ash that fell to the south, five times the mass of ash fell in the region leading to overall greater amounts of bioavailable nutrient deposition. Both the quantity and quality of ash are expected to influence algal production by providing key limiting nutrients including phosphorus (P), nitrogen (N), and micronutrients.

Task 2: Characterize the content of atmospheric particles, including composition and potential nutrient contribution for algal growth.

J. Brahey, S. Chandra, E. Suenaga, F. Scordo, C, Seitz

Ash samples collected from deposition samplers and from the ground were collected and analyzed for micro- and macro-nutrient and metal availability. A water-extractable fraction represents the immediately bioavailable fraction while the easily-oxidized fraction corresponds to the nutrients available after oxidation in the environment. Finally, total micro- and macro-nutrient and metal concentrations were determined in the residual ash, which are largely unavailable to organisms. Deposited ash was separated into a less pyrolyzed brown fraction and a heavily pyrolyzed fine grained gray ash fraction for analyses and experimentation (see Objective 3). Pyrolosis is the decomposition of materials due to high temperatures or combustion. Ash that accumulated on the ground, representing a mixture of the above, was also collected and analyzed. The less pyrolyzed ash was higher quality in that greater amounts of nutrients (P, N, Mg, Na, Cu, Fe, Mn, and Zn) were leached as compared to the more pyrolyzed ash in both the water-extractable and oxidizable fraction. The more pyrolyzed ash contained greater concentrations of Ca and K and bound-P, likely due to the formation of carbonates during pyrolization. The less-pyrolyzed ash also contained higher concentrations of toxicants, such as As, Cd, Cr, Ni, and Pb, though the water extractable concentrations remained low. Site-specific analyses revealed a high variability in ash quality and deposition rates, though in general higher quality but lower amounts of ash fell to the northern and western areas of the lake while greater amounts of more pyrolyzed ash fell to the southeast. This pattern led to greater deposition rates of oxidizable N and P in the south and east despite the lower quality composition.

Approaches

To characterize the atmospheric particles collected in our dry deposition collectors, a sequential leaching protocol was developed by Dr. Janice Brahney's laboratory at Utah State University. The bioavailable fraction of nutrients in the atmospheric particles was determined under different short (water-extractable: WE) and medium (easily oxidizable: EO) time frames. The deionized water-extractable fraction represents the nutrients and metals that are immediately available to primary producers. The easily oxidizable fraction represents the nutrients and metals available in the medium-term via the relatively rapid oxidation of ash that occurs in the high light and oxygen conditions of freshwater environments. Finally, the residual ash was digested using strong acids and oxidants to evaluate the residual nutrient and metal content of the ash.

For the water-extractable fraction, samples were freeze-dried and weighed into HDPE centrifuge tubes. Samples were shaken with deionized water for 16 hours and centrifuged. The supernatant was removed using sterile pipettes for analysis. For the easily oxidizable fraction, samples were oxidized using Hydrogen Peroxide (H_2O_2) in a water bath at 70-80°C; after 5-days sodium sulfite was added to stop the reaction. Samples were then centrifuged, and the supernatant was extracted for analysis. On each extraction the soluble reactive phosphorus (SRP) was determined using the molybdenum blue method (Murphy and Riley 1962) Nitrate (NO_3^-) concentrations were determined colorimetrically using the salicylate method after digestion in concentrated sulfuric acid (H_2SO_4) (Cataldo et al., 1975) and Ammonium (NH4+) was determined colorimetrically after KCL extractions by the salicylate method (Nelson 1983). All colorimetry was conducted on a SpectraMax® M2E spectrophotometer. Metals and total phosphorus for each extraction were run on an ICP-MS at the University of Utah. Organic (non-reactive) phosphorus was determined by subtracting SRP from total phosphorus (TP), when available. For the determination of total phosphorus and metal content, we transferred ash to PTFE digestion vials using water, then dried down the sample at 130 °C, and obtained the mass by difference. Residual nutrients and metals were measured by first digesting the ash using 2 mL of HF and 1 mL of HNO_3 at 150 °C for 24 hours and then dried and digested in 2 mL HCL for 1 day and measured on an ICP-MS as above. In some samples, substantive amounts of black carbon could not be digested. Quality assurance data for extractions are presented in Table 3.

Table 3. Quality assurance data for all analytical methods used to characterize nutrients in ash particles collected around Lake Tahoe in summer 2021.

	Calibration Curve R^2	Detection Limit mg/L	Error mg/L
DI Leachable SRP	1.000	0.02	0.001
DI Leachable TP		0.001	N/A
DI Leachable NH4	0.998	0.04	0.06
Oxidizable SRP	0.998	0.15	0.05
Oxidizable TP		0.001	N/A
OXidizable NH_4^+	0.997	1.5	0.4
Oxidizable NO_3^-	0.993	0.4	0.1

Ash chemistry and leachable nutrients

Ash samples are grouped into three categories that were used in the bioassay experiments in Objective 3 (Task 3).

- BA1, the brown ash collected from the northwestern areas that are relatively less pyrolyzed (sites CR, GB, AB, TC, TH, and RB),
- BA2, the most heavily pyrolyzed ash that fell predominantly at sites STL, STB, and TRPA in the south Tahoe area
- Ground ash (GA) that was collected directly from the ground surface near Trout Creek.

Bioavailable nutrient concentrations differed significantly between ash types reflecting the degree of pyrolization. Nitrogen (N) is easily volatilized during combustion while phosphorus (P) is not. Therefore, we would expect N to decrease in concentration and P to become progressively concentrated in the remaining ash. However, as the P is oxidized from the plant material it will bind with calcium rendering it less bioavailable (Pereira et al. 2012; Bodí et al. 2014)). As such, BA1 contained greater concentrations of water extractable reactive P, organic P, and ammonium, reflecting the lower degree of pyrolization (Figures 8, 9, 10). In contrast, almost no P was water-extractable from BA2 and the oxidizable fraction was only 4% of what was extracted from BA1. However, as predicted TP concentrations were far greater in BA2 than BA1, reaching concentrations that are 50% greater than plant material. Nitrate was below detection limits in all water extracted samples, likely due to the efficiency at which N species are volatilized during combustion (Raison 1979). Oxidizable organic P and nitrate were present in greater concentrations in BA2. The ground ash (GA) represented a mixture between these two bucket-ash extremes.

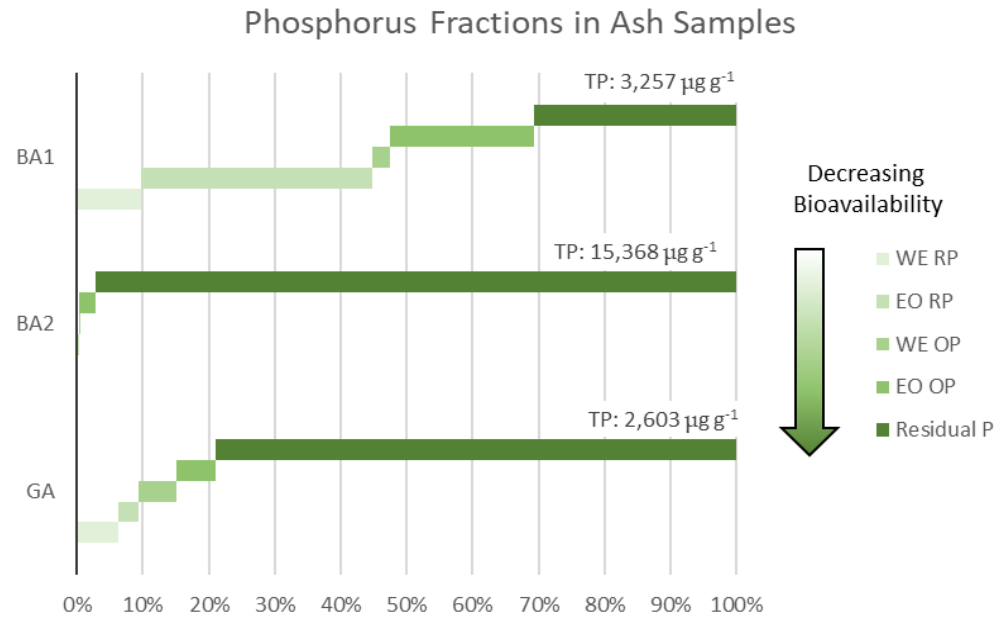

Figure 8. Bioavailability of phosphorus in ash deposition samples collected in samples placed in the northern Lake Tahoe Basin (BA1), the southern Lake Tahoe Basin (BA2), and from the ground near the lake. Bioavailable P is defined as reactive phosphorus (RP) and organic phosphorus (OP) that is either water extractable (WE) or easily oxidized (EO). **Take home:** The less pyrolyzed (thermally decomposed) BA1 ash releases substantively more bioavailable phosphorus than BA2 ash. Thus, we consider BA1 to be of higher quality since the nutrients leached by the ash is more readily available to algae and other organisms in the lake.

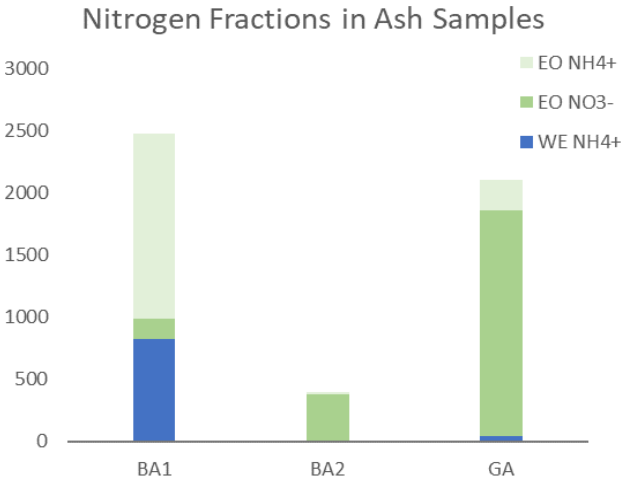

Figure 9. Nitrogen fractions in ash deposition samples collected in samples placed in the northern Lake Tahoe Basin (BA1), the southern Lake Tahoe Basin (BA2), and from the ground near the lake. All forms of nitrogen presented here are considered bioavailable. **Take home:** BA1 ash leaches substantively more nitrogen than BA2 ash.

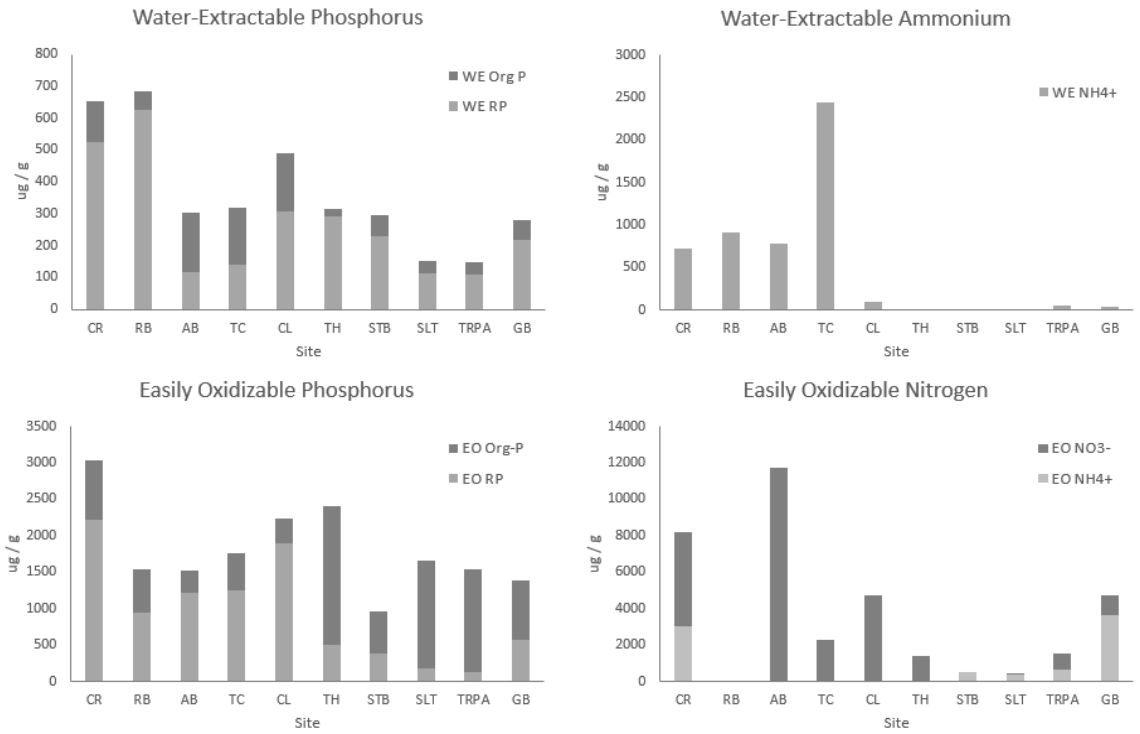

Fig 10. Deionized water-leachable and oxidizable nutrients averaged for ten sites where ash was collected from August 26th-October 7th, 2021. **Take home:** Deposition rates of nutrients were highly variable. In general, sites to the north/west had higher quality ash with greater concentrations of bioavailable nutrients.

Deposition rates of nitrogen and phosphorus

Even though total ash deposition rates were 70% lower at the northwest locations compared to the south/east (Figure 5, Table 2), the overall deposition rates of bioavailable N and P are driven by the overall deposition of material at each site and region (Figures 8-11). Bioavailable P concentrations were markedly higher leading to an average deposition of 76 µg P m^{-2} day^{-1}, which was nearly double the south/east, which averaged 42 µg P m^{-2} day^{-1}. However, TP was substantively larger in the south/east at 3,294 µg P m^{-2} day^{-1} compared to only 164 µg P m^{-2} day^{-1} in the north/west. Given that much of the TP is bound in with calcium in this fraction, this P could become available if exposed to sufficiently low pH to solubilize the material. In summary, the average bioavailable P deposition in ash was 60.8 µg P m^{-2} day^{-1}, with a maximum rate of 248 µg P m^{-2} day^{-1}. The latter at the CR site within the first week of deposition. Total P deposition was on average 1,621 µg P m^{-2} day^{-1} with a maximum deposition of 13,110 µg P m^{-2} day^{-1} at SLT during the first week of deposition. For reference, the average/maximum bioavailable and total P deposition rates from dust across the western US are 28/186 µg P m^{-2} day^{-1} and 72/394 µg P m^{-2} day^{-1} (Brahney personal communication). Global average P deposition rates are 137 µg P m^{-2} day^{-1} (Brahney et al. 2015).

Despite lower concentrations of bioavailable N in the south/east, the higher deposition rates of ash led to a doubling of the average N deposition rate. At the north/west locations the average bioavailable N deposition rate was 92.5 µg N m^{-2} day^{-1} and at the south/east 204.8 µg N m^{-2} day^{-1}. The highest N deposition rates were at GB at 654.3 µg N m^{-2} day^{-1}, during the second week of deposition.

Nutrient stoichiometry (ratio of elements like nitrogen to phosphorus) can be important for determining algal growth. The ratio of N to bioavailable P in deposition was on average 3.1 by mass (7.1 molar). At the north/western sites the ratio was 1.4 by mass (2.9 molar) and at the south/east locations 5.38 by mass (12.4 molar), the latter again driven by high N deposition rates at GB which led to a ratio of 57.

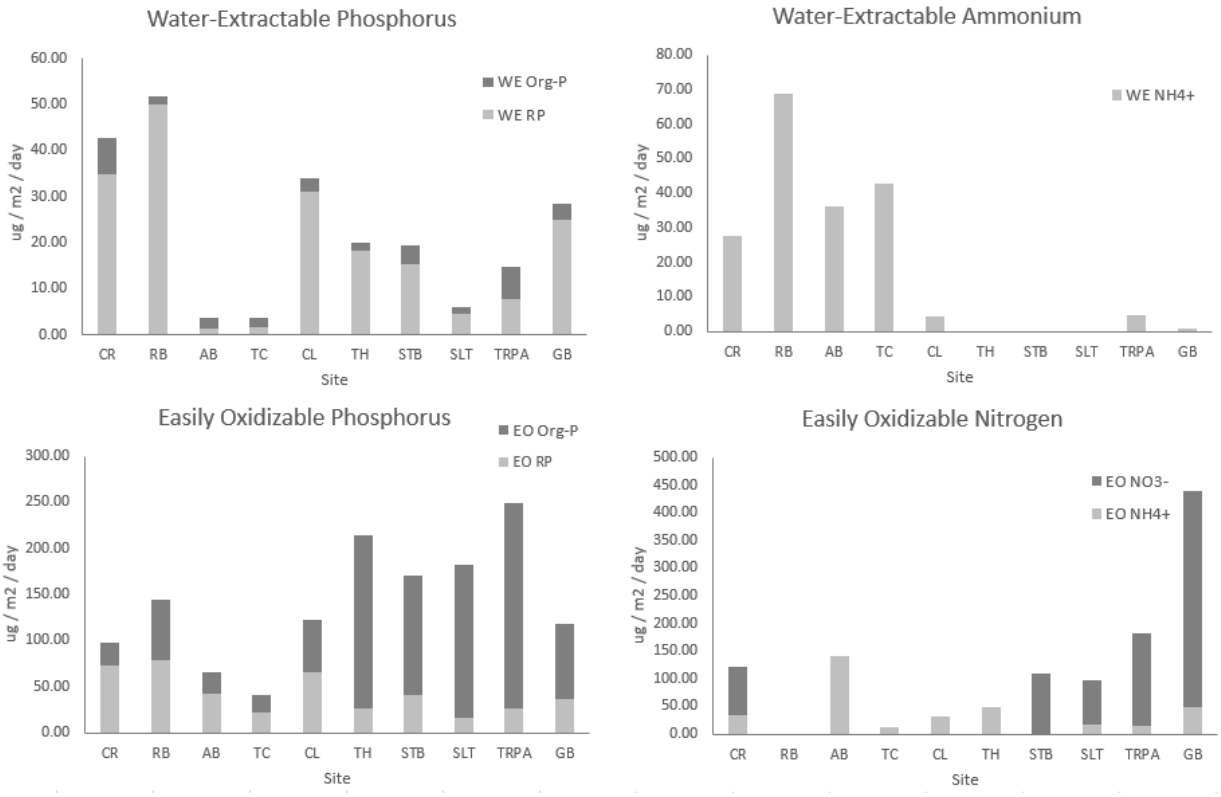

Figure 11. Deionized water-leachable and oxidizable nutrients deposition rates averaged for ten sites where ash was collected from August 26th-October 7th, 2021. **Take home:** Despite the lower quality ash (less nutrients) found in the south/east, the deposition rates were 5x higher leading to a greater total flux of bioavailable nutrients to these areas. The high deposition rates in the southeast are driven by the oxidizable fractions.

Ash concentrations of cations, micronutrients, and toxic elements

The degree of pyrolization was also evident in the amount of macro/micronutrients and toxicants found in the ash samples. For example, the macro and micronutrients, P, Na, Mg, Cu, Fe, Mn, and Zn were present at higher concentrations in the WE fraction of BA1 as compared to BA2. Many toxic elements are volatilized at higher temperatures but can be concentrated in ash from low to medium intensity fires (Wan et al. 2021, Bodí et al. 2014). Ca and K were more concentrated in the highly-pyrolized BA2, the former likely due to the formation of calcite (Figure 12).

As with the water extractable nutrients, for the most part the ground ash represented a mixture of the BA1 and BA2 extremes. The concentration of elements in the oxidizable and residual fraction were also generally higher in the BA1 ash as compared to BA2 ash, however, Ca, P, Zn, Mn, and Pb were higher in the residual BA2 ash (Table 4).

Ash composition was highly variable by site with both macro and micronutrients peaking at different locations (see Figure 1A in supplemental material). However, high deposition rates at STR, SLT, and TRPA resulted in generally the highest deposition rates of water soluble and oxidizable TP, Fe, Mg, K, Ca, Mn, Co, Cu, and Zn. Though toxicant concentrations were highest at sites CR, RB, AB, TC, and CL, the higher deposition rates at SB, SLT, TRPA, and GB led to those sites receiving the greatest loads of water extractable and residual toxicants, while concentrations within the easily oxidizable fraction were more evenly distributed (Table 5).
Take Home: Despite the lower concentrations of macro- and micronutrients and toxicants in BA2, the high deposition rates lead to higher loads of these water extractable and oxidizable elements.

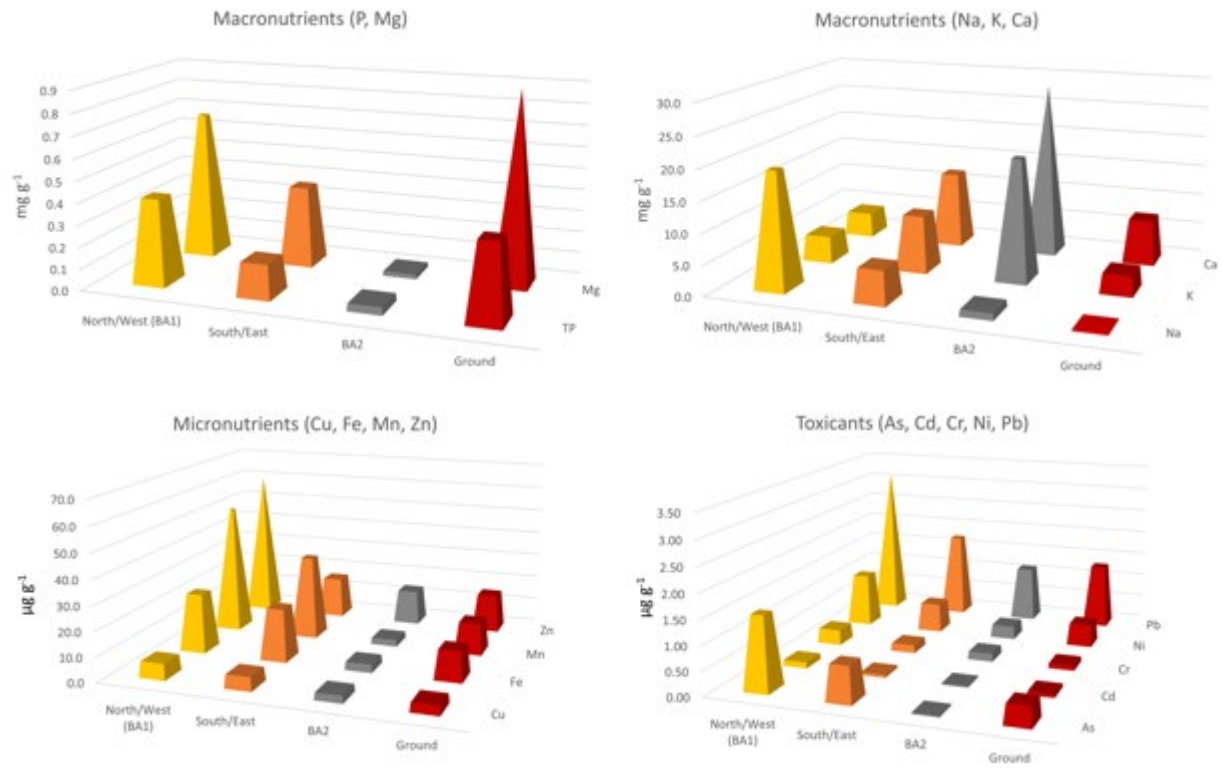

Figure 12. Summary of water-leachable macro/micronutrients and toxicant, grouped by region and experimental composition. **Take Home:** The higher quality (less pyrolized) ash (BA1) had greater concentrations of macro/micronutrients as well as toxicants.

Table 4. Summary of water-leachable, easily oxidizable, and residual elemental concentrations in ash grouped by region and experimental composition.

	Water-extractable (WE)															
	Macronutrients (mg/g)					Micronutrients (ug/g)					Toxicants (ug/g)					
	TP	Mg	K	Ca	Na	Fe	Zn	Cu	Co	Mn	As	Cd	Cr	Ni	Pb	
North/West	0.40	0.70	4.46	4.17	19.62	23.64	60.03	6.52	1.06	51.98	1.51	0.12	0.32	1.09	3.14	
South/East	0.16	0.43	7.77	9.90	7.94	21.08	16.39	5.51	0.35	33.47	0.74	0.06	0.16	0.59	1.74	
BA2	0.04	0.02	19.76	28.50	1.11	3.27	13.84	2.93	0.06	2.62	0.03	0.03	0.16	0.27	1.13	
Ground	0.34	0.89	3.28	7.34	0.22	12.13	15.15	3.77	0.06	12.76	0.41	0.07	0.10	0.46	1.32	
	Easily-oxidizable (EO)															
	Macronutrients (mg/g)					Micronutrients (ug/g)					Toxicants (ug/g)					
	TP	Mg	K	Ca	Na	Fe	Zn	Cu	Co	Mn	As	Cd	Cr	Ni	Pb	
North/West	1.72	0.60	1.70	6.80	N/A	457.27	1,006.40	39.56	3.19	223.59	0.70	0.91	14.76	71.57	15.87	
South/East	1.22	0.52	2.36	7.81	N/A	446.67	342.08	23.95	1.30	205.46	0.56	0.52	4.31	5.23	3.30	
BA2	0.41	0.53	6.47	13.01	N/A	3.66	52.50	2.03	0.09	4.14	0.08	0.04	2.11	1.69	0.13	
Ground	0.30	1.05	1.24	16.82	N/A	62.36	30.91	1.42	0.12	127.83	0.17	0.04	1.52	0.12	2.71	
	Residual															
	Macronutrients (mg/g)					Micronutrients (ug/g)					Toxicants (ug/g)					
	TP	Mg	K	Ca	Na	Fe	Zn	Cu	Co	Mn	As	Cd	Cr	Ni	Pb	
North/West	1.00	16.44	16.81	30.44	31.84	38,337	204.07	134.37	15.19	848	7.70	11.70	72.66	59.42	31.34	
South/East	6.12	16.08	17.07	57.02	21.47	33,066	224.41	70.40	14.31	3,490	4.62	2.42	84.96	40.51	30.57	
BA2	14.95	16.81	11.72	140.82	7.56	19,631	314.70	69.54	11.13	11,255	2.37	0.87	19.62	18.74	32.07	
Ground	2.13	13.15	16.74	38.72	19.44	49,453	129.43	34.04	15.41	3,380	2.11	0.73	20.80	13.38	28.29	

Table 5. Deposition rates of all fractions of macro- and micro-nutrients a well as toxicants.

Water-extractable (WE)

	Macronutrients (µg. m^{-2}.day^{-1})					Micronutrients (µg. m^{-2}.day^{-1})					Toxicants (µg. m^{-2}.day^{-1})				
	TP	Mg	K	Ca	Na	Fe	Zn	Cu	Co	Mn	As	Cd	Cr	Ni	Pb
North/West	26.5	45.9	324	257	892.1	1.23	1.79	0.32	0.06	3.27	0.09	0.01	0.01	0.05	0.13
South/East	22.0	42.7	4,419	6,294	667.6	2.26	3.89	0.99	0.04	3.86	0.03	0.01	0.04	0.09	0.33
BA2	20.9	12.6	11,793	17,019	642.1	1.94	8.53	1.71	0.04	1.52	0.02	0.02	0.10	0.16	0.64
CR	42.74	41.74	268.4	322.1	439.8	1.04	3.56	0.36	0.02	1.24	0.01	0.00	0.01	0.04	0.04
RB	51.65	113.08	1027.3	371.9	1273.9	2.71	1.26	0.48	0.25	14.13	0.21	0.01	0.02	0.07	0.11
AB	5.56	12.47	18.3	113.3	1104.9	0.73	0.32	0.33	0.01	0.06	0.07	0.00	0.01	0.04	0.09
TC	5.53	13.66	60.3	96.6	727.3	0.47	0.37	0.18	0.03	0.65	0.04	0.00	0.01	0.03	0.07
CL	33.94	52.75	315.2	387.0	758.5	0.98	4.65	0.27	0.03	1.84	0.06	0.01	0.01	0.05	0.28
TH	19.86	41.45	253.7	248.8	1048.2	1.44	0.57	0.30	0.02	1.71	0.15	0.01	0.01	0.05	0.18
STB	25.59	46.61	3777.4	5903.0	583.9	3.50	0.97	0.93	0.03	6.47	0.02	0.01	0.02	0.09	0.51
SLT	12.24	24.21	5372.6	8038.2	401.7	0.99	5.56	0.58	0.05	2.39	0.01	0.01	0.05	0.06	0.10
TRPA	22.51	31.63	6583.9	8997.4	581.0	1.90	5.53	1.18	0.03	4.20	0.02	0.01	0.06	0.12	0.37
GB	27.11	75.59	499.5	436.2	1161.3	2.88	2.39	1.14	0.03	2.13	0.09	0.01	0.02	0.09	0.31

Easily-oxidizable (EO)

	Macronutrients (µg. m^{-2}.day^{-1})					Micronutrients (µg. m^{-2}.day^{-1})					Toxicants (µg. m^{-2}.day^{-1})				
	TP	Mg	K	Ca	Na	Fe	Zn	Cu	Co	Mn	As	Cd	Cr	Ni	Pb
North/West	112.5	38.9	74	462	0.00	22.56	25.91	1.35	0.15	18.14	0.03	0.04	0.46	1.19	0.43
South/East	189.8	143.0	1,447	3,074	0.00	27.06	33.03	2.75	0.12	16.65	0.06	0.03	0.81	0.82	0.30
BA2	243.6	312.5	3,890	7,724	0.00	2.20	31.64	1.20	0.05	2.43	0.05	0.02	1.27	1.02	0.08
CR	84.7	9.0	30	93	0.00	13.55	12.79	1.43	0.05	2.83	0.02	0.02	0.32	3.85	0.29
RB	144.7	96.5	131	749	0.00	36.11	16.49	1.02	0.55	42.41	0.04	0.06	0.54	0.73	0.29
AB	66.0	17.2	65	494	0.00	25.56	29.92	3.27	0.09	3.55	0.04	0.08	0.80	1.01	1.00
TC	42.1	11.3	44	125	0.00	18.25	34.58	1.07	0.11	2.92	0.02	0.02	0.43	0.61	0.47
CL	123.1	78.3	143	988	0.00	11.62	55.31	0.58	0.07	43.16	0.03	0.02	0.54	0.77	0.42
TH	214.5	21.2	31	324	0.00	30.24	6.38	0.71	0.05	13.97	0.03	0.04	0.13	0.16	0.10
STB	170.2	128.0	1,184	2,290	0.00	25.69	29.13	3.55	0.10	22.74	0.03	0.01	0.60	0.76	0.26
SLT	182.8	126.7	2,004	2,943	0.00	35.41	60.59	1.53	0.21	6.46	0.03	0.02	0.79	0.78	0.24
TRPA	248.6	200.8	2,076	5,051	0.00	27.58	26.53	3.14	0.07	12.15	0.06	0.03	1.06	0.92	0.39
GB	118.7	78.1	103	694	0.00	19.20	20.21	2.50	0.11	28.24	0.13	0.06	0.63	0.73	0.27

Residual

	Macronutrients (µg. m^{-2}.day^{-1})					Micronutrients (µg. m^{-2}.day^{-1})					Toxicants (µg. m^{-2}.day^{-1})				
	TP	Mg	K	Ca	Na	Fe	Zn	Cu	Co	Mn	As	Cd	Cr	Ni	Pb
North/West	64	936	1049	1617	1543	2160	10.63	5.36	0.93	54	0.30	0.42	3.68	2.63	1.54
South/East	3285	4542	3636	31890	3192	6536	79.05	19.87	3.30	2,465	0.83	0.28	9.49	6.47	8.96
BA2	8950	10027	6959	84304	4494	11687	188.14	41.59	6.65	6,745	1.42	0.51	11.69	11.16	19.20
CR	119	846	799	1508	1181	2081	10.82	7.34	0.82	73	0.14	0.11	2.30	5.42	1.40
RB	47	1325	1189	2004	1573	2892	10.78	1.94	1.29	60	0.30	0.43	3.25	1.68	1.78
AB	36	513	1546	1407	2152	1880	11.00	14.59	0.69	39	0.37	1.13	7.99	4.14	1.43
TC	39	693	461	1052	941	1423	7.24	3.28	0.55	29	0.30	0.22	2.90	1.67	1.06
CL	100	975	937	1892	1798	1931	11.34	1.31	0.87	65	0.33	0.31	1.88	1.30	1.50
TH	44	1261	1363	1837	1615	2749	12.62	3.71	1.34	55	0.35	0.34	3.73	1.57	2.06
STB	2333	3754	3029	23330	2775	5337	56.99	17.71	2.47	1762	0.62	0.25	5.21	3.75	5.49
SLT	4088	4858	3224	39341	2729	6035	89.72	21.95	3.27	3149	0.79	0.27	6.20	5.06	8.98
TRPA	5242	6579	5168	49743	3916	9171	121.16	29.10	4.85	3889	1.08	0.36	9.20	8.08	13.74
GB	172	1618	2101	3245	2865	3844	20.27	4.55	1.59	112	0.67	0.20	17.51	7.94	4.44

Objective 3. Quantify the effects of smoke on algal biomass and productivity in the pelagic (Task 3 & 8) and nearshore (Task 4) zones of Lake Tahoe.

Plain Language Summary: The experiments conducted indicated that both the quality of the ash that fell as well as the altered light conditions have the potential to increase algal production. In addition, we found that the initial condition of the lake, including the lake nutrient trophic state and starting algal composition, will control the degree to which algae respond. In all experiments, the simulated reduced light environment amplified the algal response to the ash additions. The complexity of the response suggests that more experimental conditions are required to disentangle the relative role of ash composition (including micronutrient and toxin concentrations), microbial respiration, and algal production.

Task 3. Quantify the contributions of deposited ash particles to algal productivity in the offshore of Lake Tahoe and Castle Lake.

*All authors contributed equally to this effort and are listed in alphabetical order: S Chandra, J Brahney, E Carlson, S Sadro, F Scordo, E Suenaga, C Seitz

To quantify the contribution of deposited ash particles to offshore algal productivity, we collected water from two systems: Lake Tahoe and Castle Lake (a lake which mimics the productivity of Emerald Bay and other smaller lakes in the Tahoe basin). We collected water from a 20m depth in Lake Tahoe and from the pooled mixed layer at Castle Lake (equal parts 0m, 3m, and 5m). All water was filtered through 80μm mesh to remove macro zooplankton from the sample. Our experiments included treatments with added ash collected from the ground at different concentrations (GA1: low, GA2: medium, GA3: high), ash collected from our deposition bucket samplers from the north (BA1) and south (BA2) ends of the lake (Table 5), and treatments with added nutrients of concentrations above ambient lake concentrations (nitrogen, phosphorus, and both nitrogen and phosphorus (Figures 11). All the treatments were compared to the control treatment that contained lake water with no additions. Since wildfire smoke can alter atmospheric conditions of photosynthetically active radiation (visible) light at different time scales (hours, days to weeks) while also adding nutrients to lakes, we simulated conditions with reduced atmospheric/ incident light conditions and normal light conditions for the experiments.

We used multiple methods to estimates changes to algae. First, chlorophyll a which can be used as surrogate estimation of algal biomass measured. Second, we used the ^{14}C method (two light replicates, and one dark) which has been part of the long-term monitoring program to measure net productivity, and third, PreSens DO sensors for discrete dissolved oxygen measurements every ~12 hours (5 replicate jars for each treatment). All bottles were placed in a temperature-controlled chamber and exposed to cycles of 16 hours of light (UV and PAR mimicking light conditions in Lake Tahoe) and 8 hours of dark at 18°C. An identical set of treatment bottles were covered in a cloth to reduce light conditions simulating atmospheric smoke in the basin and reduced light conditions.

For the ^{14}C method we used 125mL glass bottles injected with 0.35mL of radiolabeled aqueous sodium bicarbonate and incubated the bottles for 5 days. The dark bottle treatments were placed in a box inside the temperature-controlled room to ensure similar temperature regimes across bottles. After 5 days, 50mL of sample water from each bottle was filtered through 0.45µm millipore filters, the filters were dried for over 24hrs, and radiation was counted on a beta counter at UNR which was then converted into rates of primary productivity. We compared rates of primary productivity in each of the treatments to the control using a Dunnett's test in the DescTools package in R version 3.6.3. The ^{14}C method is limited in accounting for bacterial processes, so a second method for measuring productivity was used.

The PreSens microDOTs were glued into pint-size (473mL) glass mason jars and incubated for 12 days, with measurements taken every 12 hours in the morning and evening. This method allowed us to evaluate oxygen changes over time and determine net ecosystem production (NEP), which accounts for algal and heterotrophic bacterial dynamics. Chlorophyll-a and nutrient samples were also taken from the same jars by filtering known volumes of water through Whatman GF/F filters and chlorophyll-a concentrations were measured on a Turner AU fluorometer.

Chlorophyll a after incubations under different light conditions

Chlorophyll-a increased in Lake Tahoe treatments for ash added from the BA1 (north/west)) and BA2 (south/east) under low light conditions simulating smoke conditions over the lake (Figure 14, Tables 6-9). There is generally higher variability in the BA treatments under low light conditions compared to other treatments. There are no significant differences in the additions of ash to the Tahoe treatments with normal light conditions. Ground ash (GA) stimulated chlorophyll a in Castle Lake but there is generally high variability in the treatments. In general, high light conditions did not appear to change, in a significant statistical determination, algal mass as detectable by chlorophyll a. Overall there is simply much more heterogeneity (variability) in chlorophyll a within the jars for detectable measures of changing indicating that for these experiments it is better to use rate based change estimations and chemical characteristics of the water like dissolved oxygen which is a response to changes in algal community and biomass (see below).

^{14}C estimation of productivity after incubations with under different light conditions

In Lake Tahoe, ash (BA1 north/ east) additions were significantly higher in net primary productivity with no other additions stimulating between treatments and control (Figure 15a, Table 10). The BA1 ash was collected from buckets placed on the north end of the lake and was browner in color and contained more plant material. As indicated under Objective 2, this material was generally higher in nutrient quality but loads of this material were lower into the lake. The experiments here suggest that for a comparable amount of mass added into the bottles, the smoke ash from BA1 (north/east) stimulates production. No interaction effect of light condition and treatment was detected (Table 11).

Using Castle Lake water, which represents conditions found in Emerald Bay or other smaller lakes in the region, we find significantly higher rates of primary productivity in treatments with added NP, P, GA2, BA1, and BA2 relative to the control ($p<0.05$) in the smoke-simulated light condition (Figure 15b, Tables 12, 13), but no differences were found under normal light conditions This suggests that lake conditions (trophic state, composition of algae and staring conditions when influences by smoke) along with lower light simulations affect the production in a lake regardless of the quality of ash deposition type (ground or atmosphere). Thus, the additions of ash quality (ground, higher quality from the north/west or south/ east) have a similar affect and increase net productivity. Untangling these mechanisms may be difficult but suggest that smaller more productive lakes can be influenced by smoke-ash deposition when combined with changes in light in the atmosphere.

Finally, ash deposition collected from the north/eastern shores of Lake Tahoe (BA1) was the most consistent treatment that resulted in an increase in primary productivity relative to the control. BA1 was visually observed to contain more plant material compared to the ash collected on the south shore of the lake and from the ground. This suggests that the quality of the ash is an important factor to consider when determining impacts on aquatic ecosystems. This will be further discussed again in the next sections and Objective 2. Quantifying the nutrient state of the lakes, composition of algae and bacteria, and interactions with light (PAR and UV) could be important when trying to determine the ecosystem influences from ash deposition onto a lake.

Table 5. Ash weights added to treatment jars for productivity experiments using water from Lake Tahoe and Castle Lake.

Treatment	Ash concentrations
GA1 (low)	10 mg L-1
GA2 (medium)	25mg L-1
GA3 (high)	50mg L-1
BA1 (North)	25mg L-1
BA2 (South)	25mg L-1

Figure 13. Left: incubations bottles for dissolved oxygen PreSens sensors and 14C method in the lab at the University of Nevada Reno, and right: Dr. Steve Sadro leads a team to fill incubation bottles with lake water from Lake Tahoe and Castle Lake.

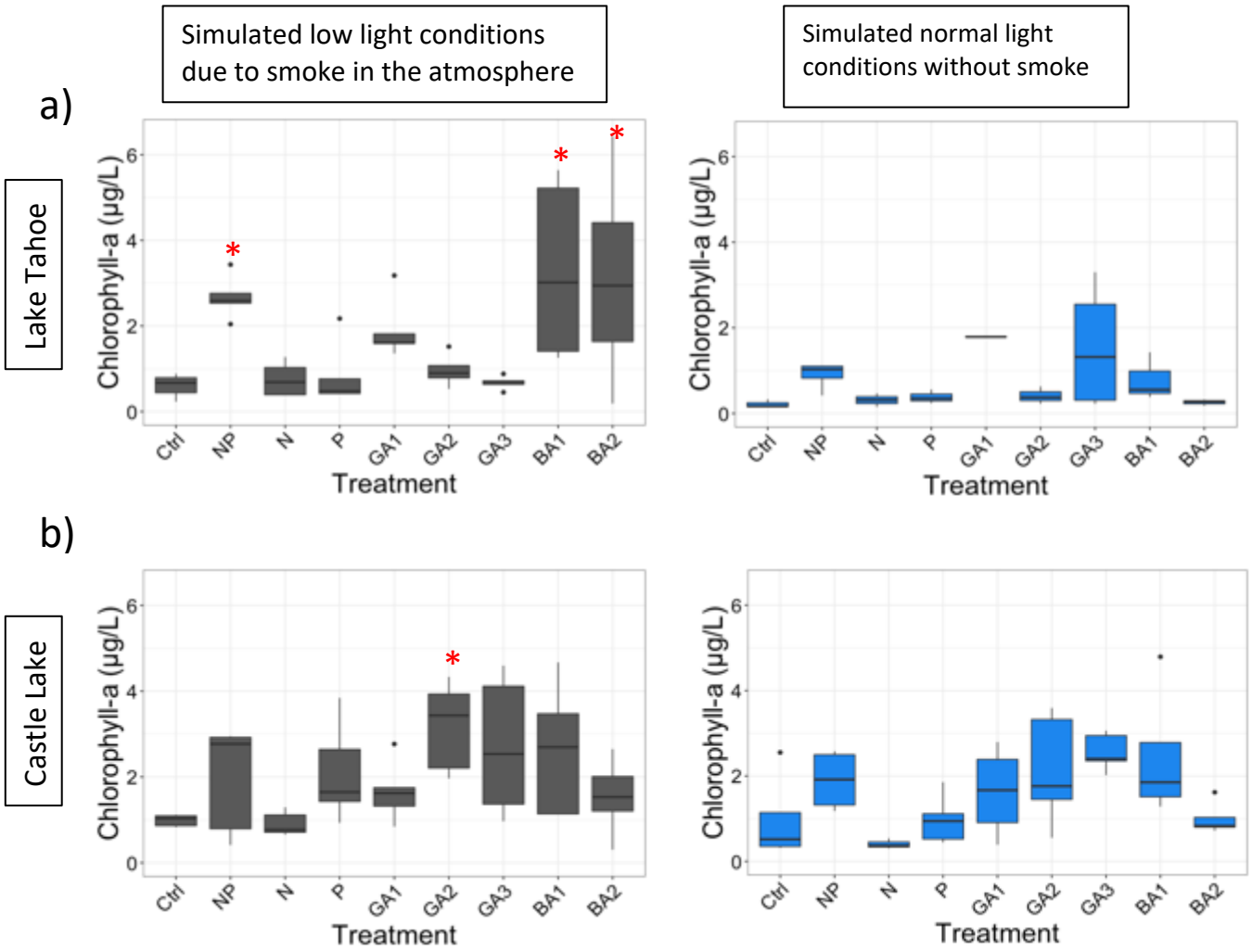

Figure 14. Chlorophyll-a concentrations (mg L^{-1}) after a 12-day incubation in 473mL glass jars under simulated smoke light conditions (grey) and simulated normal light (blue) conditions for a) Lake Tahoe and b) Castle Lake in July 2022. Treatment amendments included the additions of nitrogen and phosphorus (NP), nitrogen (N), phosphorus (P), ground ash at low (GA1), medium (GA2), and high (GA3) concentrations, and ash collected in bucket collectors around the north end (BA1) and south end (BA2) of Lake Tahoe during the Caldor Fire in 2021. Red asterisks indicate significant differences between treatment and control determined using a Dunnett's Test ($p<0.05$). Red points indicate p-values <0.1. **Take home:** Chlorophyll a can be a coarse measure of algal biomass and does not reflect compositional changes of algae over time. There can be high variability in treatment responses with ash and nutrient additions indicating less detectable changes in algae likely due to the high variability in compositional changes to the algal community. Some treatments like ash additions under simulated conditions with low light did seems to stimulate detectable changes in algal mass.

Table 6. Dunnett's test results for chlorophyll-a concentrations (mg L^{-1}) in Lake Tahoe water (20m) in treatments exposed to a) simulated smoke light conditions and b) simulated normal light conditions without smoke. Asterisks denote significance of $p<0.05$.

a)

Treatment	% of control	Lower CI	Upper CI	P-value
N + P	199.2	0.010	4.126	0.048*
N	92.0	-1.907	2.208	1.000
P	212.3	-1.810	2.305	0.999
GA1	167.9	-0.751	3.365	0.374
GA2	321.1	-1.825	2.540	0.999
GA3	274.7	-1.992	2.123	1.000
BA1	265.3	0.648	4.763	0.006*
BA2	155.8	0.461	4.576	0.011*

b)

Treatment	% of control	Lower CI	Upper CI	P-value
N + P	194.6	-0.880	2.237	0.712
N	41.5	-1.768	1.956	1.000
P	100.0	-1.503	1.829	0.999
GA1	167.0	-0.786	3.926	0.297
GA2	218.9	-1.473	1.859	0.999
GA3	262.0	-0.237	2.880	0.118
BA1	250.5	-1.096	2.236	0.877
BA2	102.4	-1.626	1.706	1.000

Table 7. Results from two-way ANOVA for testing interaction between simulated light conditions and treatments for chlorophyll-a concentration in Lake Tahoe.

	DF	Mean Sq	F-value	P-value
Treatment	8	33.36	3.925	0.001**
Light	1	14.88	13.964	<0.001**
Treatment:Light	8	22.61	2.652	0.016*

Table 8. Dunnett's test results for chlorophyll-a concentrations (mg L^{-1}) in Castle Lake water (0-5m) in treatments exposed to a) simulated smoke light conditions and b) simulated normal light conditions without smoke. Asterisks denote significance of $p<0.05$.

a)

Treatment	% of control	Lower CI	Upper CI	P-value
N + P	199.2	-0.909999	2.870	0.587
N	92.0	-1.969	1.810	1.000
P	212.3	-0.779	2.999	0.456
GA1	167.9	-1.218	2.561	0.886
GA2	321.1	0.296	4.075	0.017*
GA3	274.7	-0.162	3.617	0.086
BA1	265.3	-0.255	3.523	0.115
BA2	155.8	-1.337	2.442	0.955

b)

Treatment	% of control	Lower CI	Upper CI	P-value
N + P	194.6	-0.946	2.792	0.623
N	41.5	-2.589	1.448	0.957
P	100.0	-1.773	1.773	1.000
GA1	167.0	-1.215	2.522	0.884
GA2	218.9	-0.613	2.933	0.333
GA3	262.0	-0.192	3.354	0.097
BA1	250.5	-0.400	3.337	0.174
BA2	102.4	-1.846	1.892	1.000

Table 9. Results from two-way ANOVA for testing interaction between simulated light conditions and treatments for chlorophyll-a concentration in Castle Lake.

	DF	Mean Sq	F-value	P-value
Treatment	8	4.743	4.615	<0.001**
Smoke light	1	3.616	3.518	0.065
Treatment:Light	8	0.439	0.427	0.901

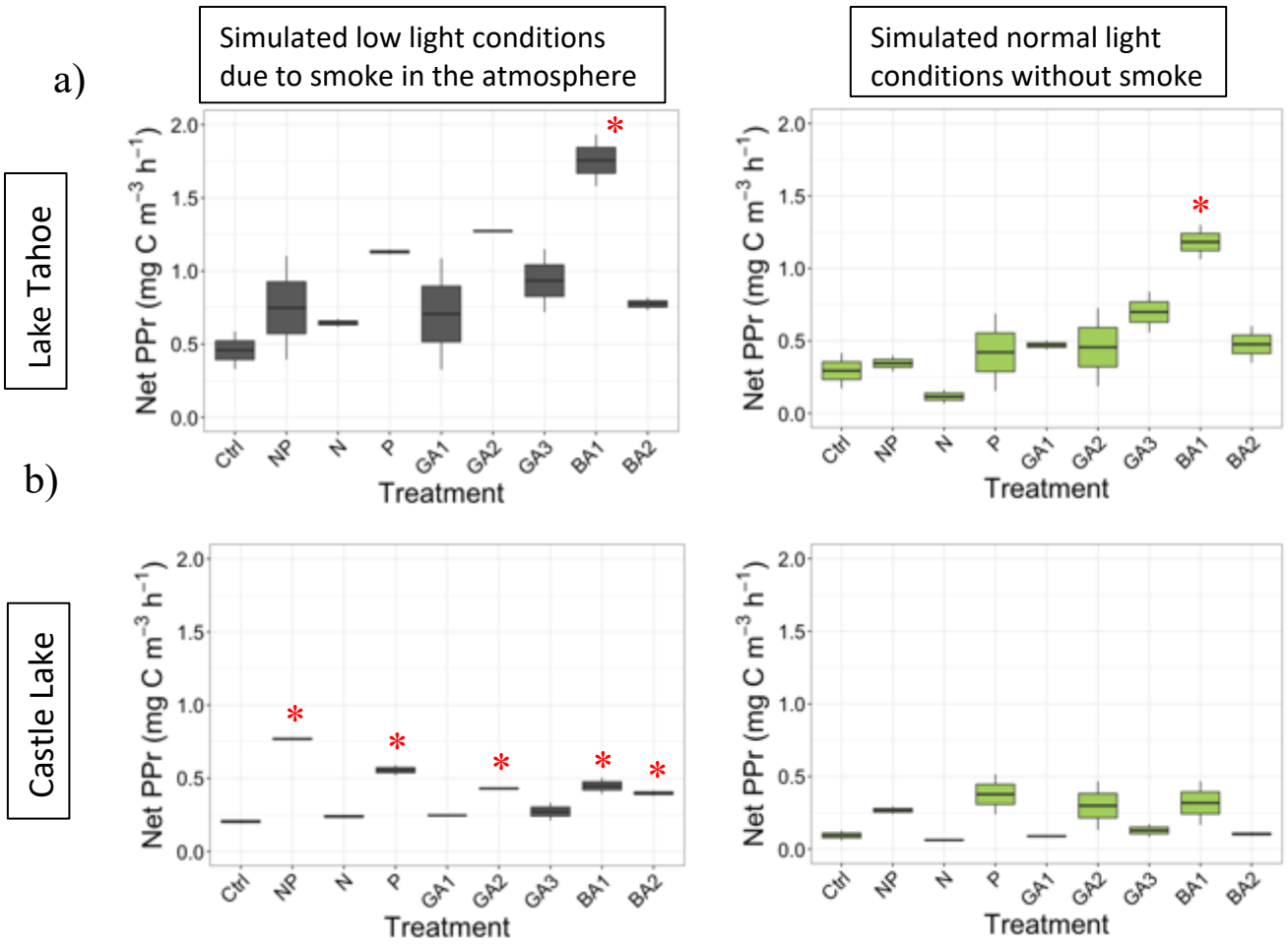

Figure 15. Net primary productivity (mg C m^{-3} h^{-1}) after a 5-day incubation in 125mL bottles for smoke light (grey) and full light (green) treatments for Lake Tahoe and Castle Lake in July 2022. Treatment amendments included the additions of nitrogen and phosphorus (NP), nitrogen (N), phosphorus (P), ground ash at low (GA1), medium (GA2), and high (GA3) concentrations, and ash collected in bucket collectors around the north end (BA1) and south end (BA2) of Lake Tahoe during the Caldor Fire in 2021.Red asterisks indicate significant differences between treatment and control determined using a Dunnett's Test ($p<0.05$). Red points indicate p-values <0.1. **Take home:** Lakes have differential responses to the additions of ash which can depend on the lake type, quality of ash introduced into waters, and light conditions in the atmosphere. In Lake Tahoe, net primary production increases only with higher quality ash deposited on the lake from the north/east deposition buckets under all light conditions whether simulating smoke in the atmosphere and thus reduced light entering the lake or normal light conditions. The higher quality ash means it is greater in bioavailable nitrogen, phosphorus, and metals as demonstrated from the extraction experiments. In smaller lakes (e.g., Castle Lake) with different conditions (like algal community structure, nutrient conditions) net primary production occurs with many types of ash sources (burned ground ash or different smoke ash deposits of low and high quality) under reduced atmospheric light conditions due to smoke in the atmosphere. This shows that lakes can have complex responses to smoke ash

deposits and under different atmospheric light conditions. Quantifying the nutrient state of the lakes, composition of algae and bacteria, and interactions with light (PAR and UV) could be important when trying to determine the ecosystem influences from ash deposition onto a lake.

Table 10. Dunnett's test results for net primary productivity measurements in Lake Tahoe water (20m) in treatments exposed to a) simulated smoke light conditions and b) simulated normal light conditions without smoke. Asterisks denote significance of $p<0.05$.

a)

Treatment	% of control	Lower CI	Upper CI	P-value
N + P	163.3	-0.644	1.225	0.864
N	140.8	-0.748	1.121	0.982
P	246.6	-0.262	1.607	0.193
GA1	154.0	-0.687	1.182	0.928
GA2	277.6	-0.120	1.749	0.093 .
GA3	203.7	-0.459	1.410	0.480
BA1	383.0	0.363	2.232	0.008*
BA2	168.9	-0.618	1.251	0.816

b)

Treatment	% of control	Lower CI	Upper CI	P-value
N + P	117.3	-0.666	0.768	1.000
N	39.2	-0.896	0.538	0.945
P	143.2	-0.590	0.844	0.991
GA1	160.1	-0.540	0.893	0.948
GA2	155.2	-0.555	0.879	0.966
GA3	237.8	-0.312	1.122	0.384
BA1	402.1	0.171	1.605	0.016*
BA2	162.0	-0.525	0.899	0.940

Table 11. Results from the two-way ANOVA for testing interaction between simulated light conditions and ash/nutrient treatments in Lake Tahoe.

	DF	Mean Sq	F-value	P-value
Treatment	8	0.442	6.813	<0.001**
Light	1	1.750	26.973	<0.001**
Treatment:Light	8	0.053	0.812	0.601

Table 12. Dunnett's test results for net primary productivity measurements in Castle Lake water (combined 0m, 3m, and 5m) in treatments exposed to a) simulated smoke light conditions and b) simulated normal light conditions without smoke. Asterisks denote significance of $p<0.05$.

a)

Treatment	% of control	Lower CI	Upper CI	P-value
N + P	376.3	0.419	0.711	<0.001**
N	116.9	-0.111	0.181	0.957
P	271.5	0.205	0.497	<0.001**
GA1	120.6	-0.104	0.188	0.897
GA2	210.1	0.079	0.371	0.004**
GA3	133.2	-0.078	0.214	0.564
BA1	219.3	0.098	0.390	0.002**
BA2	194.7	0.048	0.339	0.010*

b)

Treatment	% of control	Lower CI	Upper CI	P-value
N + P	283.7	-0.246	0.593	0.669
N	66.0	-0.452	0.387	1.000
P	400.6	-0.136	0.793	0.236
GA1	94.6	-0.425	0.414	1.000
GA2	317.2	-0.215	0.624	0.519
GA3	136.6	-0.385	0.454	0.999
BA1	337.5	-0.196	-.643	0.435
BA2	110.5	-0.410	0.429	1.000

Table 13. Results from the two-way ANOVA for testing interaction between simulated light conditions and ash/nutrient treatments in Castle Lake.

	DF	Mean Sq	F-value	P-value
Treatment	8	0.081	8.718	<0.001**
Light	1	0.369	39.931	<0.001**
Treatment:Light	8	0.015	1.674	0.173

PreSens dissolved oxygen sensors evaluate changes in water quality and productivity

Ash and nutrient additions stimulated increased metabolic activity, but the magnitude and direction of the effect changed over the course of the experiment. Net oxygen flux was negative in the control and all treatments at the beginning of the experiment, which indicates the ecosystem is consistently net heterotrophic (Figure 16). Most of the treatments remained heterotrophic throughout the entire experiment, with dissolved oxygen (DO) declining linearly through time (Figure 16a). In many treatments, net heterotrophy was lower after 200 hours (T2) than during the first 200 hours of the incubation (T1), signifying an increase in the phytoplankton metabolic activity after ash sits in the bottles (Figure 16b). In some treatments, the system became net autotrophic, signifying that phytoplankton production was eventually stimulated (Figure 16c).

In the jars with smoke-simulated light conditions, production seemed to be somewhat stimulated, resulting in NEP to be less negative in both Lake Tahoe and Castle Lake (Figure 17). Mean rates of oxygen consumption were slightly higher in jars with simulated normal light (full PAR light) compared to the smoke-light simulated jars, with a magnitude of the difference larger in the Lake Tahoe than Castle Lake, perhaps reflecting the greater sensitivity of the 20m Tahoe community to effects of light. The rates of oxygen consumption were lower in T2 than T1 in both light treatments in both lakes. In Castle Lake, the effect of light on NEP was small compared to the effect of nutrients (i.e., differences in mean between smoke-simulated and normal light jars is considerably smaller than between T1 and T2). However, in Lake Tahoe, the effects of light were similar to effects with nutrients (i.e., the difference between smoke-simulated and normal light is comparable between T1 and T2).

The mean net change in DO across treatment types and light levels ranged from -0.035 to +0.005 in replicate jars. Chemical oxygen demand ranged from -0.007 to -0.002mgDO hr^{-1} across all treatments, which was an order of magnitude lower than the rate of change in DO within treatments with ash and nutrients (Figure 18). The control treatments did not show a difference between the first 200h (T1) and the last 150h (T2). However, in all other treatments, rates of oxygen consumption were on average lower during T2 than T1, reflecting an increase in production associated with treatment effects that took >200h to begin. Ash deposits from the north/west (BA1), south/ east (BA2), and ground ash stimulated bacterial heterotrophic responses initially in Lake Tahoe and Castle Lake with a change after 8 days of incubation to more phytoplankton/ autotrophic dominated responses. It takes time to detect measurement responses in dissolved oxygen conditions using laboratory experiments and likely from lake conditions in the pelagic zone of low productive ecosystems.

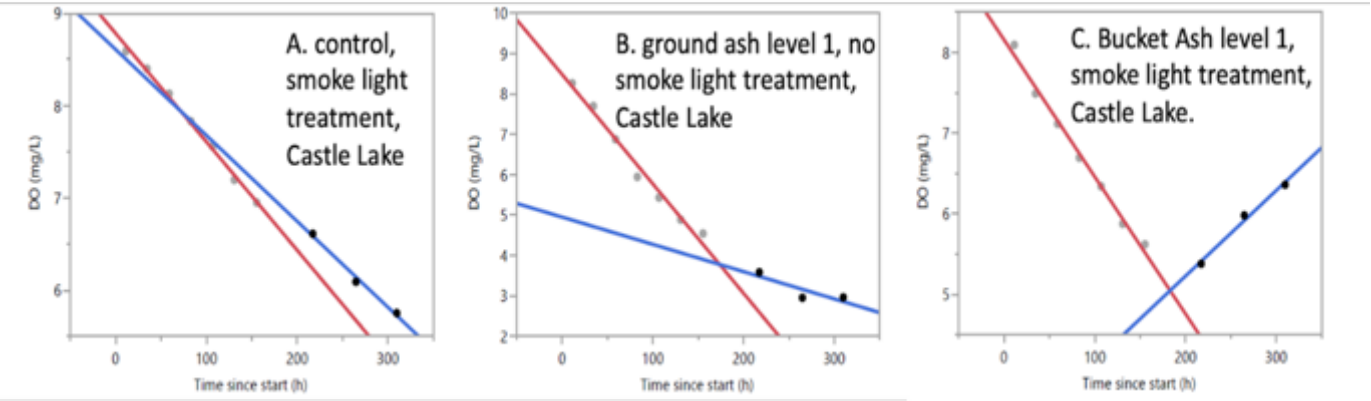

Figure 16. Changes in the dissolved oxygen (DO) through time illustrate the net metabolic dynamics associated with phytoplankton and bacterioplankton metabolism through successive diel light/dark cycles (~16h light and 8h dark). Measurements shown are of dissolved oxygen within incubation jars collected daily after a period of darkness. Rates of change in the DO over the course of the experiment were calculated as the slope of the change in DO over the first 200h (red line) and the last ~150h (blue line). Panel A (control, simulated smoke light treatment, Castle Lake) illustrates the consistent net rate of decline in DO. Panel B and C illustrate the pattern from jars that showed a treatment effect after about 200h, where the net change in DO either became less negative but still heterotrophic (panel B, ground ash level 1, normal light simulation, Castle Lake) or switched to become positive illustrating an increase in GPP (panel C, bucket ash level 1, simulated smoke light treatment, Castle Lake). **Take home:** Water quality, dissolved oxygen concentrations demonstrate: 1) a consistent net rate of decline in oxygen in waters under light and dark conditions suggest heterotrophic activity is important with and without ash additions. Oxygen responses take time to manifest likely due to the activation of phytoplankton and heterotrophic community assemblages where after 8 days (200 hours), there is a change in conditions depending on the type and quality of ash added to the waters (ground versus high quality ash from the north/east BA1). Ash from the buckets seems to have a great stimulatory response to the balance of the autotrophic (phytoplankton)/ heterotrophic community perhaps due to the higher quality ash as determined in Objective 2.

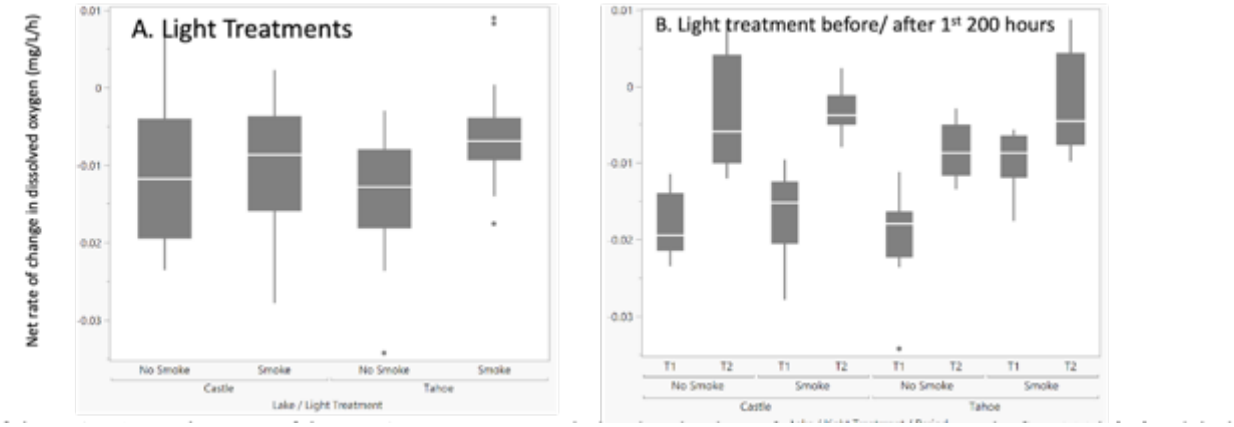

Figure 17. Rates of change in dissolved oxygen (DO) over the course of the 14-day experiment. Rates were calculated as the slope of the change in DO over the first 200h (T1) and the last ~150h (T2). Panel A compares differences in NEP between light treatments for each lake (smoke-simulated- reduced atmospheric light conditions simulated normal light atmospheric conditions) for Lake Tahoe and Castle Lake. Panel B compares differences in light treatment in both lakes during T1 and T2 independently. **Take home:** Using the rate of change in dissolved oxygen to determine net ecosystem productivity indicates that Lake Tahoe and Castle waters exhibit net heterotrophic conditions (bacterial and respiratory metabolic processes dominate over autotrophic-phytoplankton oxygen production with little changes in oxygen due to chemical demand. Smoke simulated conditions in the atmosphere thus reducing light seems to stimulate phytoplankton or autotrophic attributes particularly after 8 days of incubations suggesting a change from bacterial dominated metabolic process to phytoplankton.

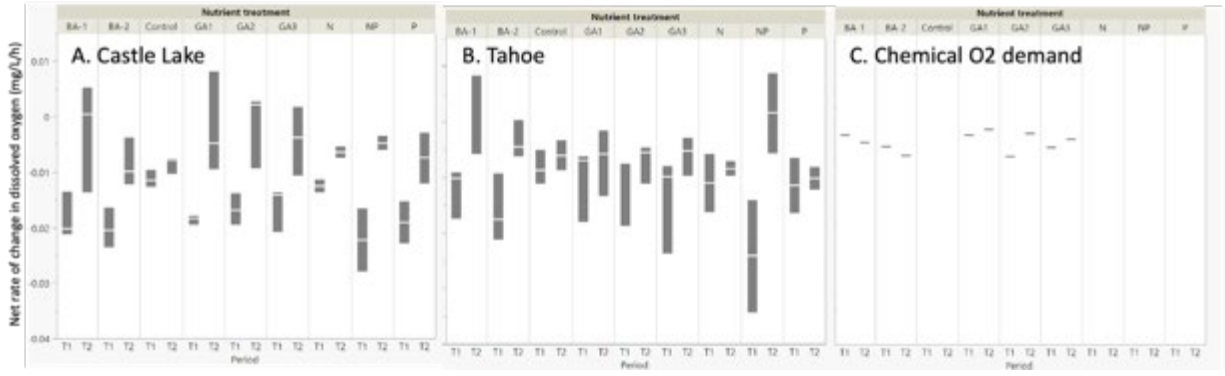

Figure 18. Rates of change in dissolved oxygen (DO) over the course of the 14-day experiment. Rates were calculated as the slope of the change in DO over the first 200h (T1) and the last ~150h (T2) in a) Castle Lake, b) Lake Tahoe. **Take home:** Ash deposits from the north/west (BA1), south/ east (BA2), and ground ash stimulated bacterial heterotrophic responses initially in the lakes suggesting a dominance of organic carbon consuming bacterial activity and respiration with a shift after 8 days to phytoplankton/ autotrophic dominated responses. It takes time to detect measurement responses in dissolved oxygen conditions using laboratory experiments and likely from lake conditions in the pelagic zone of low productive ecosystems.

Task 8. Quantify the effects of prolonged smoke cover on metabolic rates and photosynthetic efficiency of phytoplankton and nearshore periphyton through laboratory incubations.

S. Sadro

Plain language summary: The goal of this task was originally focused on understanding the extent to which long term smoke cover, and the resulting reduction in phytoplankton exposure to ultraviolet and photosynthetically active radiation (PAR) wavelengths of light, altered the photosynthetic efficiency of phytoplankton. Unfortunately, by the time resources became available the majority of smoke had cleared from the Tahoe Basin, leaving us without the ability to test for change. Consequently, effort was re-directed into a collaborative project with the UNR task associated with quantifying the combined effect of ash and smoke on algal productivity using the ^{14}C PPR method. That experiment was expanded to include oxygen metabolism and additional treatments and the results reported with that task. However, we did carry out two experiments aligned with the original UCD task that provided useful information.

Our experiment showed that: 1) phytoplankton in surface waters are more sensitive and inhibited by light than phytoplankton collected from depths near the chlorophyll-a maximum (50-60 meters); 2) the maximum photosynthetic rate (P_{max}) of phytoplankton from within the chlorophyll-a maximum was 16 ug oxygen L^{-1} h^{-1}, corresponding to light levels of 260 PAR (I_{max}); 3) although we were not able to accurately measure P_{max} or I_{max} for phytoplankton in surface waters because the level of production was near detection limits and because our preliminary experiment did not focus on light levels that were low enough, our experiment suggests the maximum photosynthetic rate corresponds to light levels <250 PAR (evidence that these phytoplankton are photo-inhibited by high light levels); and 4) photosynthetic efficiency of phytoplankton from within the chlorophyll-a maximum was computed as 0.03 ug oxygen L^{-1} h^{-1} per unit PAR.

Main conclusions: Although limited to only two experiments, this analysis provides extremely useful information about phytoplankton sensitivity to variation in light. It has been decades since these types of experiments have been carried out in Lake Tahoe, and the data provide valuable methodological information for continuing to carry out further experiments. These results clearly demonstrate differences in sensitivity to light in phytoplankton with depth and the data provide a baseline estimate of photosynthetic efficiency for phytoplankton from within the chlorophyll-a maximum. Perhaps most importantly, the results suggest similar experiments will allow researchers to more accurately parameterize phytoplankton growth for the Tahoe Lake Clarity model, reflecting the current phytoplankton community structure found within the lake rather than literature values, and importantly, incorporate variation with depth associated with differences in light sensitivity and resulting photosynthetic efficiency.

Methods

The methods used for this task correspond to those previously described in Task 3, as summarized below.

• Collected phytoplankton from surface waters and the deep chlorophyll maximum

• Incubated samples under ambient water temperatures at 6-8 light levels (100% irradiance to 1% irradiance, and in the dark.

• Measured changes in dissolved oxygen within incubation chambers and compute metabolic rates (net ecosystem production, gross primary production, and ecosystem respiration).

• Used the variation in metabolic rates with light levels to compute Photosynthesis-Irradiance (P-I) parameters, maximum photosynthetic rate, saturation irradiance, the growth efficiency, and the sensitivity to photo-inhibition.

Results and discussion

The original intent of this task (i.e., P-I incubations) was to explore the effect of prolonged exposure to smoke from the Caldor fire on different elements of phytoplankton growth efficiency. Prolonged exposure to smoke may alter either the physiological growth efficiency or the community growth efficiency of primary producers by altering exposure to UV and photosynthetically active radiation. The hypothesis is that reduced UV and PAR will increase the growth efficiency of phytoplankton. However, by the time TRPA resources became available, the bulk of smoke from the Caldor fire had already cleared from the Tahoe basin, affecting our ability to characterize changes in photosynthetic efficiency associated with variability in duration of smoke cover.

Consequently, the scope of the original UCD task was re-aligned with the UNR task associated with quantifying the combined effect of ash and smoke on algal productivity using the 14C PPR method. By combining both dissolved oxygen and 14C methods of measuring productivity over the course of a long-term incubation experiment, we gained a much clearer understanding of phytoplankton responses at time scales that the 14C method alone does not capture. The substantive UCD contribution to the incubation experiments that sought to disentangle the differential effects of ash as a source of nutrients to phytoplankton and smoke as a mechanism reducing light available to phytoplankton are described in the UNR Task: Quantify contributions of deposited particles to algal productivity.

Here, we describe the results from two P-I incubation experiments that were carried out during the tail end of the Caldor Fire in the summer of 2021 associated with the original UCD task.

3.1 Collect phytoplankton from the deep chlorophyll maximum

Water samples were collected from the long-term TERC pelagic monitoring station in Lake Tahoe on 9/9/2021 from 15m and 50m, corresponding to near surface waters and the deep

chlorophyll-a maximum. A second sample was collected from the same site in Lake Tahoe on 9/15/2021 from 65m, corresponding to the chlorophyll-a maximum. Samples were immediately transported to UC Davis and incubated at in situ temperatures.

3.2 Incubate under ambient water temperature across a range of PAR spanning from 100% to ~1% light.

On both dates, water samples were returned to the UC Davis incubation facility within 12h of collection. 500mL borosilicate incubation jars fitted with PreSens DO sensor spots were filled and allowed to equilibrate at in situ temperatures overnight prior to the start of each experiment. Mean water column temperature for 15-50m depth interval was used for the first experiment (~14 degrees C) and the *in situ* temperature from 65m was used in the second experiment (~8 degrees C). Light levels for the first experiment were 12%, 25%, 50%, and 100% of surface PAR (~1200 µmol m2 s-1). To better characterize the linear range of increase in production with light, levels for the second experiment were increased to 9 intervals, focusing on the range of PAR <10% but ranging up to 91%.

In both experiments, each light level had 5 replicate incubations jars, from which DO measurements were made 2-4 times over 24-48h periods for both light and dark treatments.

3.3 Measure changes in dissolved oxygen in incubations and compute metabolic rates

Rates of change in DO were computed for each jar over the interval measurements were taken. Change in DO in jars during intervals of light corresponds to net ecosystem production (NEP), change in DO during dark intervals corresponds to ecosystem respiration (ER), and gross primary production (GPP) as computed as GPP = NEP – ER where ER is treated as a negative value.

Metabolic rates from the five replicate jars for each light treatment were averaged (Table 14) to smooth data and account for measurement error in jars. Mean metabolic rates for each light level were then plotted as photosynthesis (i.e., GPP) – irradiance curves for water samples from each depth (Figure 19).

3.4 Based on metabolic rates, compute photosynthetic-irradiance parameters.

P-I curves, which characterize changes in phytoplankton production with light, were successfully made for the samples collected from 3 depths over 2 dates in mid-September 2021, after skies had already been clear from smoke in the Tahoe basin for 1-2 weeks.

Although these results cannot be used to characterize phytoplankton responses to the Caldor fire directly because sampling was not carried out prior to and throughout the period of smoke cover, they nevertheless remain informative of phytoplankton sensitivity to light, and together with the collaborative experiment with UNR where light and ash levels were manipulated concurrently, inform how phytoplankton in different parts of the water column respond to changes in light from smoke cover.

The photosynthetic efficiency of phytoplankton (α) is computed as the slope of the linear portion of increase in GPP with irradiance. Photosynthetic efficiency increased with depth, with α highest for the 65m sample (0.03) and slightly lower for the 50m sample (0.02). The negative slope observed over the PAR range we measured in experiment 1 for the near surface water sample (15m) indicates P-max was already exceeded and α cannot be computed across the range of light used.

Phytoplankton collected from 15m had lower rates of production than those collected from the deep chl-a maximum, perhaps reflecting both differences in phytoplankton abundance and adaptation to light. The irradiance of maximum photosynthesis (I-max) was fairly consistent for phytoplankton collected at the deep chl-a maximum (260 – 275 µmol m2 s-1). The lower I-max of the phytoplankton in surface waters may reflect a population that is stressed by higher exposure to UV or other effects of photo-inhibition.

Key Conclusions

• Rates of primary production and photosynthetic efficiency were higher for phytoplankton collected in deeper waters corresponding to the lower light environment where the chlorophyll-a maximum occurs.

• Rates of production in surface waters were lower, with phytoplankton showing greater sensitivity to light (lower I-max) than phytoplankton collected from the deep chlorophyll-a maximum.

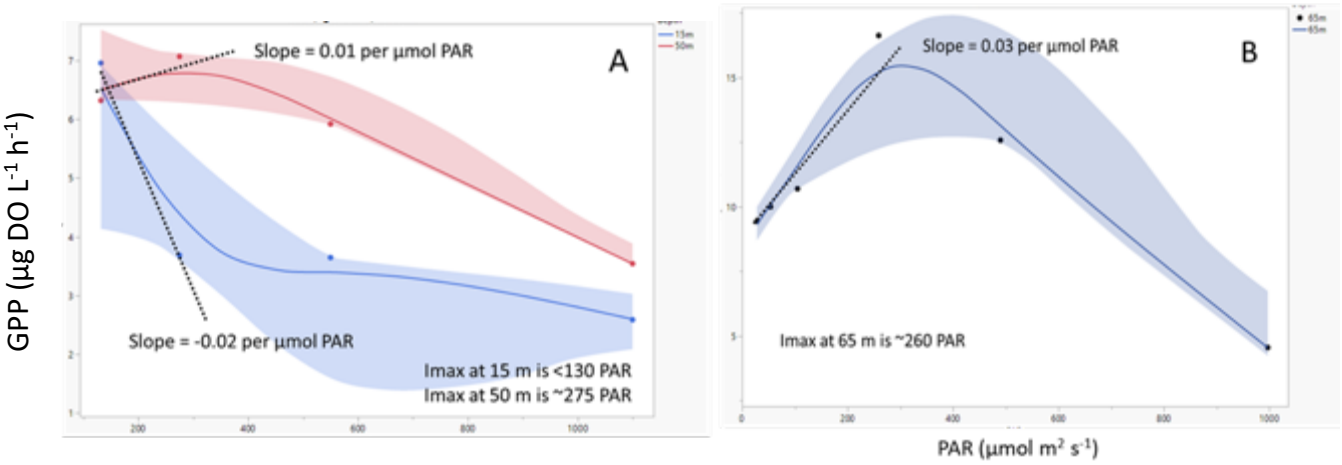

Figure 19. Photosynthesis-Irradiance curves for water samples collected from 15m and 50m on September 9, 2021 (A) and from 65m on September 15, 2022 (B) from Lake Tahoe.

Table 14. Metabolic rates computed from 3-5 replicate jars incubated at various light levels. Values represent mean rates computed from 5 replicate incubation jars for each light level. Light incubations were carried out first for 24-48h, and change in DO used to compute NEP, followed by dark incubations, which change in DO over 24-48h was used to compute ER. GPP was computed as NEP – ER.

Collection date	Depth	PAR	Light (%)	NEP (ug L-1 h-1)	ER (ug L-1 h-1)	GPP (ug L-1 h-1)
9/9/2021	15m	132	12	3.96	-3.00	6.96
9/9/2021	15m	275	25	2.76	-0.93	3.69
9/9/2021	15m	550	50	2.60	-1.04	3.65
9/9/2021	15m	1100	100	1.41	-1.18	2.59
9/9/2021	50m	132	12	4.17	-2.15	6.32
9/9/2021	50m	275	25	5.33	-1.74	7.07
9/9/2021	50m	550	50	4.11	-1.81	5.92
9/9/2021	50m	1100	100	3.13	-0.42	3.54
9/15/2021	65m	28	3	6.11	-3.33	9.44
9/15/2021	65m	54	5	7.78	-2.22	10.00
9/15/2021	65m	105	10	7.67	-3.04	10.70
9/15/2021	65m	126	11	7.33	-3.37	10.69
9/15/2021	65m	157	14	5.86	-2.24	8.10
9/15/2021	65m	259	24	14.31	-2.33	16.63
9/15/2021	65m	490	45	9.61	-2.97	12.58
9/15/2021	65m	997	91	3.56	-0.99	4.55

Task 4. Quantify the effects of smoke on algal productivity in the nearshore of Lake Tahoe

F Scordo, J Blaszczak, K Loria

We estimated metabolic rates using a modeling approach based on Phillips (2020) and Lottig et al. (2021). This model requires high-frequency measurements of DO concentration (mg L-1), water temperature (℃), PAR (µmol m-2 s-1), wind speed (m s-1), and barometric pressure (mbar). The model generates daily estimates (mmol O2 m-3 d-1) of GPP, R, and NEP (NEP = GPP - R). A detailed description of the model can be found in Lottig et al. (2021). Metabolism estimates were calculated from August 1st to September 27nd for two littoral sites on the west coast of the lake (Blackwood) and two littoral sites on the east coast of the lake (Glenbrook).

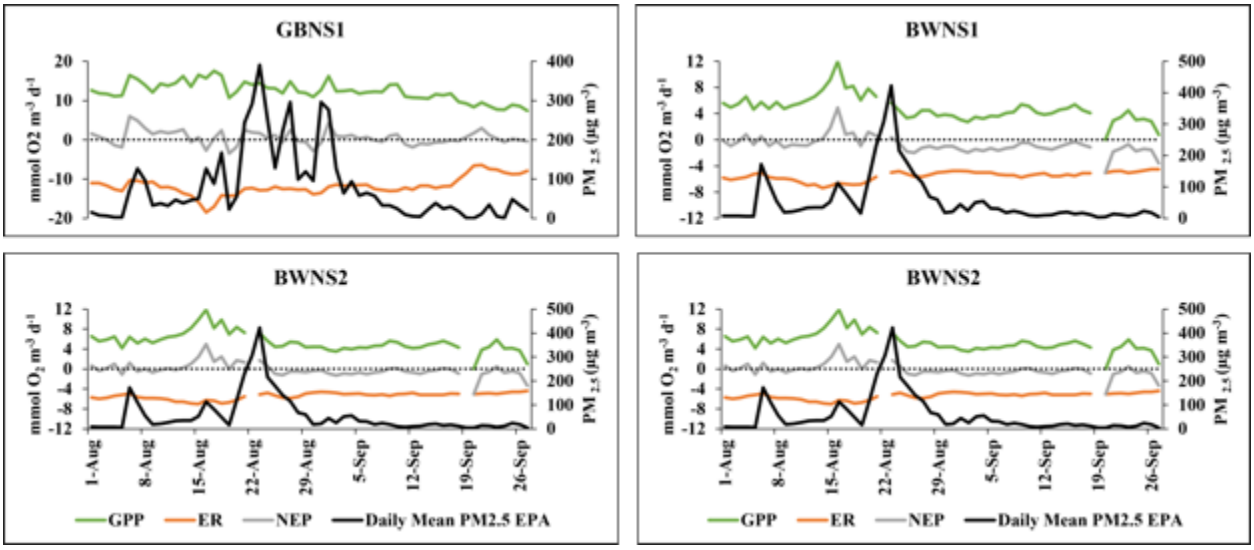

Figure 20. Gross primary production (GPP), ecosystem respiration (ER), and net ecosystem production (NEP) from a) Glenbrook (GBNS1), b) Blackwood (BWNS1 & 2) modeled using dissolved oxygen sensors in the littoral area of Lake Tahoe. The black line indicates PM2.5 concentrations during the sampling period to track smoke in the watershed. **Take home:** We observed small increases in gross primary production and ecosystem production (bacterial and periphyton) in the nearshore of Lake Tahoe in two locations in the first small pulse of smoke cover in the basin, but no major changes in metabolism during the heavy smoke-cover period. This increase may occur due to a reduction in ultraviolet light and photosynthetically active radiation. {Published work from Castle Lake suggests that production in the nearshore does not change significantly under reduce light conditions from atmospheric smoke possibly reflecting adaptation of algal and bacterial species to high-intensity UV-B light in these habitats. Having longer-term measures of dissolved oxygen and modeled lake metabolic process in the nearshore which is more heterogenous in habitat structure could lend to understanding the influences of ash deposits to the lake condition over time.

Objective 4: Task 5. Using long-term monitoring data to assess changes in water quality (temperature, nutrient concentrations) in comparison to years without prolonged smoke coverage

Background: As part of the UC Davis ongoing monitoring programs, offshore of Lake Tahoe, water quality profiles were be collected and used to understand changes to water quality. Water quality profiles include particle size, temperature, oxygen, chlorophyll-*a*, conductivity, light, and primary productivity using 14C. Additional water quality profiles for oxygen, temperature, chlorophyll-*a*, conductivity, light (a minimum of five additional times) were collected during fire season (presumably from September to October) to understand the finer time scale changes to water quality as light and particle deposition changes occurred on the lake.

Introduction: The smoke impacts from the Caldor Fire, together with the earlier Tamarack Fire and Dixie Fire, were the focus of this amendment. Conditions at Lake Tahoe were unprecedented – the 2007 Angora Fire that was wholly within the Tahoe Basin – was of far shorter duration, burned far less acreage and had a far lower impact on air quality. These conditions led many in both the science and management communities to question what the impacts on the wildfire smoke were, and what they might mean for the anticipated future wildfires in the western US.

The rapid scientific response required to sample while the fires were still occurring was challenging but was achieved through the dedication of our field and laboratory staff. Outside conditions were extremely unhealthful. The rapidity needed meant that there was not time to hire additional staff – instead existing staff had to work extra days and weeks to accomplish all the required tasks. Most importantly, some of the work was actually commenced prior to the funding being in place, thereby extending the record forward to some of the most intense periods of smoke.

4.1 Lake Profiling

Lake profiles are collected using a Seabird SBE 25 or 25Plus profiler, a LISST 100X or 200 profiler, and a BIC PAR and UV sensor. Data from the LTP station are presented here, as those data are taken more frequently, and provide more detail on the upper water column that was impacted by the wildfire smoke. Measured variables include temperature, electrical conductivity, dissolved oxygen, chlorophyll fluorescence, turbidity, PAR attenuation and light transmission.

The data are presented as color contours of each variable (Figure 21). The dashed vertical lines indicate the date at which the individual vertical profiles were taken.

A)

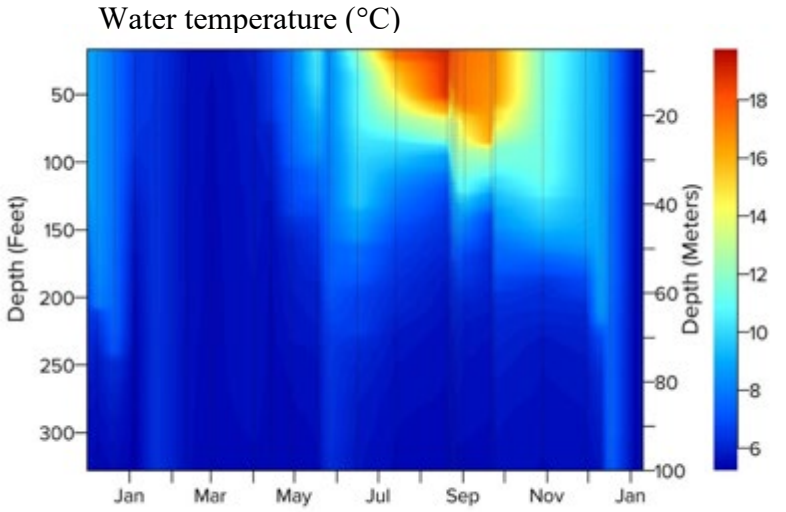
Water temperature (°C)
Depth (Feet)
50
100
150
200
250
300
Depth (Meters)
20
40
60
80
100
Jan
Mar
May
Jul
Sep
Nov
Jan
18
16
14
12
10
8
6

B)

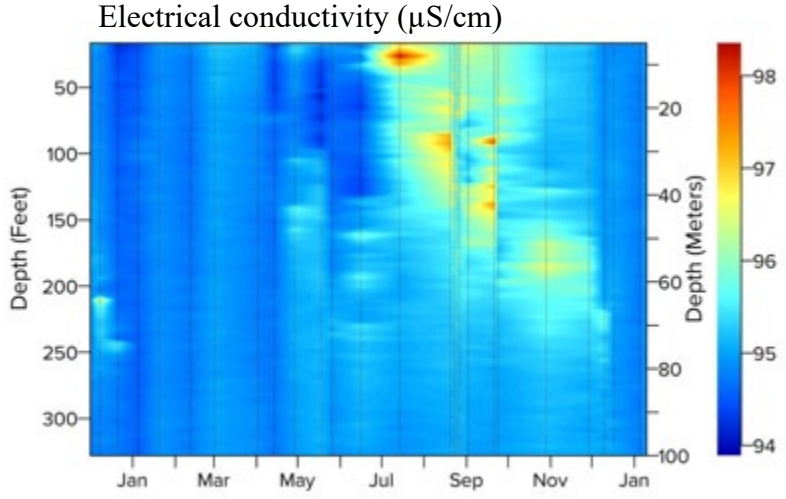
Electrical conductivity (µS/cm)
Depth (Feet)
50
100
150
200
250
300
Depth (Meters)
20
40
60
80
100
Jan
Mar
May
Jul
Sep
Nov
Jan
98
97
96
95
94

C)

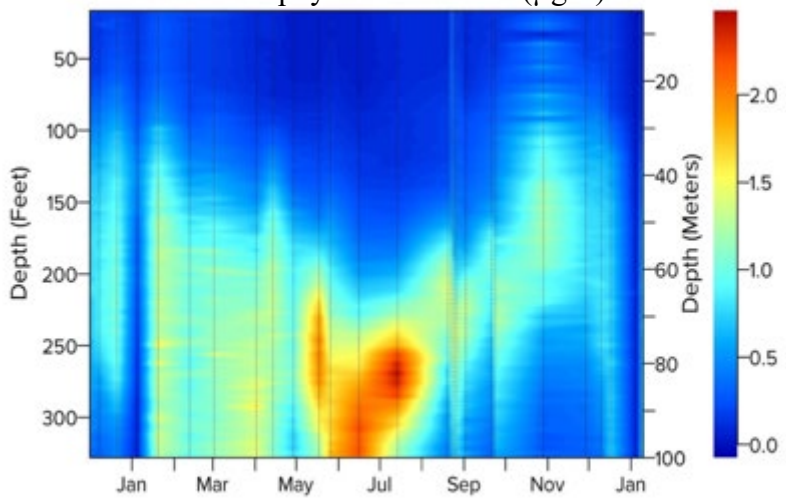
In situ chlorophyll fluorescence (µg/L)
Depth (Feet)
50
100
150
200
250
300
Depth (Meters)
20
40
60
80
100
Jan
Mar
May
Jul
Sep
Nov
Jan
2.0
1.5
1.0
0.5
0.0

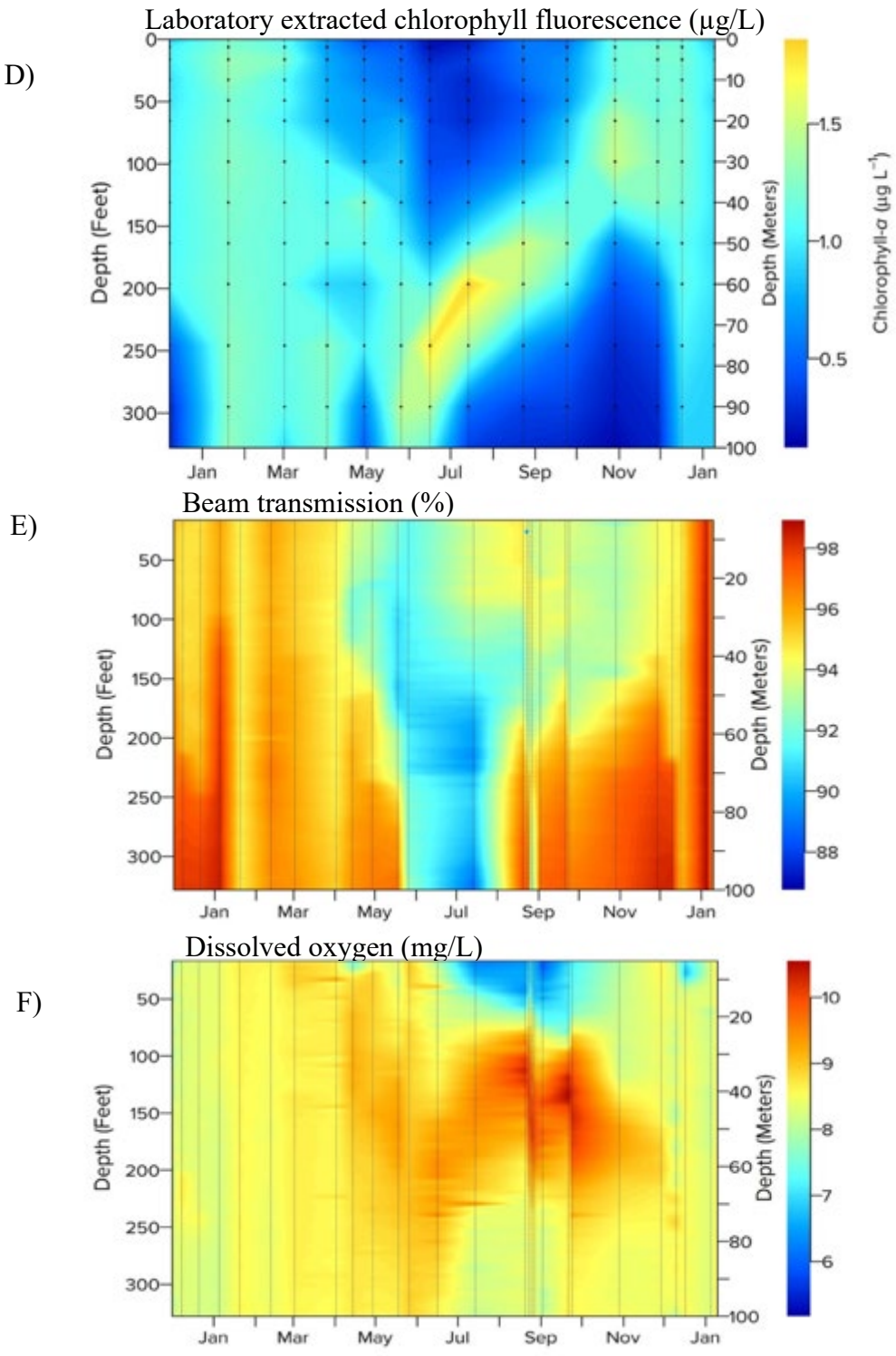

Figure 21. A) Water temperature, B) electrical conductivity (µS/cm), C) *in situ* chlorophyll fluorescence (µg/L), D) laboratory extraction chlorophyll fluorescence (µg/L), E) beam transmission (%), F) dissolved oxygen (mg/L) from January 2021 through January 2022. **Take home:** Dominant feature of 2021 lake profiles at the long-term LTP site was a rise (shoaling) in the level of the deep chlorophyll maximum during the wildfire smoke period.

Plain language summary: Increased temporal monitoring of Lake Tahoe during the Caldor fire showed the system's general response to the combination of light and UV reductions, and nutrient and fine particle additions at the surface. Even with the increased frequency, however, the observed patterns are dominated by interpolation over days at a time.

The most dominant features of lake profiles were the rise in the level of the deep chlorophyll maximum and the change in the algal speciation. The rise in the depth of maximum chlorophyll was evident in both fluorescence profiles, and in water samples where chlorophyll was laboratory extracted. Early in the spring, before wildfire smoke was an issue, the chlorophyll maximum layer was at its normal summer depth of 60- 80 m.

4.2 The Light Environment

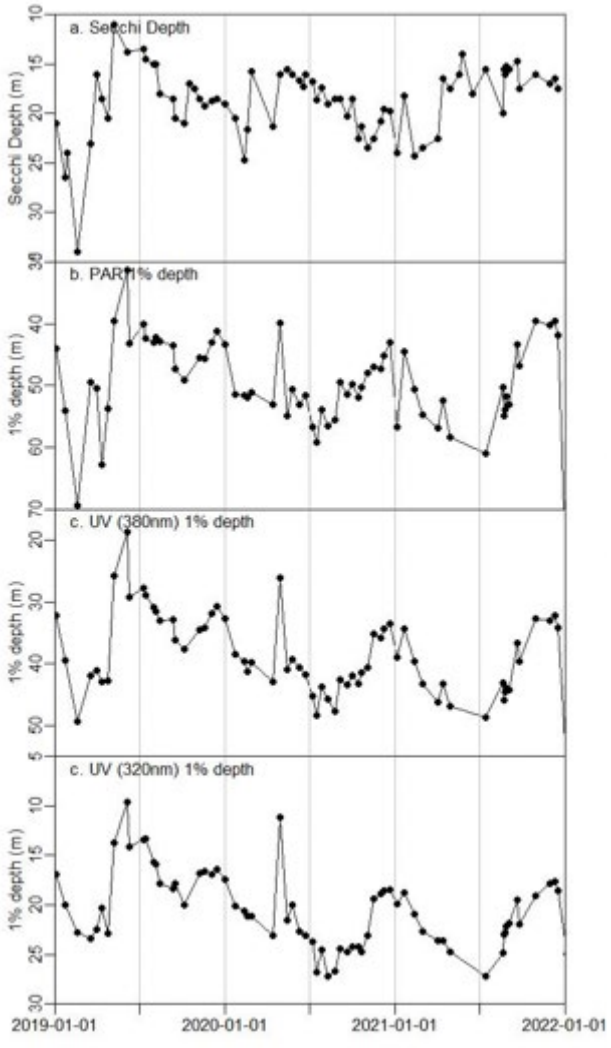

Figure 22. Light Field 2019-2021

Take home: In the period of heavy smoke cover in 2021, we observe shallower light penetration measured by Secchi, and 1% depths of different wavelengths of light.

Plain Language Summary: There was a decline in Secchi depth, associated with the wildfire smoke, a result of the reduced ambient light levels and the increase in particulates and the small *leptolyngbya* cells that were dominant in the upper waters

4.3. Particulates

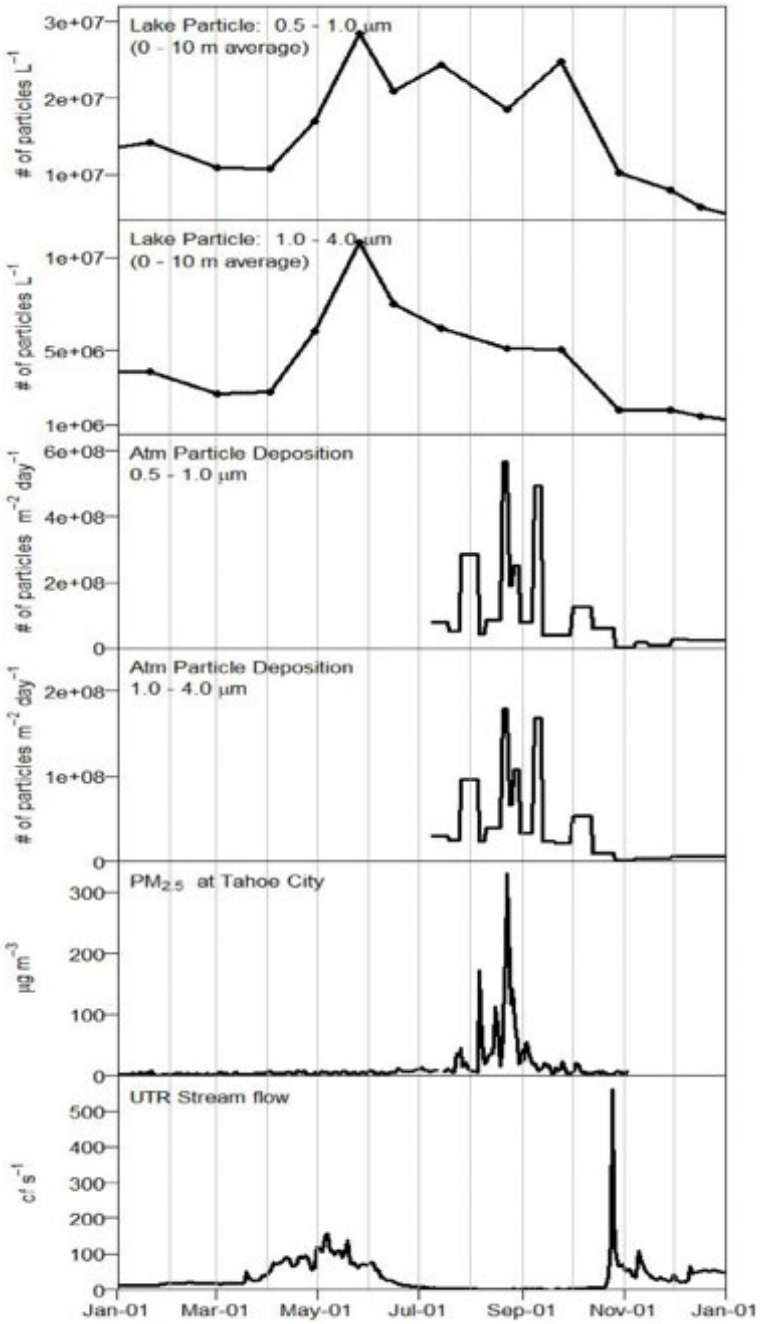

Figure 23. Particles from 2021. A) Lake particles 0-10m, 0.5-1.0µ; B) lake particles 0-10m, 1.0-4.0µ; C) on-lake atmospheric particle deposition 0.5-1.0µ; D) on-lake atmospheric particle deposition 1.0-4.0µ; E) PM2.5 at Tahoe City; F) Upper Truckee River stream flow. **Take home:** We observed an increase in particle deposition rates during the Caldor Fire in and on Lake Tahoe and along the Truckee River. Particles in the smallest size range are ones that contribute to the loss of clarity at Lake Tahoe.

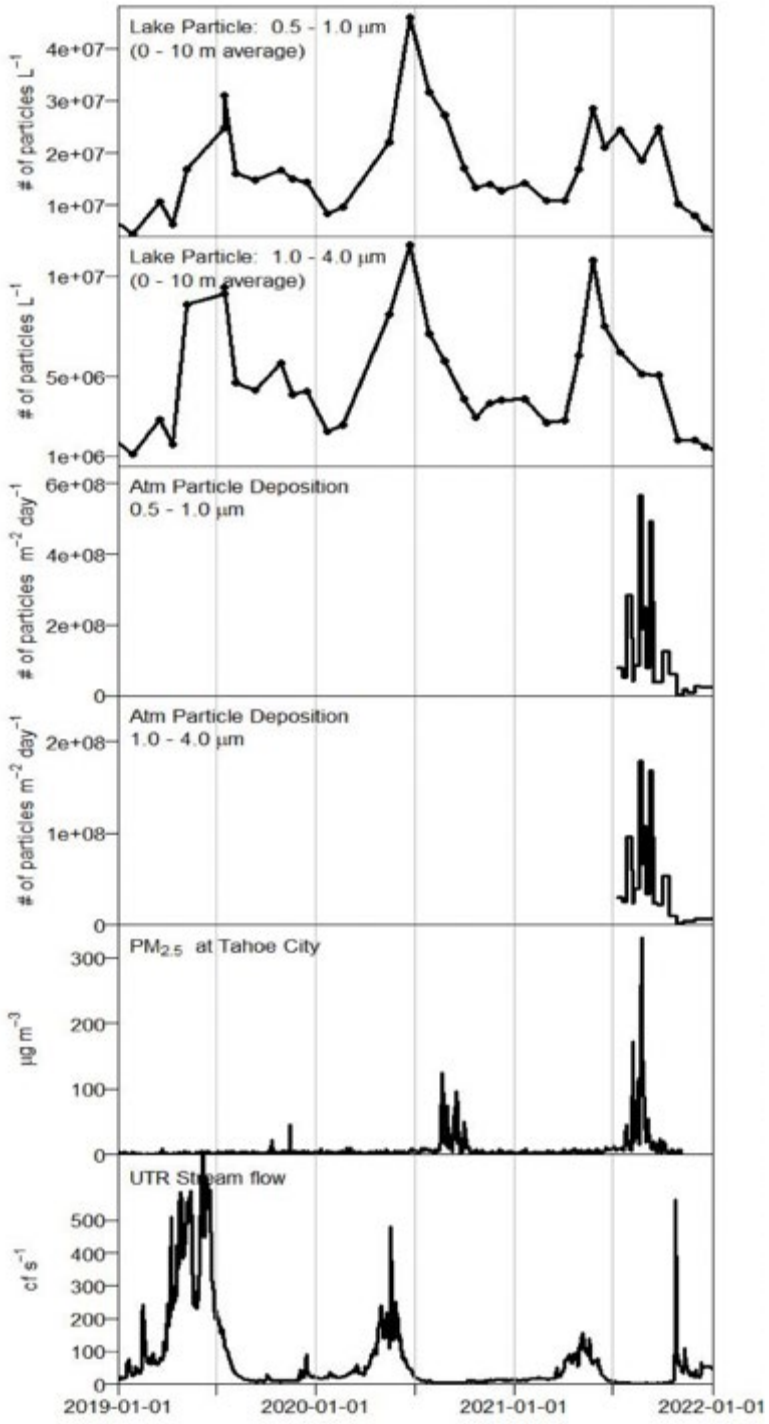

Figure 24. Particles 2019-2021. A) Lake particles 0-10m, 0.5-1.0µ; B) lake particles 0-10m, 1.0-4.0µ; C) on-lake atmospheric particle deposition 0.5-1.0µ; D) on-lake atmospheric particle deposition 1.0-4.0µ; E) PM2.5 at Tahoe City; F) Upper Truckee River stream flow.

Plain language summary: The wildfire smoke added particulates to the upper (0-10 m) part of the lake in the clarity-critical size range of 1-6 microns, at a time of year when such inputs would not normally occur. The peak concentrations were lower than those produced by streams during the spring runoff period. It should be noted that 2021 was a record low year for stream inputs, so normal stream particle loads are significantly higher than those shown. When compared with data from the last 3 years, the fine particle concentrations in the lake can be seen to be lower, but with higher concentration later in the year (September – December) than normally observed.

4.4 Phytoplankton Response to Wildfires

Phytoplankton enumeration and identification took place monthly (4x greater than contract) and at six depths (2x greater than contract). This higher frequency made it possible to detect both seasonal changes throughout the year and responses to wildfire smoke.

The total number of algal cells from different groups vary from year to year. Diatoms are generally the most common type of algae. In 2021, there was a major shift in the phytoplankton composition, with an abrupt increase in the abundance of the cyanobacteria *Leptolyngbya sp.* that extended from September through the end of the year (Figure 25). This was the only year on record in which a single taxon belonging to the cyanobacteria group dominated the phytoplankton assemblage. *Leptolyngbya* is a simple filamentous genus that in Lake Tahoe that includes an extremely narrow species, generally with cells 1–2 microns (µ) wide, this makes them potentially important for clarity (Figure 26). Individual filaments display a visible sheath comprised of dozens of individual cells and can be over 200µ in length.

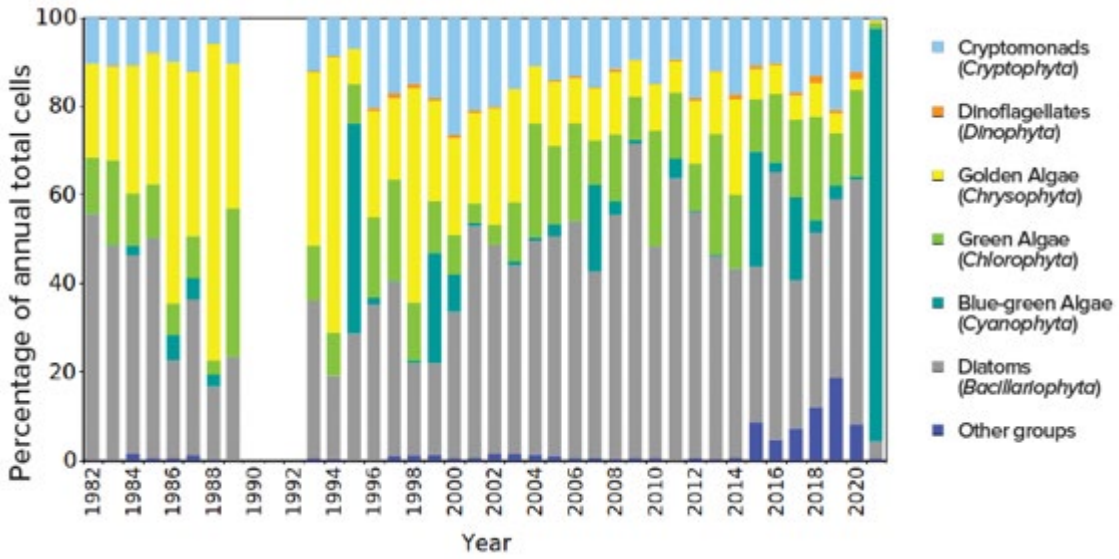

Figure 25. Annual distribution of algal groups. **Take home:** In 2021, we observed an abrupt shift in the phytoplankton community to be dominated by blue-green algae. In Lake Tahoe, the algal community has always been predominantly diatoms, so this shift could have consequences for higher trophic levels who are unable to consume blue-green algae.

Figure 26. *Leptolyngbya sp.* (blue-green algae)

The response of *Leptolyngbya* to the wildfire smoke can be seen from its monthly vertical distribution in the water column in Figure 27. Note the variation of the horizontal scale that helps to better show the spatial distribution. The monthly distributions had low maximum abundances from January through August, with peak values of less than 5,000 filaments/liter. In the September sampling, peak values increased by a factor of ten, and then from October through November, they increased further by a factor of 30 approaching abundances of 1.5 million filaments/liter. The high abundances were confined to the upper 130ft (40m) of the lake. In December, the abundances were still high, but spread through a greater depth due to fall mixing. The reason for the *Leptolyngbya* is likely due to its preference for the higher N:P ratios associated with wildfire smoke (Mackey et al. 2013).

Both the high concentrations and the spatial distributions can be better appreciated, if the same scale is used for the number of filaments. This is shown in Figure 28 at depths of 20m (top graph) and 40m (bottom graph) at the LTP monitoring station.

The total biovolume of different algal genera vary month to month as well as year to year, as shown in Figure 29. In 2021, despite the domination of cyanobacteria in algal abundance based on the number of individual cells, diatoms again dominated the biovolume (proportional to the mass) of the phytoplankton community in every month. The peak in the monthly average biovolume occurred in April and May 2021. This “spring bloom” is a typical occurrence in Lake Tahoe. This was 4–5 months before any wildfire smoke was present in the Tahoe basin. Despite the very “average” whole lake chlorophyll concentration, the peak biovolume was over 1,300 cubic millimeters per cubic meter, six times the usual peak biovolume (see Figure 30). There was also a smaller “fall bloom” in November, likely related to wildfire smoke effects. The red dots indicate the average total biovolume for years 2012 and 2015–2020. Other years had incomplete data sets and were not used in the calculation of the average.

Despite these huge changes in both the biovolume and the algal abundance in 2021, the annual average chlorophyll concentration (based on laboratory extractions) was unremarkable, as shown in Figure 30.

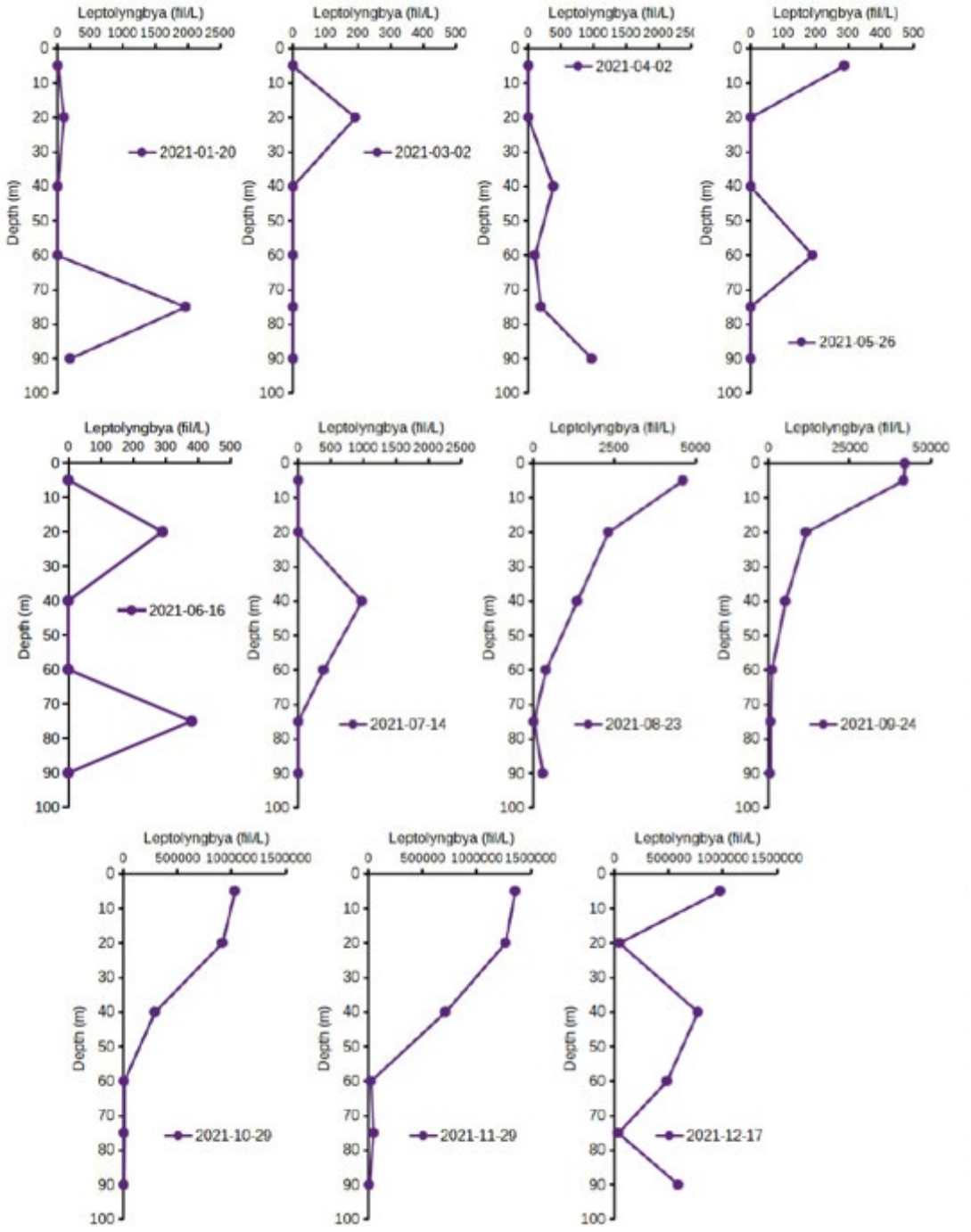

Figure 27. *Leptolyngbya* filaments per litre at each sampling at the LTP site. Note that the horizontal scale varies between plots. **Take home:** As seen by the horizontal scale, we observed a large increase in the blue-green algal species, *Leptolyngbya*, during and after the period of smoke cover in Lake Tahoe. The highest abundances were observed in the upper 40m of the lake.

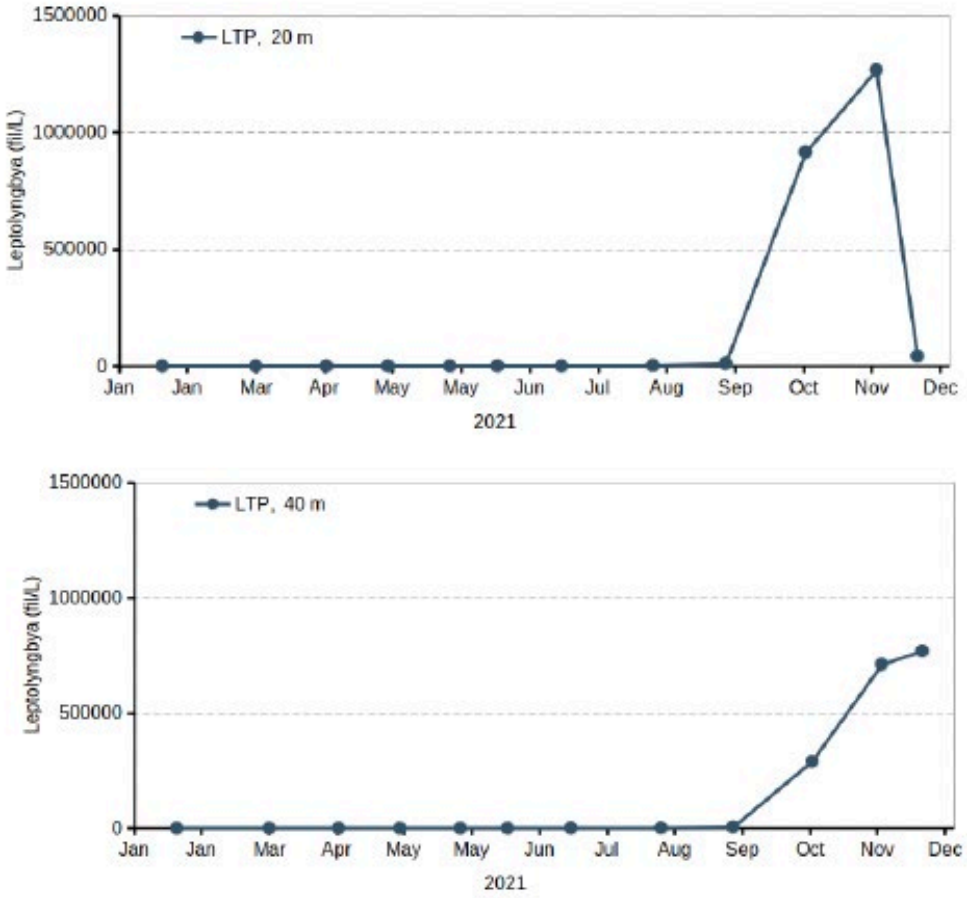

Figure 28. *Leptolyngbya* filaments per litre at each sampling at the LTP depths of 20 meters (top) and 40 meters (bottom).

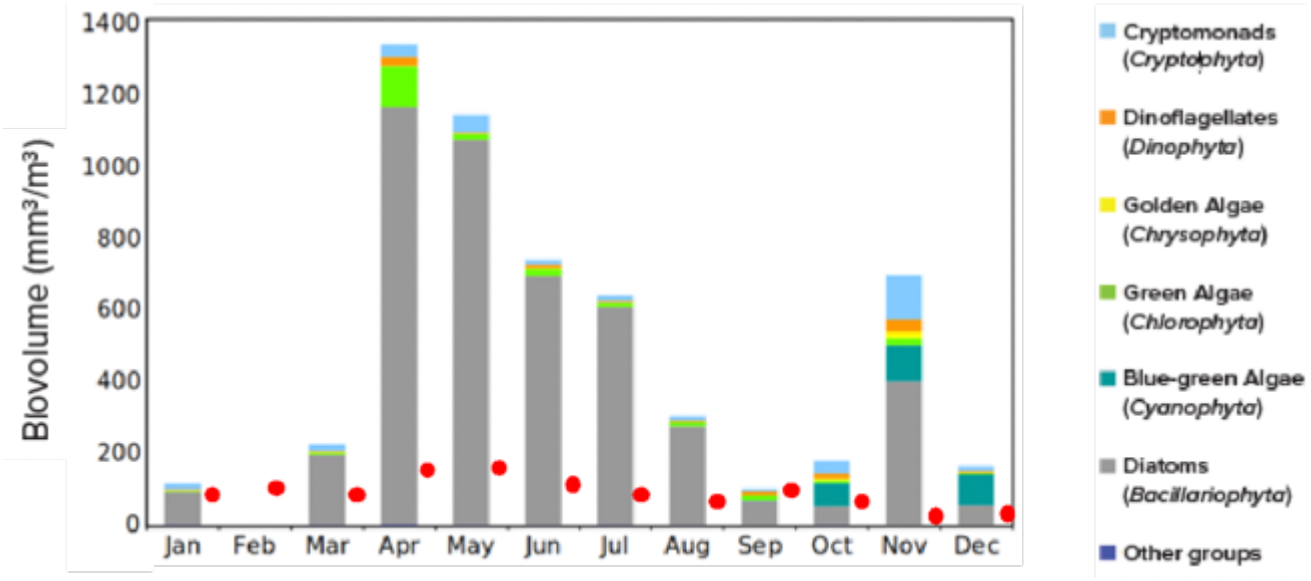

Figure 29. Algal groups as a fraction of total biovolume in 2021 (bars). The red dots indicate the average total biovolume for years 2012 and 2015-2020.

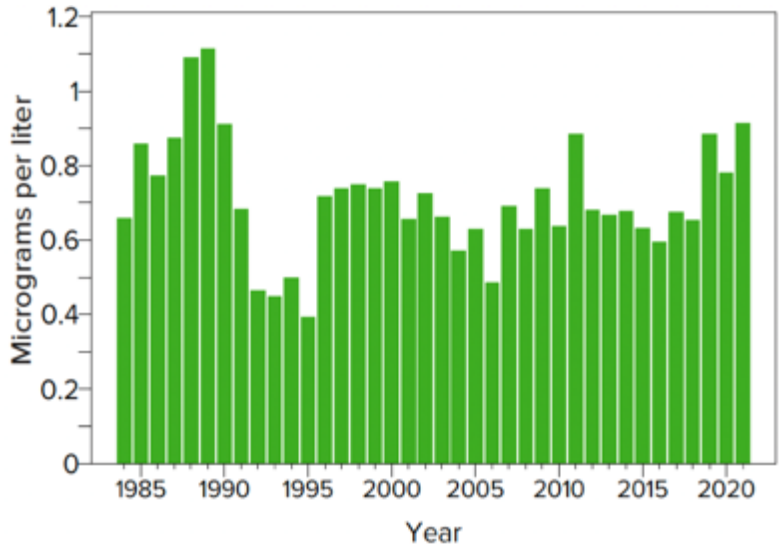

Figure 30. Annual whole lake, depth-averaged chlorophyll-a concentration in Lake Tahoe.

Plain language summary: The cause of the rise in the chlorophyll maximum depth, which commenced in September, is believed to be due to a combination of reduced light levels and a change in the nutrient loading ratio between nitrogen and phosphorus. This favors the growth of the cyanobacteria *leptolyngbya*, which has been shown to be favored by high N:P. In late 2021, the dominant alga (over 90%) by cell number was *leptolyngbya*. This is the only time this has occurred since continuous phytoplankton monitoring commenced in 1982.

The algal biovolume was at a record high level in 2021, mostly in April-July. There was an increase in November, but significantly lower that the spring (pre-fire) biovolumes. The

principal cause is unknown as nutrient inputs were low. One could speculate that climate change may have played a role, although a clear causal mechanism is lacking.

4.5 Primary Productivity (PPr)

Annual average PPr for 2021 was 334 grams of Carbon per square meter per year (gC $m^{-2}yr^{-1}$) (Figure 31). While still provisional, this value is the highest annual value ever recorded. The value is 20% higher than the previous high of 282 gC m^{-2} recorded in 2019. This is consistent with the very high algal abundance in 2021, and with the occurrence of very high cell counts of *leptolyngbya*.

Looking at seasonal changes of PPr from 2015–2021 (Fig 32), the large spring (April) and summer (July) 2021 peaks are clearly visible as well as a smaller (but very significant) peak in the late summer (September), likely driven by wildfire smoke added nutrients.

Figure 32 shows the daily PPr at each sampling from 2015 through 2021. Figure 33 shows the values at each depth during PPr measurement in 2021 (as well as the last value in 2020 and the first value in 2022). The highest value was in spring, with peak PPr at around 30 meters. From July onwards there was a noticeable increase in PPr in the water column suggestive of the impact of atmospherically added nutrients (and reduction of ambient PAR values). The PM2.5 data from Tahoe City (see Figure 34) confirms that July and August were when the impacts of wildfire smoke started to be observed in the northern part of Lake Tahoe.

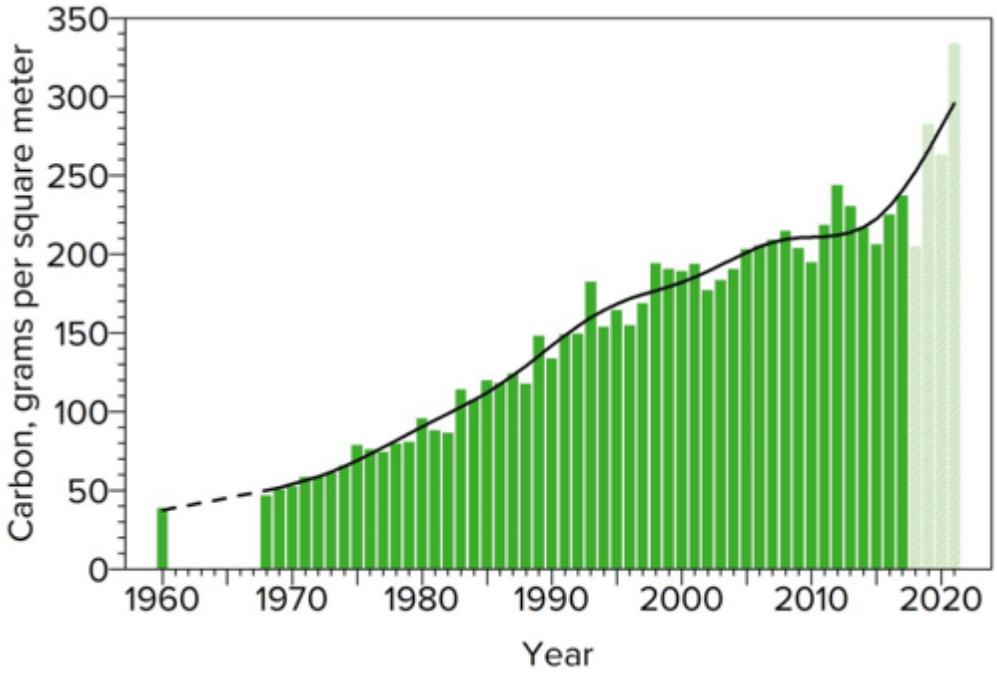

Figure 31. Annual average PPr in Lake Tahoe 1960-2021 in units of carbon uptake per square meter per year. The curve is plotted with a GAM with df=4.

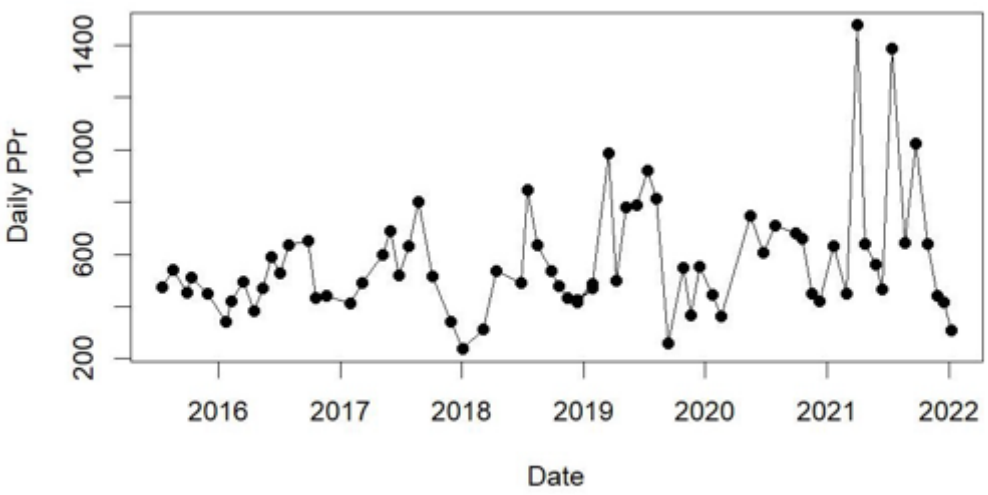

Figure 32. Daily PPr in Lake Tahoe 2015-2021 in units of carbon uptake per square meter per day.

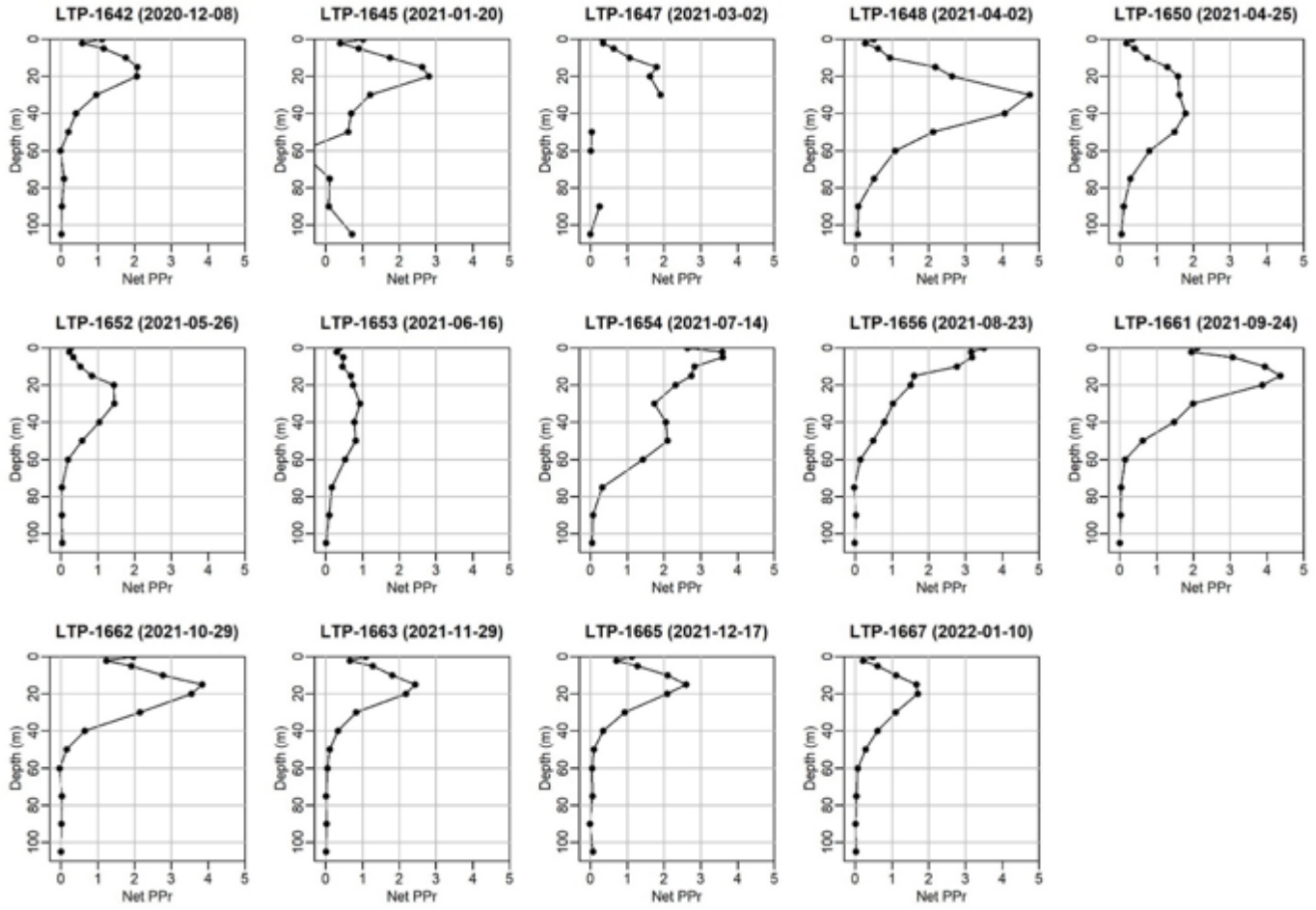

Figure 33. Primary productivity profiles in Lake Tahoe in 2021.

Plain language summary: Primary productivity (as measured by ^{14}C uptake) was at a record high level in 2021. However, the two highest peaks occurred prior to the heavy wildfire smoke period and are likely associated with nutrient inputs from the watershed. This observation is puzzling, although consistent with the previously noted high biovolume observations. as noted previously, stream nutrient loads were very low.

4.6 Measured Particulate Atmospheric Deposition

In July 2021, TERC initiated the measurement of the atmospheric deposition of particulates on Lake Tahoe at buoy TB4. This unfunded effort was in addition to the funded measurement of atmospheric deposition of nutrients at buoy TB1. The daily averaged total fine particle input (0.5–16μm) was highest at a value of 7.8×10^8 particles m^{-2} day^{-1} (Fig 34 top) when wildfire smoke as represented by PM2.5 measurements at Tahoe City was at its maximum (Figure 34 bottom).

Based on these deposition data, the cumulative number of particles falling on the lake in the period July 26 to September 12, 2021 was 1.6×10^{10} particles m^{-2}. Note, that this is assuming that the value recorded in the deposition bucket can be extrapolated over the entire area of the lake. These data are sub-divided into two size classes, small and medium, and summarized in Table 15.

Under the assumption that particles (in the range 0.5–16 μm) deposited on the lake surface are mixed uniformly into the top 20 meters of the lake and that particle size is not transformed through aggregation or other processes, the 7.8×10^8 particles m^{-2} day^{-1} of particle input results in a maximum particle concentration increase over this 20m depth of 3.9×10^4 particles L^{-1} day^{-1}, as shown in Figure 35. The mean particle concentration input over this 20-meter depth was about half this value.

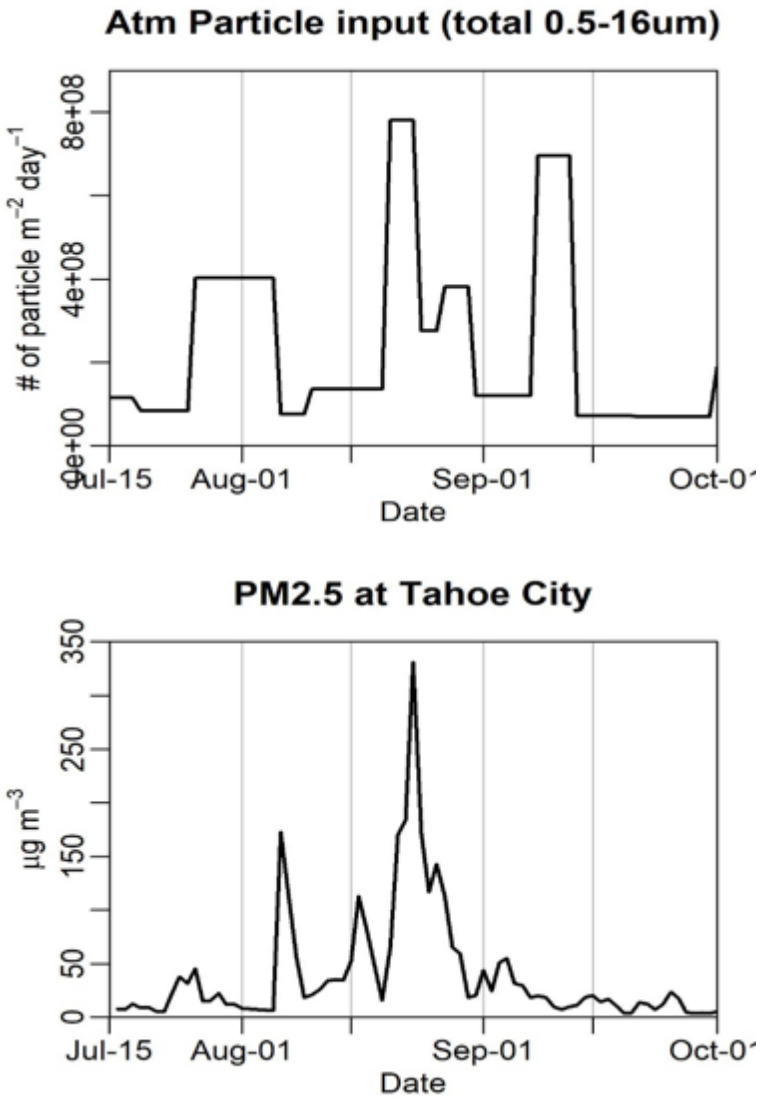

Figure 34. The top figure shoes the daily atmospheric particle flux measured at buoy TB4. The horizontal line indicates the length of the sampler deployment. The bottom figure shows the measured PM2.5 at Lake Tahoe.

Table 15. Summary of particle deposition for each size range.

	Total (0.5-16µm)	Small (0.5-1.0µm)	Medium (1.0-4.0µm)
Maximum Daily value	7.8×10^{8} m^{-2} day^{-1}	5.6×10^{8} m^{-2} day^{-1}	1.8×10^{8} m^{-2} day^{-1}
Cumulative Jul 26 – Sep 12	1.6×10^{10} m^{-2}	1.1×10^{10} m^{-2}	0.4×10^{10} m^{-2}

How much did atmospheric deposition of particles contribute to the number of particles in the upper 20 meters of the lake?

The highest daily atmospheric input accounts for the addition of 0.4% ($3.9 \times 10^4 / 1.0 \times 10^7$) of the particles in the surface layer, and closer to 0.2% over the period. zoom

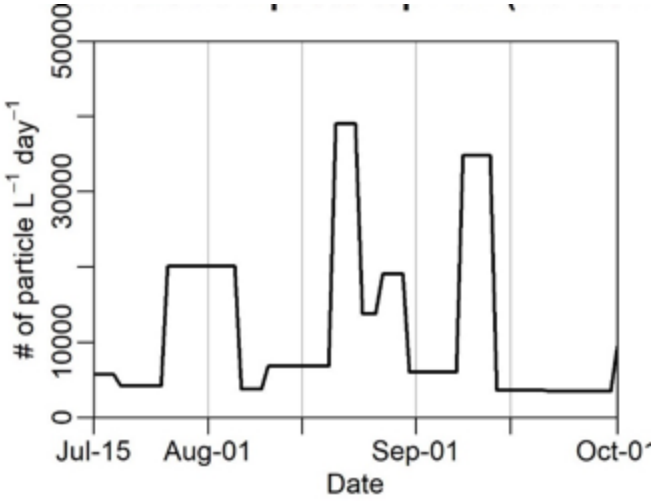

Figure 35. Loading rate of fine particles into the upper 20 meters of Lake Tahoe based on TB4 sampler data in 2021.

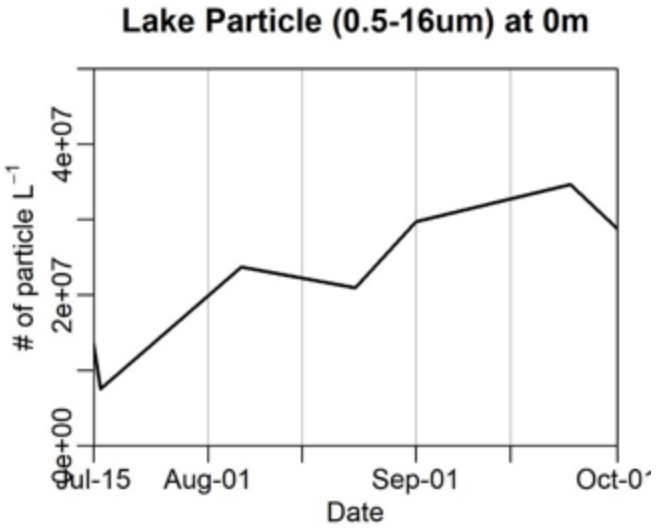

Figure 36. Fine particle concentrations (0.5-16µm) at the surface of Lake Tahoe in 2021.

How did atmospheric deposition of fine particles compare to input via stream inflows?

The Upper Truckee River accounts for approximately 25% of the streamflow into Lake Tahoe. In 2021, the year shown, streamflow was one of the lowest flow years and particle concentrations on record, as shown in Figure 37.

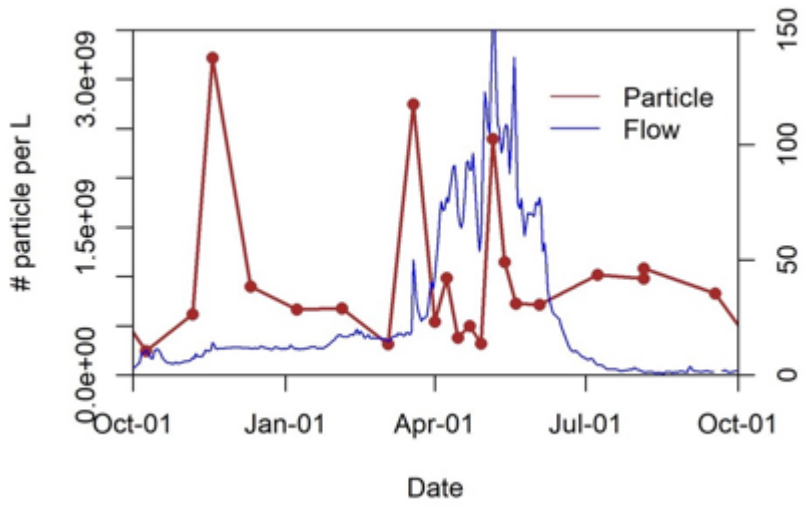

Figure 37. The Upper Truckee River particle concentration and flow.

An approximate flux can be calculated to yield the following plot (Figure 38) of the estimated daily flux. The estimated fine (0.5–16µm) particles added by the UTR in WY2021 was 2.1 x 10^{19} particles. The cumulative number of particles added by atmospheric deposition in the period Jul 26 to Sep 12 was 1.6 x 10^{10} particles m^{-2}. With lake surface area of 490 km^2 the total number of particles added was 7.8 x 10^{18} particles.

Therefore, the atmospheric deposition of particles from the most extensive wildfire smoke event on record, was equivalent to 37% of the particle input from the Upper Truckee River in the near-driest year on record, or an estimated 9% of the input from all streams.

In summary, atmospheric deposition of particles was a relatively small contributor to lake particles overall. During the smoky period, the mean addition of particles was approximately 0.2% of the population of particles in the upper 20 meters of the lake each day. It is not known what fraction of the in-lake particle number was organic or inorganic. The wildfire particles are assumed to be largely inorganic. Nutrient inputs from smoke appear to have stimulated algal growth in the small phytoplankton (and likely picoplankton) and may have produced new organic particles in the upper 20 meters of the lake. The reduced PAR from the smoke may have played a role in this.

Even in this smokiest of years and lowest stream inflow years, stream-borne particles contributed an order of magnitude, more fine particles (although the timing of the two inputs was separated by many months). In other words, the sky is not falling.

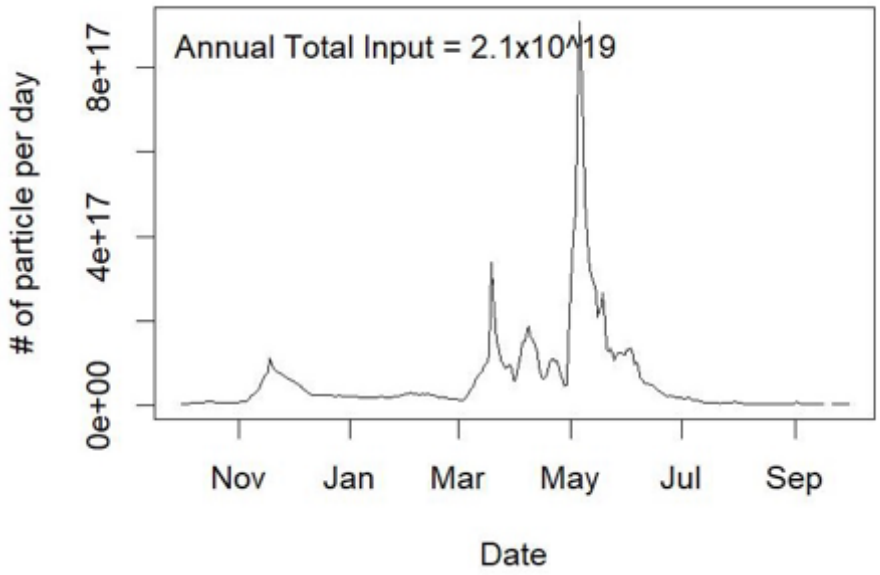

Figure 38. Estimated Upper Truckee River particle flux to Lake Tahoe in 2021.

Objective 5: Task 6. Quantify the particle size distribution, volumetric concentration, and algal biomass measured as chlorophyll-a in the water column affecting clarity and compare it with historical information (Task 6)

Use glider to collect repeat profiles across the lake to augment traditional particle size sampling methods with prototype LISST-200X.

• Glider repeat transects both East-West (approximately 15 hours) and North-South (approximately 24 hours).

• Compare particulate data with previous glider deployments (2018, 2021).

5.1 Autonomous Underwater Glider Payload

As part of the wildfire study, UC Davis deployed their Slocum G2 autonomous underwater glider "Storm Petrel" (a.k.a. Stormy) in Lake Tahoe during the Caldor Fire (Figure 39). The glider was equipped with a buoyancy pump rated for dives up to 200 meters in depth. The glider was equipped with a SeaBird 41CP conductivity, temperature, and depth (CTD) sensor, a WetLabs Eco Puck Triplet (measuring chlorophyll-*a* fluorescence, CDOM, and optical backscatter), and a glider-LISST 200X (measuring particle size distributions, volume concentrations from 1–500µm, and water clarity in terms of 670nm wavelength (red) light attenuation). The equipped payload allowed measurement of several environmentally relevant physical parameters which help characterize the impacts of wildfire smoke on Lake Tahoe's particulate matter concentrations, water clarity, and algal biomass.

The glider was deployed in Lake Tahoe on September 3, 2021, during the peak level of atmospheric fine particulate matter concentrations in the Lake Tahoe Basin. The glider continuously operated while collecting data until September 25 when its battery dropped low enough to necessitate recovery. The glider deployment allowed for continuous high-resolution observations of conditions in Lake Tahoe for over three weeks both during and after atmospheric deposition of smoke and ash particulates from the Caldor Fire.

5.2 Programmed Glider Mission

The glider's navigation behaviors were programmed to accomplish the objectives of repeating transects across the full extent of Lake Tahoe (both E-W and N-S transects) as shown in Figure 40, augmenting traditional particle size sampling methods. While navigating laterally along the programmed transects, the glider continuously repeated dive/climb cycles between the water surface and 150-meter depth while averaging horizontal speeds of 0.5 kt. This maximum dive depth was chosen to increase the amount of data collected in the epilimnion wherein fine particle concentrations, water clarity, and chlorophyll-*a* have the greatest variability and greatest impacts on ecological dynamics in the photic zone.

5.3 Algal Biomass Measured as Chlorophyll-*a*

Chlorophyll-*a* distributions were consistent with previous years' observations for late summer in Lake Tahoe, exhibiting a distinct vertical structure but with very little lateral variability across the lake transects (Figure 41). Chlorophyll-*a* was most highly concentrated in a layer below the thermocline at approximately 50m depth referred to as the deep chlorophyll maximum (DCM). Chlorophyll-*a* concentrations near the DCM (from 40–60m depth) were observed in the range of 1–1.5µg/l, with significantly lower concentrations both above and below this layer. These observations are in excellent agreement with the vertical profiles of chlorophyll-*a* presented in Section 4.1. A very gradual trend of DCM shoaling can also be seen over time, which is more clearly pronounced across the longer-term data provided in Section 4.1.

Figure 39. The UC Davis glider being recovered from Lake Tahoe with the equipped science payload.

5.4 Lateral Variability along Transects

One advantage of autonomous gliders in supplementing traditional vertical profiling techniques is the ability to collect data spanning large areas with a high degree of spatial resolution. This can reveal the degree to which measured parameters vary spatially. For this deployment, despite the heterogeneity of atmospheric particulate concentrations and deposition rates, negligible lateral variability in particulate concentrations or chlorophyll-*a* was observed in the glider data. Magnitudes of particulate concentrations typically varied less than one order of magnitude along transects and did not exhibit any discernable spatial pattern (Figure 41).

Instead, variation in particulate concentrations was primarily dependent on depth and time. It is assumed that lake mixing by wind and large-scale water currents was responsible for rapid dispersion of atmospherically deposited particles in the surface layer, which led to the observed lateral homogeneity.

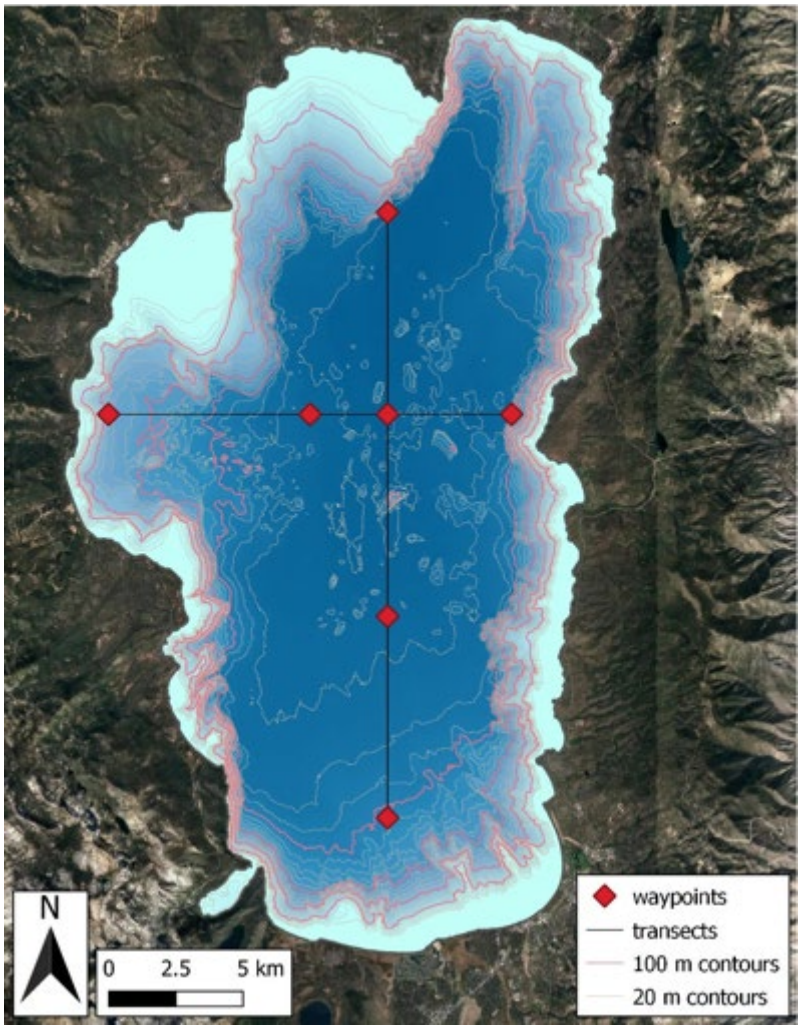

Figure 40. Glider transects and waypoints used for the wildfire study. The glider alternated between a N-S transect at constant longitude and E-W transect at constant latitude. Bathymetric contours of Lake Tahoe are shown for context. Bathymetric data sourced from NOAA satellite.

5.5 Vertical Structure

Profiles of temperature, optical backscatter, chlorophyll-*a* concentrations, fine particulate matter concentrations, and light attenuation are plotted for the entirety of the glider deployment period (Figure 42). The overall vertical profile of temperature stratification was typical for late summer in Lake Tahoe and similar to vertical profiler temperature observations presented in Section 4.1, with a distinct thermocline/metalimnion present around 25 m depth.

Optical backscatter was also greatest near the DCM, with marginally lower backscatter in the epilimnion above and significantly lower backscatter in the hypolimnion below. Because optical backscatter is often greater for particles of organic matter, this result suggests that organic particles are mainly confined to the region at or above the DCM.

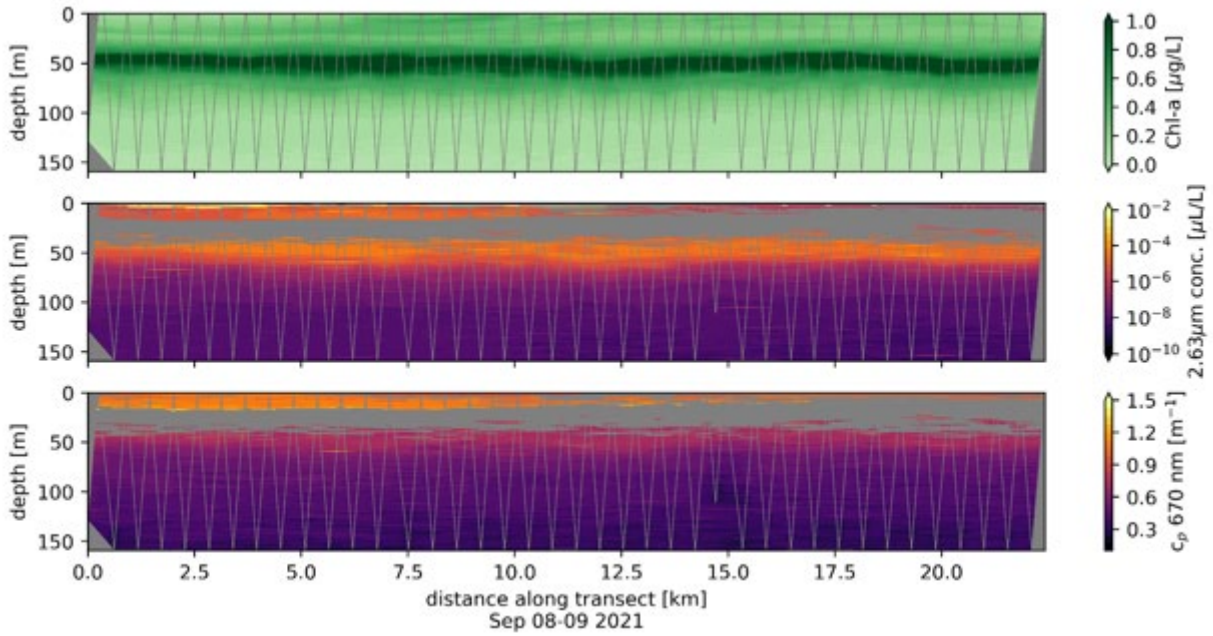

Figure 41. Chlorophyll-a, volume concentration of 2-3µm diameter particles, and light extinction coefficient measured across a South-North glider transect (South on left, North on right) as shown in the map of Figure 40. Gray lines indicate the glider dive/climb profiles between which data are interpolated. The horizontal gray stripe in particle concentrations and extinction coefficient measurements are areas that were excluded due to high stratification which skews LISST measurements.

5.6 Particle Size Distributions and Volume Concentrations

Total volume concentrations of suspended particulate matter (as opposed to number concentrations, which skews towards smaller particles) as measured by the glider LISST-200X (1–500µm diameter size range) were dominated by medium-sized particles in the 10–200µm size ranges. The total volume concentration (sum of concentrations for all size classes) was nearly homogeneous and did not change significantly during the glider deployment period (Figure 43). However, while the total volume of particulate matter in Lake Tahoe was dominated by larger particles, these large particles have a relatively negligible impact on water

clarity compared to small particles in the 1–10µm size range. Despite larger particles occupying more volume, small particles (< 10µm) were more numerous (higher number concentrations) and more efficiently scatter light in the visible wavelength range. Consequently, the dynamics of small particle concentrations in the 1–10µm range have a much greater impact on water clarity compared to large size classes for a given volume concentration, therefore an emphasis is given to particles within this size range. Deposition of these fine particulates from runoff or atmospheric deposition can have significant impacts on water clarity despite having a relatively minor impact on overall suspended particulate matter volume concentrations.

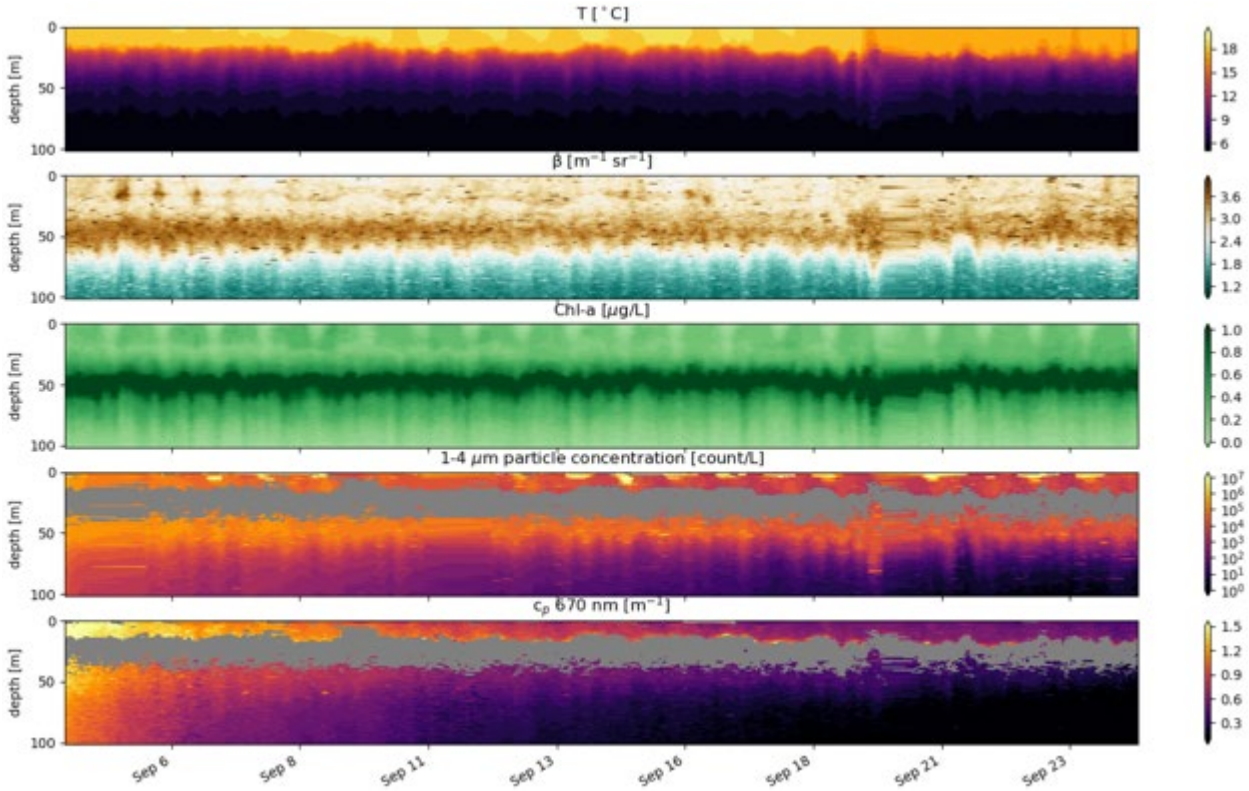

Figure 42. Profiles of measured variables versus depth and time: temperature, optical backscatter, chlorophyll-a concentration, 1-4µm particle number concentration, and beam attenuation coefficient. Greyed out regions in the last two plots are regions of high stratification where schlieren effects create erroneous LISST measurements.

Figure 44a shows the median particle size distribution for each day, taken from all valid measurements over the 0–150m depth range. Concentrations have been converted from volume concentrations to number concentrations (per unit bin width) assuming spherical particles of the median diameter for each size bin. The normalization per unit bin width ensures that integrating this curve over a range of diameters gives the total number of particles within that size range. Median concentrations throughout the water column each day indicate particles between 1–10µm were present in excess of 10^6 particles/L on September 3 but had dropped by an order of magnitude to 10^5 particles/L by September 25.

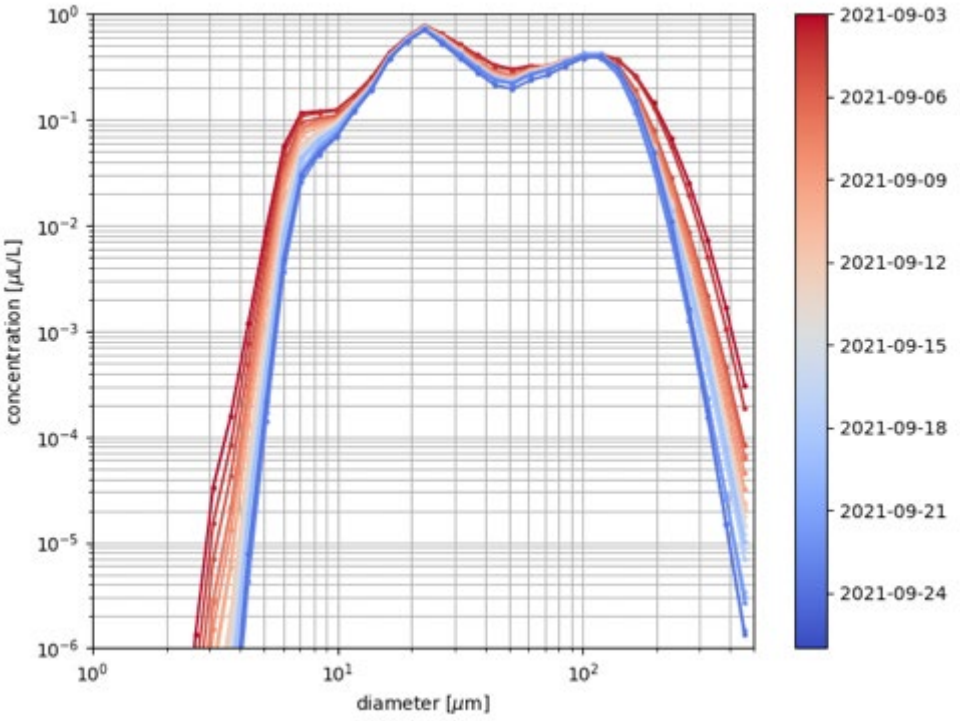

Figure 43. Median daily volume concentrations for each of the 36 logarithmically-spaced particle size bins from 1-500µm measured by the glider LISST-200X throughout the deployment. Note that both axes are log-scaled. One line is plotted giving the median volume concentrations for each day of the glider deployment, averaged over the 0-150m depth range.

5.7 Particulate Matter Dynamics and Comparison with Historical Information

The gradual, rapid decrease in fine suspended particulate matter concentrations observed throughout the glider deployment indicated that these particulates quickly cleared from the water. As atmospheric particulate concentrations waned in early September, concentrations of small particles in Lake Tahoe followed a similar trend with little lag, indicating that these small particles swiftly settled out of the water column or were sequestered by other processes.

The particulate light attenuation coefficient (m^{-1}) as measured by the glider-LISST represents the amount of light intensity from a 670nm wavelength laser beam lost to scattering and absorption by particles as it propagates a given distance through the water. Thus, an attenuation coefficient of 0 corresponds to a perfectly clear water body, while greater attenuation coefficients indicate diminished clarity. Generally speaking, attenuation is inversely proportional to Secchi disk depth, though attenuation can vary vertically while Secchi depth is a bulk parameter characterizing the surface waters as a whole.

On September 3, particulate light attenuation in the upper waters of Lake Tahoe were nearly three times higher (1.4m^{-1}) than typical values observed with a LISST-100X during previous summers (0.4–0.6m^{-1} in September 2010) (Figure 44b). By September 25, light attenuation both in the upper 30 meters and in the upper 150 meters had recovered to typical summertime epilimnetic and hypolimnetic attenuation values of 0.4–0.6m^{-1} and 0.1m^{-1}, respectively (Andrews, 2010). The lag between clearing of atmospheric particulates in the Lake Tahoe Basin and the recovery of Lake Tahoe's water clarity to historical seasonal values (as measured by the 670nm particulate light attenuation coefficient) was approximately two weeks. In January 2022, Secchi depth measurements were near a record high, further suggesting that the influx of atmospherically deposited fine particles from the Caldor Fire had a short-lived residence time and impact on water clarity.

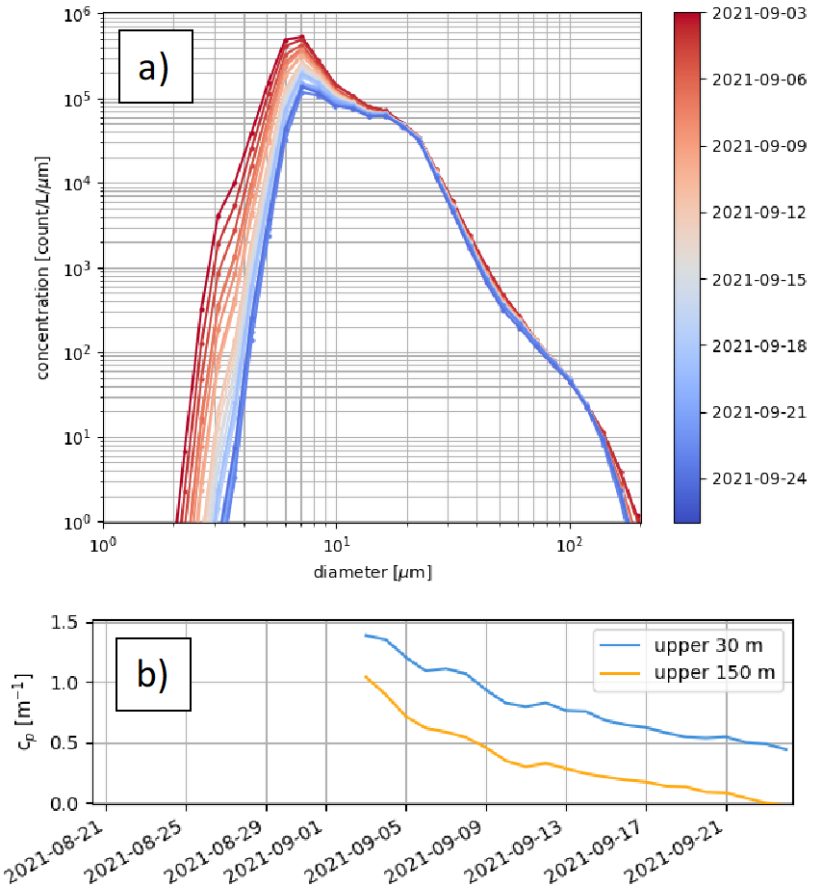

Figure 44. Temporal dynamics of particle concentrations and light attenuation. A) Each line represents the daily median particle size distribution represented as number concentration per unit bin width and colored from red to blue with increasing time. B) average values of the attenuation coefficient taken over the upper 30 meters (blue) and upper 150 meters (yellow) of the water column.

LITERATURE CITED

Andrews, S.W. 2010. Measurement and Interpretation of Light Scattering by Suspended Particulates in an Oligotrophic Lake. PhD dissertation, University of California, Davis. https://www.proquest.com/openview/f493735362eba3c929e52ff8da305923/

Bodí, M. B., D. A. Martin, V. N. Balfour, C. Santín, S. H. Doerr, P. Pereira, A. Cerdà, and J. Mataix-Solera. 2014. Wildland fire ash: Production, composition and eco-hydro-geomorphic effects. Earth-Science Reviews 130:103–127. https://doi.org/10.1016/j.earscirev.2013.12.007

Brahney, J., N. Mahowald, D. S. Ward, A. P. Ballantyne, and J. C. Neff. 2015. Is atmospheric phosphorus pollution altering global alpine Lake stoichiometry? Global Biogeochemical Cycles 29:1369–1383. https://doi.org/10.1002/2015GB005137

Cataldo, D. A., M. Maroon, L. E. Schrader, and V. L. Youngs. 1975. Rapid colorimetric determination of nitrate in plant tissue by nitration of salicylic acid. Communications in Soil Science and Plant Analysis 6:71–80. https://doi.org/10.1080/00103627509366547

Goldman, C. R., A. D. Jassby, and E. de Amezaga. 1990. Forest fires, atmospheric deposition and primary productivity at Lake Tahoe, California-Nevada. SIL Proceedings, 1922-2010 24:499–503. https://doi.org/10.1080/03680770.1989.11898787

Goldman, C. R., A. Jassby, and T. Powell. 1989. Interannual fluctuations in primary production: Meteorological forcing at two subalpine lakes: Interannual lake variability. Limnology and Oceanography 34:310–323. https://doi.org/10.4319/lo.1989.34.2.0310

Jassby, A. D., T. M. Powell, and C. R. Goldman. (n.d.). Interannual Fluctuations in Primary Production: Direct Physical Effects and the Trophic Cascade at Castle Lake, California:19. https://doi.org/10.4319/lo.1990.35.5.1021

Liu, J. C., A. Wilson, L. J. Mickley, F. Dominici, K. Ebisu, Y. Wang, M. P. Sulprizio, R. D. Peng, X. Yue, J.-Y. Son, G. B. Anderson, and M. L. Bell. 2017. Wildfire-specific Fine Particulate Matter and Risk of Hospital Admissions in Urban and Rural Counties. Epidemiology (Cambridge, Mass.) 28:77–85. https://doi.org/10.1097/EDE.0000000000000556

Lottig, N. R., Phillips, J., Batt, R. D., Scordo, F., Williamson, J. T., Carpenter, S. R., et al. (2021). Estimating primary production in lakes: Comparison of ^{14}C incubation and free-water O_2 approaches. *Limnology and Oceanography: Methods*. https://doi.org/10.1002/lom3.10471

Mackey, K. R. M., D. Hunter, E. V. Fischer, Y. Jiang, B. Allen, Y. Chen, A. Liston, J. Reuter, G. Schladow, and A. Paytan. 2013. Aerosol-nutrient-induced picoplankton growth in Lake Tahoe: aerosol-induced picoplankton growth. Journal of Geophysical Research: Biogeosciences 118:1054–1067. https://doi.org/10.1002/jgrg.20084

Melack, J. M., S. Sadro, J. O. Sickman, and J. Dozier. 2021. Lakes and Watersheds in the Sierra Nevada of California: Responses to Environmental Change. First edition. University of California Press. https://doi.org/10.2307/j.ctv17hm9sr

Murphy, J., and J. P. Riley. 1962. A modified single solution method for the determination of phosphate in natural waters. Analytica Chimica Acta 27:31–36. https://doi.org/10.1016/S0003-2670(00)88444-5

Nelson, D. W. 1983. Determination of ammonium in KCl extracts of soils by the salicylate method. Communications in Soil Science and Plant Analysis 14:1051–1062. https://doi.org/10.1080/00103628309367431

Park, S., M. T. Brett, A. Müller-Solger, and C. R. Goldman. 2004. Climatic forcing and primary productivity in a subalpine lake: Interannual variability as a natural experiment. Limnology and Oceanography 49:614–619. https://doi.org/10.4319/lo.2004.49.2.0614

Pereira, P., X. Úbeda, and D. A. Martin. 2012. Fire severity effects on ash chemical composition and water-extractable elements. Geoderma 191:105–114. https://doi.org/10.1016/j.geoderma.2012.02.005

Phillips, J. S. (2020). Time-varying responses of lake metabolism to light and temperature. *Limnology & Oceanography*, *65*(3), 652–666. https://doi.org/10.1002/lno.11333

Raison, R. J. 1979. Modification of the soil environment by vegetation fires, with particular reference to nitrogen transformations: A review. Plant and Soil 51:73–108.

Reheis, M. C. 1997. Dust deposition downwind of Owens (dry) Lake, 1991–1994: Preliminary findings. Journal of Geophysical Research: Atmospheres 102:25999–26008. https://doi.org/10.1029/97JD01967

Sadro, S., J. O. Sickman, J. M. Melack, and K. Skeen. 2018. Effects of Climate Variability on Snowmelt and Implications for Organic Matter in a High-Elevation Lake. Water Resources Research 54:4563–4578. https://doi.org/10.1029/2017WR022163

Scordo, F., S. Chandra, E. Suenaga, S. J. Kelson, J. Culpepper, L. Scaff, F. Tromboni, T. J. Caldwell, C. Seitz, J. E. Fiorenza, C. E. Williamson, S. Sadro, K. C. Rose, and S. R. Poulson. (n.d.). OPEN Smoke from regional wildfires alters lake ecology. Scientific Reports:15. https://doi.org/10.1038/s41598-021-89926-6

Strub, P. T., T. Powell, and C. R. Goldman. 1985. Climatic Forcing: Effects of El Niño on a Small, Temperate Lake. Science 227:55–57. https://doi.org/10.1126/science.227.4682.5

Urmy, S. S., C. E. Williamson, T. H. Leach, S. G. Schladow, E. P. Overholt, and J. D. Warren. 2016. Vertical redistribution of zooplankton in an oligotrophic lake associated with reduction in ultraviolet radiation by wildfire smoke: Wildfire Changes UV and Zooplankton Depth. Geophysical Research Letters 43:3746–3753. https://doi.org/10.1002/2016GL068533

Wan, X., C. Li, and S. J. Parikh. 2021. Chemical composition of soil-associated ash from the southern California Thomas Fire and its potential inhalation risks to farmworkers. Journal of Environmental Management 278:111570. https://doi.org/10.1016/j.jenvman.2020.111570

Williamson, C. E., E. P. Overholt, J. A. Brentrup, R. M. Pilla, T. H. Leach, S. G. Schladow, J. D. Warren, S. S. Urmy, S. Sadro, S. Chandra, and P. J. Neale. 2016. Sentinel responses to droughts, wildfires, and floods: effects of UV radiation on lakes and their ecosystem services. Frontiers in Ecology and the Environment 14:102–109. https://doi.org/10.1002/fee.1228

SUPPLEMENTAL MATERIAL

Objective 2: Task 2. Deposition rates of water-extractable and easily oxidizable micronutrients and metals measure on ash collected in bucket collectors at 10 sites around Lake Tahoe.

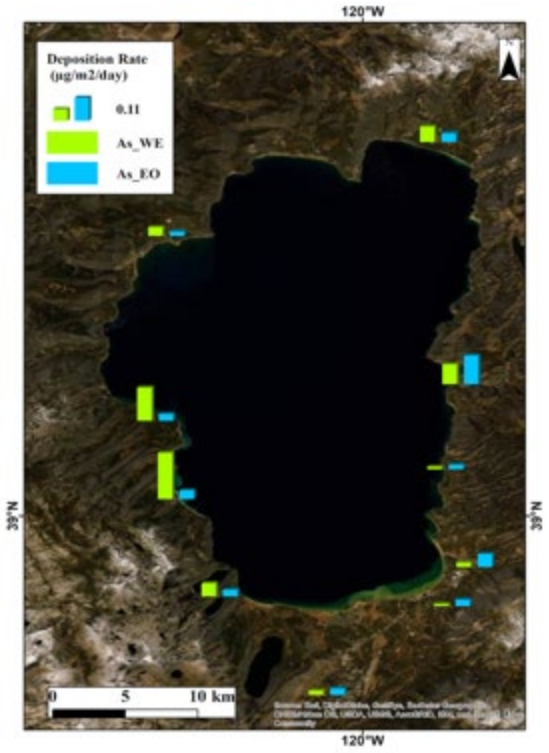

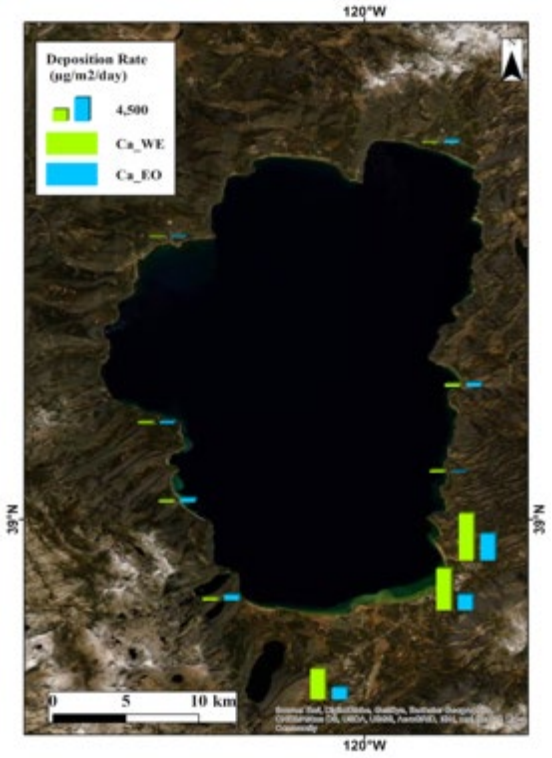

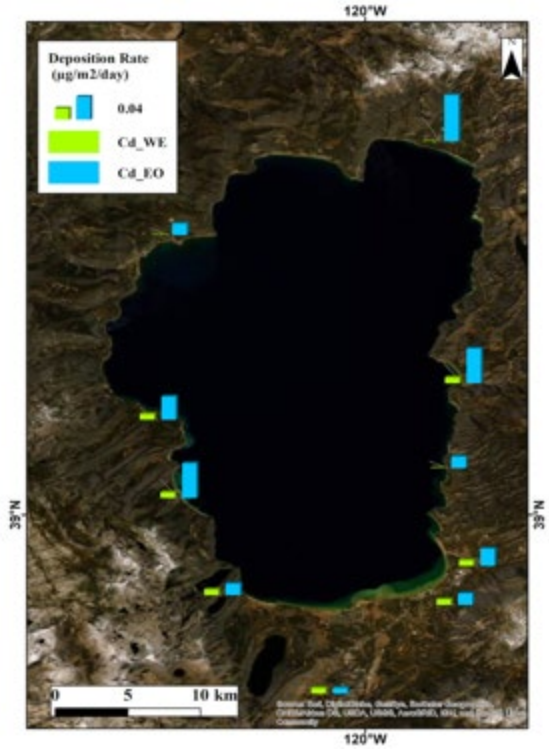

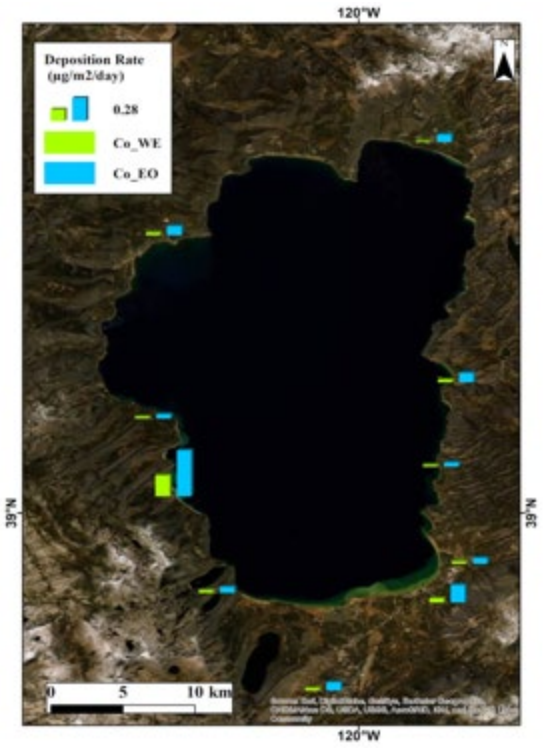

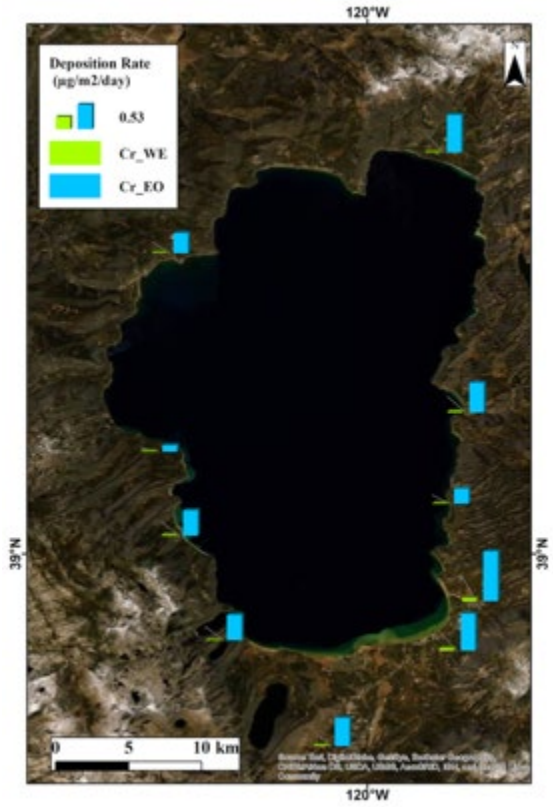
120°W
Deposition Rate
(µg/m2/day)
0.53
Cr_WE
Cr_EO
N
39°N
0 5 10 km
120°W

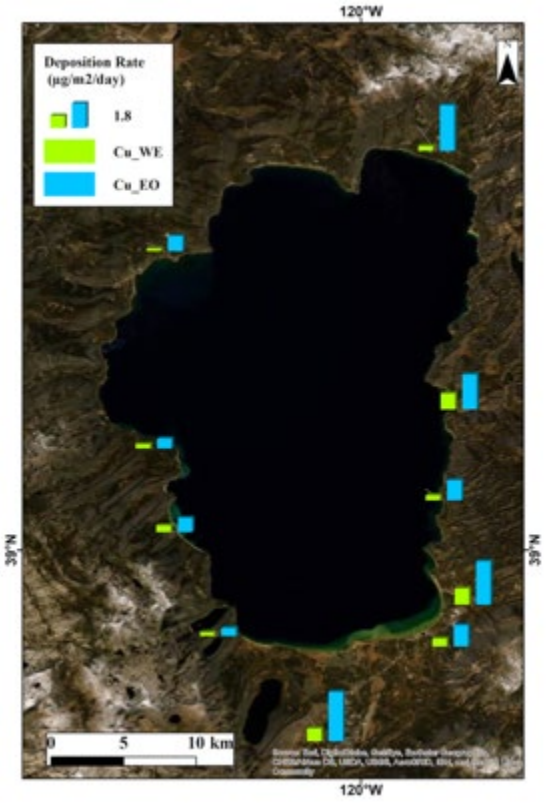
120°W
Deposition Rate
(µg/m2/day)
1.8
Cu_WE
Cu_EO
N
39°N
0 5 10 km
120°W

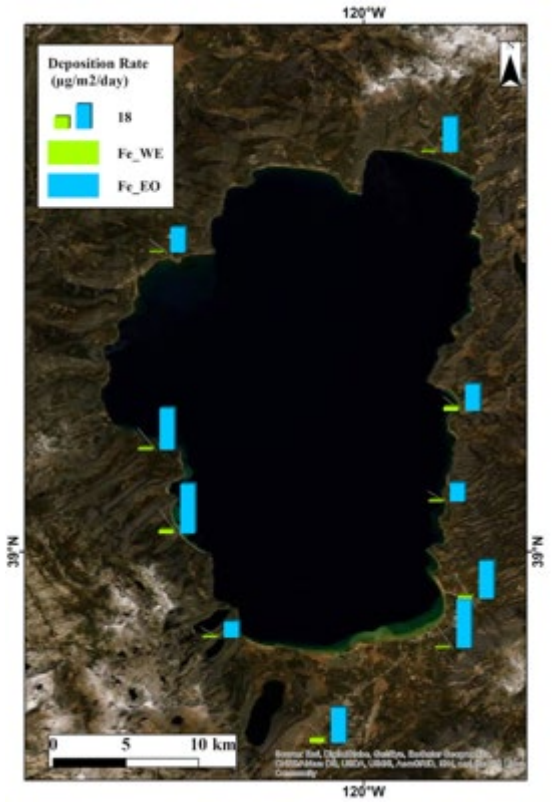
120°W
Deposition Rate
(µg/m2/day)
18
Fe_WE
Fe_EO
N
39°N
0 5 10 km
120°W

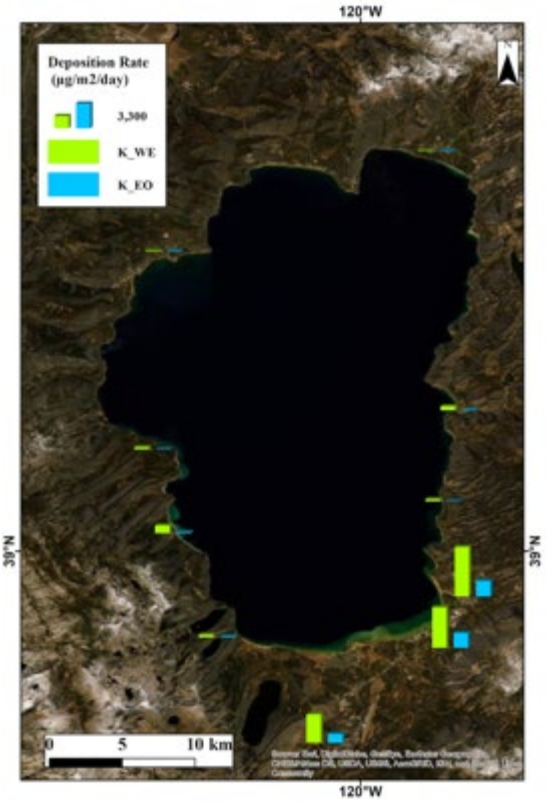
120°W
Deposition Rate
(µg/m2/day)
3,300
K_WE
K_EO
N
39°N
0 5 10 km
120°W

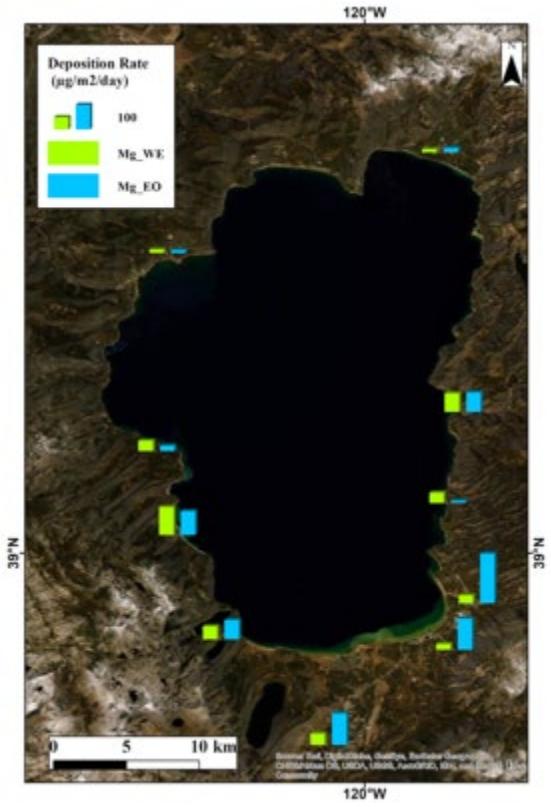
120°W
Deposition Rate
(µg/m2/day)
100
Mg_WE
Mg_EO
39°N
0 5 10 km
120°W

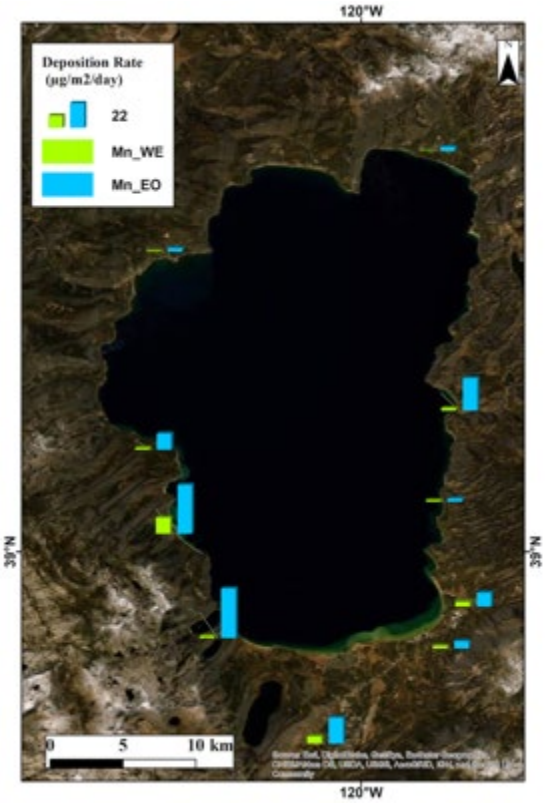
120°W
Deposition Rate
(µg/m2/day)
22
Mn_WE
Mn_EO
39°N
0 5 10 km
120°W

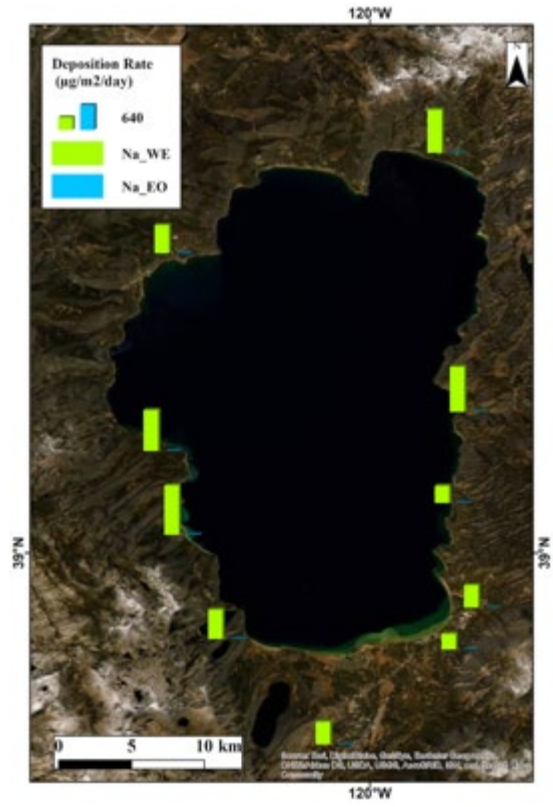
120°W
Deposition Rate
(µg/m2/day)
640
Na_WE
Na_EO
39°N
0 5 10 km
120°W

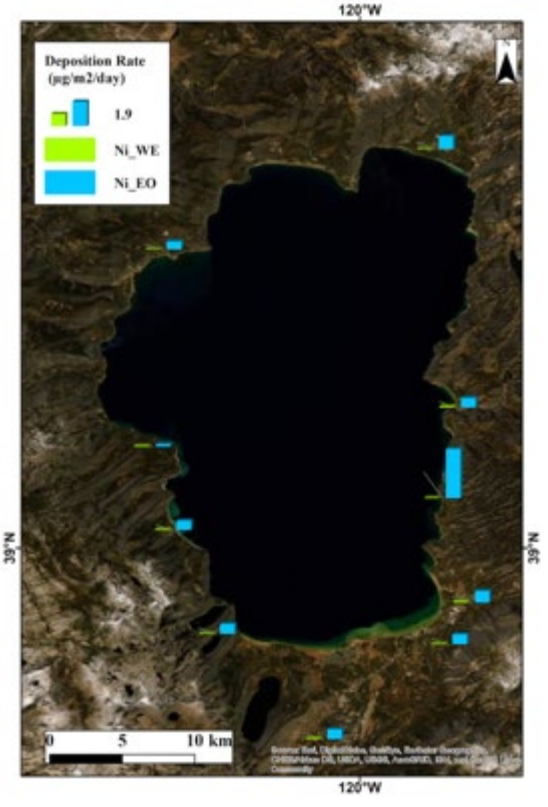
120°W
Deposition Rate
(µg/m2/day)
1.9
Ni_WE
Ni_EO
39°N
0 5 10 km
120°W

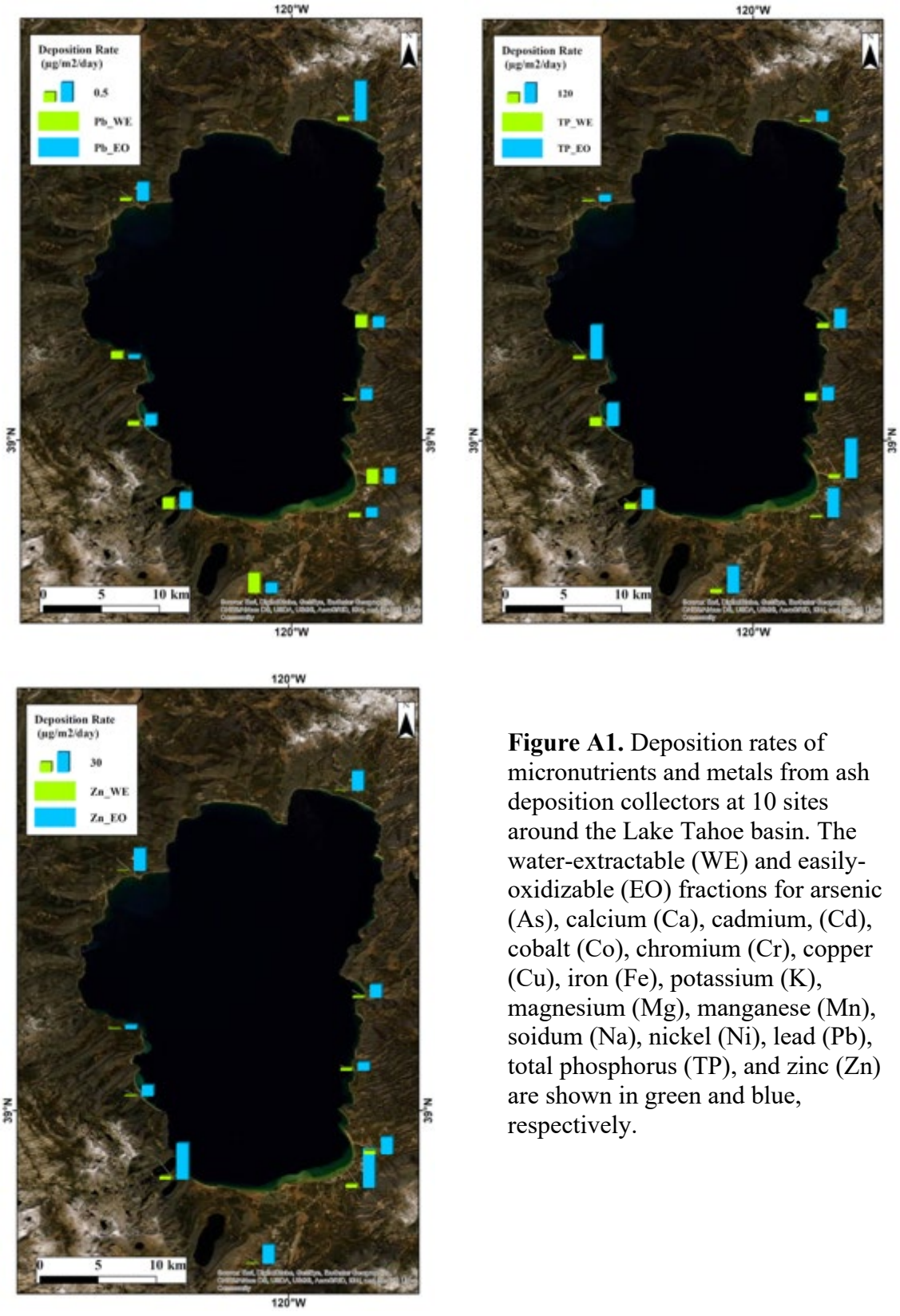

Figure A1. Deposition rates of micronutrients and metals from ash deposition collectors at 10 sites around the Lake Tahoe basin. The water-extractable (WE) and easily-oxidizable (EO) fractions for arsenic (As), calcium (Ca), cadmium, (Cd), cobalt (Co), chromium (Cr), copper (Cu), iron (Fe), potassium (K), magnesium (Mg), manganese (Mn), soidum (Na), nickel (Ni), lead (Pb), total phosphorus (TP), and zinc (Zn) are shown in green and blue, respectively.